RNA Polymerase I Transcription Inhibition: A novel therapeutic strategy for osteosarcoma

CHANG WON KANG

A THESIS SUBMITTED FOR THE DEGREE OF MASTER OF PHILOSOPHY
THE AUSTRALIAN NATIONAL UNIVERSITY

JULY 2020

Declaration

All experimental work presented in this thesis was performed and analysed by the author unless otherwise stated in the text. Dr Lucy Coupland, Dr Kate Hannan and A/Prof. Blackburn supervised the student, assisted in the design and conduct of the experiments and were involved in editing the thesis.

This thesis conforms to The Australian National University guidelines and regulations. The work contained within has not been submitted for the purpose of obtaining any other degree at this or other universities.

Chang-won Kang
(Author, MPhil candidate)

Dr Lucy Coupland
(Supervisor)

Dr Kate Hannan
(Co-supervisor)

A/Prof Anneke Blackburn
(Co-Supervisor)

Cancer and Vascular Biology Group
ACRF Department of Cancer Biology and Therapeutics
The John Curtin School of Medical Research
The Australian National University

JULY 2020

Acknowledgement

Firstly, I would like to appreciate to my supervisors, Lucy Coupland, Kate Hannan and Anneke Blackburn. Thanks to all of your dedicate support, I was able to finish my research project. Also, I would like to express a special thanks to Chris Parish for giving me the chance to undertake an advanced research project in his laboratory and invaluable support.

I also greatly thankful to all the members (past and present) of Parish Lab. Thank you for all the help and good memories you have given me over the past year. Including Ben, Farzi, Anna Orlov, Anna Browne, Dillon, Claudia and Jinsoo for the help, care and discussions (scientific and otherwise). Special thanks to also go to Harpreet, Mick and Cathy of the Imaging and Cytometry Facility for the assistance with In Vivo Imaging System and flow cytometry. I am also thankful to the animal husbandry staff of the Australian Phenomics Facility that provided excellent animal care. I would also like to appreciate The John Curtin School of Medical Research, The Australian National University and The Australian Government for financial support in my search programme.

Most importantly, I would like to thank my special people Nan-hee and my family in Korea for your unconditional love, care and support to on this study and my life.

Thank you to the many other people that I know I have not mentioned individually, but have all helped in countless invaluable ways.

Chang-Won Kang

Abstract

Osteosarcoma (OS) is the most commonly occurring primary bone cancer in the young. A combination of surgery and chemotherapy is the most effective therapeutic strategy, however, the survival rate for patients with metastatic disease is less than 20% at 5 years, a statistic that has not changed for over 30 years.

To support the rapid cell growth and proliferation that are characteristic of cancer cells, the rate of ribosome biogenesis must increase, and the transcriptional activity of RNA Polymerase (Pol) I plays a key role in this process. RNA Pol I transcription activity in normal cells is maintained at a lower rate compared to that observed in cancer cells, which is mediated by a wide range of regulators such as p53, RB, MYC, AKT, S6K and MAPK. In OS, however, these regulators themselves can be dysregulated, for example *TP53* and *RB1* are frequently mutated, whereas c-*Myc* and *MDM2* are amplified. c-Myc can enhance RNA Pol I transcription as can MDM2 by promoting degradation of p53, albeit indirectly. This combination of molecular alterations reported in OS led to the proposal that RNA Pol I transcription is likely to be enhanced, similar to many other cancers, hence its inhibition may prove an effective therapeutic avenue in OS.

CX-5461 and PMR-116 are novel RNA Pol I transcription inhibitors (RNA Pol Ii) in the early stages of clinical development. The anti-tumour effects of CX-5461 have been demonstrated in Phase I clinical trials for breast cancer, lymphoma, leukaemia and prostate cancer. PMR-116 has proven effective in murine leukaemia, prostate cancer and myeloma models, but has not yet been tested in humans. The overall aim of this study was to investigate the therapeutic potential of RNA Pol Ii, CX-5461 and PMR-116, for the treatment of OS.

Experiments in Chapter 3 describe the molecular characterization of 10 human OS cell lines. The expression status of p53, c-Myc, MDM2 and RB1 in these cell lines was assessed. The results of this work suggest three potential mechanisms through which RNA Pol I transcription activity and ribosome biogenesis are enhanced, thus promoting OS cell proliferation.

In Chapter 4, the effects of CX-5461 and PMR-116 on 10 human OS cell lines were evaluated *in-vitro*. Both drugs proved cytotoxic demonstrating anti-proliferative effects on all the OS cell lines tested. Both drugs inhibited their primary target, rDNA transcription, however CX-5461 showed a more pronounced anti-tumour effect through G2 cell cycle arrest in comparison to PMR-116.

In Chapter 5, the *in-vivo* effects of RNA Pol Ii were investigated using xenograft models of OS in Rag 2 knockout mice. The maximum tolerated drug doses in this mouse strain were established as 30 mg/kg for CX-5461 thrice-weekly and 80 mg/kg of PMR-116 twice-weekly. CX-5461 demonstrated significant tumour growth inhibitory effects in the xenografts using the human OS tumour 143B-Luc and SJSA-1-Luc, that are p53 mutant and p53 wild type respectively.

In conclusion, these *in-vitro* studies proposed three possible mechanisms contributing to enhanced ribosome biogenesis in OS. Also, it demonstrated that CX-5461 and PMR-116 can suppress rDNA transcription and exerted an anti-proliferative effect on OS cell lines via G2 cell cycle arrest. In addition, CX-5461 demonstrated a significant reduction in OS tumour growth *in-vivo*. This research suggests that inhibition of RNA Pol I transcription is certainly worth pursuing as an additional therapeutic weapon in the fight against this aggressive cancer.

Table of Contents

List of Figures and Tables

Appendix

Abbreviations

-/-	Knockout
Ab	Antibody
ANOVA	Analysis of variance
B6	C57BL/6 mouse strain
BrdU	Bromodeoxyuridine
DMSO	Dimethyl sulfoxide
DNA	Deoxyribonucleic acid
DNase	Deoxyribonuclease
DMEM	Dulbeccos's Modified Essential Media
EDTA	Ethylenediaminetetraacetic acid
ELISA	Enzyme-linked immunosorbent assay
FACS	Fluorescence activated cell sorting
FBS	Fetal Bovine serum
FITC	Fluorescein isothiocyanate
FSC	Forward scatter
G	Gauge
GIC_{50}	Half maximal growth inhibitory concentration
HBSS	Hank's Balance Salt Solution
HEPES	4-(2-hydroxyethyl)-1-piperazineethanesulfonic acid
IC_{50}	Half maximal inhibitory concentration
i.p.	Intraperitoneal injection
KO	Knockout
Luc	Luciferase
mAb	Monoclonal antibody
MTT	MTT-based cell proliferation assay
MEM	Minimum Essential Media
mRNA	Messenger RNA
Mut	Mutant type
nM	Nanomolar
P	*P*-value

PBS	Phosphate-buffered saline
PI	Propidium iodide
PIC	Pre-Initiation Complex
qPCR	Quantitative Real-Time PCR
RNA Pol Ii	RNA polymerase I transcription inhibitor/s
RPMI	RPMI 1640 Media
RT	Room temperature
S	Second
SD	Standard deviation
SEM	Standard error of the mean
SSC	Side scatter
s.c.	Subcutaneous injection
tIC_{50}	Half maximal rDNA transcription inhibitory concentration
UBF	Upstream Binding Factor
Wt	Wild type

Meetings at which this work has been presented

Poster Presentations

CW Kang, K. Hannan, D. Drygin, M Addach, R. Hannan, C. Parish & L. Coupland. RNA Polymerase I transcription inhibitors as novel therapies for Osteosarcoma. Australian Society for Medical Research (ASMR). ACT, Australia. 2018

CW Kang, K. Hannan, A. Blackburn, D. Drygin, R. Hannan, C. Parish & L. Coupland. Inibition of RNA Polymerase I: A Novel Therapeutic Avenue for Osteosarcoma. Australia and New Zealand Sarcoma Association (ANZSA), ACT, Australia. 2019.

Chapter One

Ribosome Biogenesis and RNA Polymerase I Transcription in Cancer

1. Introduction

Osteosarcoma (OS) is the most common primary cancer of the bone, occurring most frequently between the ages of 0-24 and >60 years of age. The survival rate of OS patients was poor, less than 20% at 5 years post diagnosis, before advances in surgical techniques and chemotherapy increasing this to 60-70% in patients with localised disease (Kansara et al., 2014). Methotrexate, cisplatin and doxorubicin are used as standard chemotherapeutic agents and are combined with surgical removal of the tumour with/without limb sparing depending on the location of the tumour (Luetke et al., 2014, Lamplot et al., 2013). Although these strategies have increased the cure rate to 60-70%, 30% of patients with localised disease have tumours that are chemotherapy resistant mediated by an unknown mechanism (Luetke et al., 2014, He et al., 2014). In addition, chemotherapy did not improve the overall cure rate in OS patients with metastatic disease (Jaffe et al., 1974, Meyers et al., 2011) who have a survival rate of <20% at 5 years. Even recent international trials with more targeted therapies such as trastuzumab (Ebb et al., 2012) along with methotrexate, doxorubicin, and cisplatin (MAP) plus pegylated interferon alpha-2b (IFN-α-2b) (Bielack et al., 2015), or MAP with ifosfamide and etoposide (MAPIE) (Marina et al., 2016) in children with OS disappointingly have not improve outcomes. As these results prove, the survival rate in OS patients has not changed for three decades and new effective therapeutic strategies for improving the outcome in OS are urgently needed. This thesis will show the potential of inhibiting RNA Pol I transcription as a new therapeutic strategy for OS patients.

1.1 Bone and osteosarcoma (OS)

To uncover new strategies of drug development for OS we need to understand the biology involved in generating and maintaining normal bone. Bone is a specialised connective tissue that provides essential functions for vertebrate life, supporting and protecting muscles and organs, providing mobility to the joint system and a microenvironment for haematopoietic tissues (Grabowski, 2009). The homeostasis of human bones is maintained by two types of cells, osteoblasts and osteoclasts. (Sims and Martin, 2014). Both cells have opposite activities, bone production by osteoblasts and bone reabsorption by osteoclasts (Gronthos et al., 1999, Roodman, 1999). Under normal bone homeostasis, the balance between osteoblast and osteoclast activity results in a healthy skeletal structure. When the balance is disrupted, however, bone-related diseases arise including osteosarcoma. A small percentage of OS cases occur in people with Paget's disease (1%), Li-Fraumeni syndrome (12%) and other germline mutations in *TP53* or *RB1* (Smith et al., 1984, Kansara et al., 2014). The majority of OS cases, however, are associated with somatic mutations, particularly in the tumour suppressor genes *TP53* (80%) and *RB1* (30%) (Chen et al., 2014, Wunder et al., 2005).

Human OS is the most common primary malignant neoplasm of human bone (Kansara et al., 2014, Biermann et al., 2013) and accounts for 5 – 10% of malignancies in children, and 0.2% of all cancers (Biermann et al., 2013). The average international incidence of OS is two to four cases annually per million for all ages combined (Rosenberg, 2013). There are two incidence peaks at ages <24 years and greater than 60 years, especially it is frequently observed in male and paediatric patients and young adults when the skeleton is growing most rapidly (Rosenberg, 2013, Lindsey et al., 2017, Gianferante et al., 2017, Mirabello et al., 2009). The most commonly occurring sites are the distal femur, the

proximal tibia and the proximal humerus which are nearest to the metaphyseal growth plates in arm and leg bones. Less commonly occurring sites are the skull, jaw and pelvis (Rosenberg, 2013). Interestingly, approximately 10-20% of OS patients are diagnosed with metastatic disease which occurs most commonly in the lung (90% of cases) (Lindsey et al., 2017, Luetke et al., 2014). The specific factors contributing the OS development have not been clarified. However, disruption of the balance between two major bone cells, osteoblast and osteoclast (Kansara et al., 2014, Thomas et al., 2004), is considered one of the main features for OS development and it is proposed to be the consequence of dysregulated cell cycle in osteoblast differentiation by altered key factors, such as p53 and RB1 (Berman et al., 2008, Miller et al., 1996, He et al., 2015, Velletri et al., 2016).

1.1.1 Molecular features of OS

A genetic feature of OS is chromosomal instability with high levels of somatic structure variations and copy number alterations and it is associated with development and proliferation of OS (Bayani et al., 2007, Chen et al., 2014). As mentioned above the most frequently reported genetic mutations in OS occur in the retinoblastoma 1 (*RB1*) and tumour protein 53 (*TP53*) genes (Kansara et al., 2014, Morrow and Khanna, 2015). In the absence of mitogenic stimuli, RB1 binds to the E2F transcription factors and prevents cell cycle progression from G1 to S phase progression. Under normal mitosis, RB1 is phosphorylated by cyclin-dependent kinase 4 (CDK4) and then releases E2F. E2F increases transcription of genes that will promote cell cycle progression from G1 to S phase (Nevins, 2001), critical cell cycle regulatory elements such as Cyclin Dependent Kinase 1 (CDK1), Cell Division Cycle 25 (CDC25) and Cyclin E. The most frequent mutation of *RB1* in OS is a deletion resulting in a loss of function, thus removes the G1 to S phase cell cycle checkpoint (Miller et al., 1996). Loss-of-function *RB1* mutations are

observed in up to 70% of OS cases (Miller et al., 1996, Benassi et al., 1999). Various rearrangements found in RB1 exons lead to the truncation or deletion of the transcripts resulting in loss of RB1 protein expression (Lorenz et al., 2016). *TP53* is a key transcription factor which protects cells in response to cellular stresses, such as endoplasmic reticulum stress, oxidative stress, hypoxia and DNA damage (Harris and Levine, 2005). In a healthy cell wild type p53 is maintained at a low level by its negative regulator MDM2 which mediates its ubiquitination degradation (Michael and Oren, 2003). When cellular stress is detected, one response is to release p53 from MDM2, thus p53 is phosphorylated and accumulates which results in activation of various responses, such as cell cycle arrest, apoptosis, autophagy, DNA repair and senescence, which prevent the replication of damaged cells (Levine and Oren, 2009). Similar to *RB1*, about 80% of OS cases contain a loss-of-function *TP53* mutation (Martin et al., 2012). Interestingly, *TP53* gene rearrangements appear to be highly specific to OS, being detected in 16-40% of cases, but were not found in 1090 samples of other tumour types analysed. These rearrangements are frequently observed to occur in intron 1 and intron 9. Intron 1 rearrangements lead to loss of exons 1 to 3 resulting in loss of the transactivation domain (Ribi et al., 2015, Lorenz et al., 2016). Intron 9 rearrangements induce loss of exon 9 containing the oligomerization domain (Lorenz et al., 2016). Consequently, these rearrangements lead to p53 protein inactivation. Another highly mutated gene is cellular myelocytomatosis (*c-Myc*) which is a proto-oncogene that codes for a transcription factor and is a member of the *Myc* family, which includes *L-Myc* and *N-Myc*. c-Myc is amplified in 43% of OS (Morrow and Khanna, 2015). Other mutated genes include E3 ubiquitin-protein ligase MDM2 (*MDM2*) and cyclin-dependent kinase inhibitor 2A (*CDKN2A*) (Chen et al., 2014, Sadikovic et al., 2009). Although a correlation between OS and genetic mutations has not yet been revealed, these genetic mutations are considered to be the

major contributors to OS development by induction of abnormal cell cycle progression and dysregulation of osteoblast differentiation (Lindsey et al., 2017, Kansara et al., 2014, Mutsaers and Walkley, 2014, Chen et al., 2014, Thomas et al., 2004). All these reports about highly mutated genes in OS are summarised in Table 1.1.

Table 1.1 Mutated genes in OS

Genes	Names	Frequency
TP53	Tumour protein P53	80%
RB1	Retinoblastoma 1	62%
c-Myc	Cellular myelocytomatosis	43%
MDM2	E3 ubiquitin-protein ligase Mdm2	6%
CDKN2A	Cyclin-Dependent Kinase inhibitor 2A	20%

The table was generated from data presented in (Chen et al., 2014, Lonardo et al., 1997, Stock et al., 2000, Miller et al., 1996)

1.1.2 Current therapeutic strategies for OS

The current standard treatment for OS patients includes a wide surgical resection of the primary tumour with significant efforts made to salvage the limb, chemotherapy and, in limited circumstances, radiotherapy (Lindsey et al., 2017, Luetke et al., 2014). These treatment strategies are depending upon the tumour site (Luetke et al., 2014).

Prior to advanced imaging techniques, a margin of 5-cm around the tumour was the goal to minimise tumour recurrence and metastasis; however, this extent of tissue excision often eliminated the opportunity to salvage the limb or leave a sufficient appendage for prosthetic attachment (Lamplot et al., 2013). Advanced imaging techniques, such as Magnetic Resonance Imaging (MRI) and Computed Tomography (CT)-scanning, have permitted the reduction of the surgical margin and, combined with chemotherapy, has resulted in a decrease in tumour recurrence and increased opportunities for limb reconstruction (Jaffe et al., 1974, Luetke et al., 2014).

The current standard chemotherapies used are high-dose methotrexate, doxorubicin and cisplatin (MAP) (Luetke et al., 2014, Lamplot et al., 2013). Methotrexate binds to dihydrofolate reductase preventing the synthesis of thymidylate which is essential for cell growth and proliferation (Jaffe, 2009). Doxorubicin intercalates into DNA inducing topoisomerase II-mediated single-and double-strand breaks. Cisplatin is a platinum-containing chemotherapeutic agents that crosslinks purine bases in DNA causing damage, preventing replication and inducing cell apoptosis (Dasari and Tchounwou, 2014). All 3 drugs are most often administered intravenously (Lamplot et al., 2013) and pre- and/or post-surgical tumour resection (Luetke et al., 2014).

While improvements have been made for patients with localised disease, the prognosis for patients with metastatic disease has not changed over the last thirty years. In a recent effort, four collaborative groups, the Children's Oncology Group (COG), Cooperative Osteosarcoma Study Group (COSS) of the German Society for Paediatric Oncology and Hematology (GPOH), European Osteosarcoma Intergroup (EOI) and Scandinavian Sarcoma Group (SSG) formed the EURAMOS (European and American Osteosarcoma Studies) and conducted clinical trials. They found that IFN-α-2β and ifosfamide with etoposide also showed good histological response in OS patients and then conducted clinical trials combining it with standard chemotherapy (Whelan et al., 2010, Goorin et al., 2002). Specifically, they compared MAP, MAP with IFN-α-2β or with ifosfamide and etoposide to improve the survival rate in OS patients. Unfortunately, no significant improvements were observed in the event-free survival rate for primary or metastatic cases when compared with MAP alone (Carrle and Bielack, 2009, Marina et al., 2016, Bielack et al., 2015). Mifamurtide, an immunomodulator which activates macrophages and monocytes, was combined with standard chemotherapy (Methotrexate, doxorubicin

and cisplatin: MAP) in Phase I-III clinical trials in OS (Meyers et al., 2005, Murray et al., 1989, Kleinerman et al., 1992, Anderson et al., 2014, Chou et al., 2009). Although mifamurtide was well tolerated and demonstrated a small but significant improvement in event-free survival (EFS) in non-metastatic cases, it unfortunately had no beneficial effect in patients with metastatic disease (Jimmy et al., 2017). The results of these trials came as a great disappointment to everyone in the field and emphasises the need new therapeutic strategies to improve the outcome for OS patients.

Chemotherapy can have significant unintended toxic effects including myelosuppression, mucositis, cardiac failure, hearing loss, nephrotoxicity, gonadal dysfunction. In addition, long-term chemotherapy can cause types of secondary cancers, such as leukaemia, myelodysplastic syndrome, breast cancer, central nervous system (CNS) tumours, carcinomas of various types and soft-tissue and bone sarcoma (Luetke et al., 2014, Janeway and Grier, 2010, Jaffe, 2009, Marina et al., 2016).

Radiotherapy has been one of the most efficient therapeutic strategies for most cancers. However, for OS patients, the use of radiotherapy is carefully considered as OS tends to be a radio-resistant tumour (Schwarz et al., 2009, DeLaney et al., 2005). In addition, it has been reported that 3% of secondary OS arise from prior radiotherapy fields (Kansara et al., 2014). Despite this, radiotherapy is administered to OS patients with unresectable or incompletely resected tumours (Ciernik et al., 2011). Also, it can be an important option when tumours occur in inoperable sites including the spine or the base of the skull. (Schwarz et al., 2009, Dai et al., 2011).

New therapeutic strategies are desperately needed to improve outcomes for OS patients especially those with treatment-resistant and metastatic disease, and to reduce the short- and long-term side effects of chemotherapies for patients who achieve remission. Recently a first in class novel drug has successfully undergone a Phase I clinical trial, CX-5461. CX-5461 targets RNA Polymerase I transcription activity and ribosome biogenesis which may have efficacy for all cancers, including OS.

1.2 Ribosome biogenesis and RNA polymerase (Pol) I transcription

Cell proliferation (an increase in cell number) and cell growth (an increase in cell mass) are exquisitely linked (Grummt, 2013). Cell growth is a pre-requisite for cell proliferation, and they both require a significant increase in protein production by ribosomes (Drygin et al., 2010). Ribosome biogenesis is one of the most complex and energy consuming processes in the cell (Figure. 1.1) (Hein et al., 2013). In humans, the ribosome is composed of two subunits, the 40S subunit which incorporates the 18S ribosomal RNA (rRNA) and 33 distinct ribosomal proteins (RPs) and the 60S subunit including three rRNA (5S, 5.8S and 28S rRNA) and 47 distinct RPs (Bywater et al., 2013). Three RNA polymerases, RNA polymerase (Pol) I, II and III are required to generate a ribosome. Among these RNA polymerases, its Pol I that transcribes what is considered as the key component of ribosome, pre 47S rRNA which is processed to generate the 5.5S, 18S and 28S rRNA, from rDNA promoter regions within the nucleolus (Drygin et al., 2010). For the initiation of rDNA transcription, assembly of multiprotein complexes are required on rDNA promoter region containing RNA Pol I and pre-initiation complex. Two RNA Pol I-specific factors, Selective factor 1 (SL-1) and upstream binding factor (UBF), bind to rDNA promoter and lead to the assembly of the pre-initiation complex. Assembled RNA Pol I complex transcribes the rDNA generating

the pre 47S rRNA which is processed to the 5.5S, 18S and 28S rRNA which all occurs within the nucleolus. In the nucleus, RNA Pol II transcribes messenger RNA (mRNA) that encodes ribosomal proteins (RPs). The mRNA is translated to ribosomal proteins (RPs) by the ribosome in the cytoplasm and RNA Pol III transcribes 5S rRNA in the nucleus. These products are translocated into the nucleoplasm and assembled along with 5.5S, 18S, and 28S rRNA to form the 90S processome. This complex is further processed to form the 40S and 60S subunits that are exported to the nucleoplasm. From there the two subunits are exported to the cytoplasm where they form the mature 80S ribosome (Figure 1.1). The main function of the 40S subunit is to bind, unwind and scan the messenger RNA (mRNA). In contrast, the 60S subunit is involved in peptide bond formation and quality control of peptides (Shen et al., 2015).

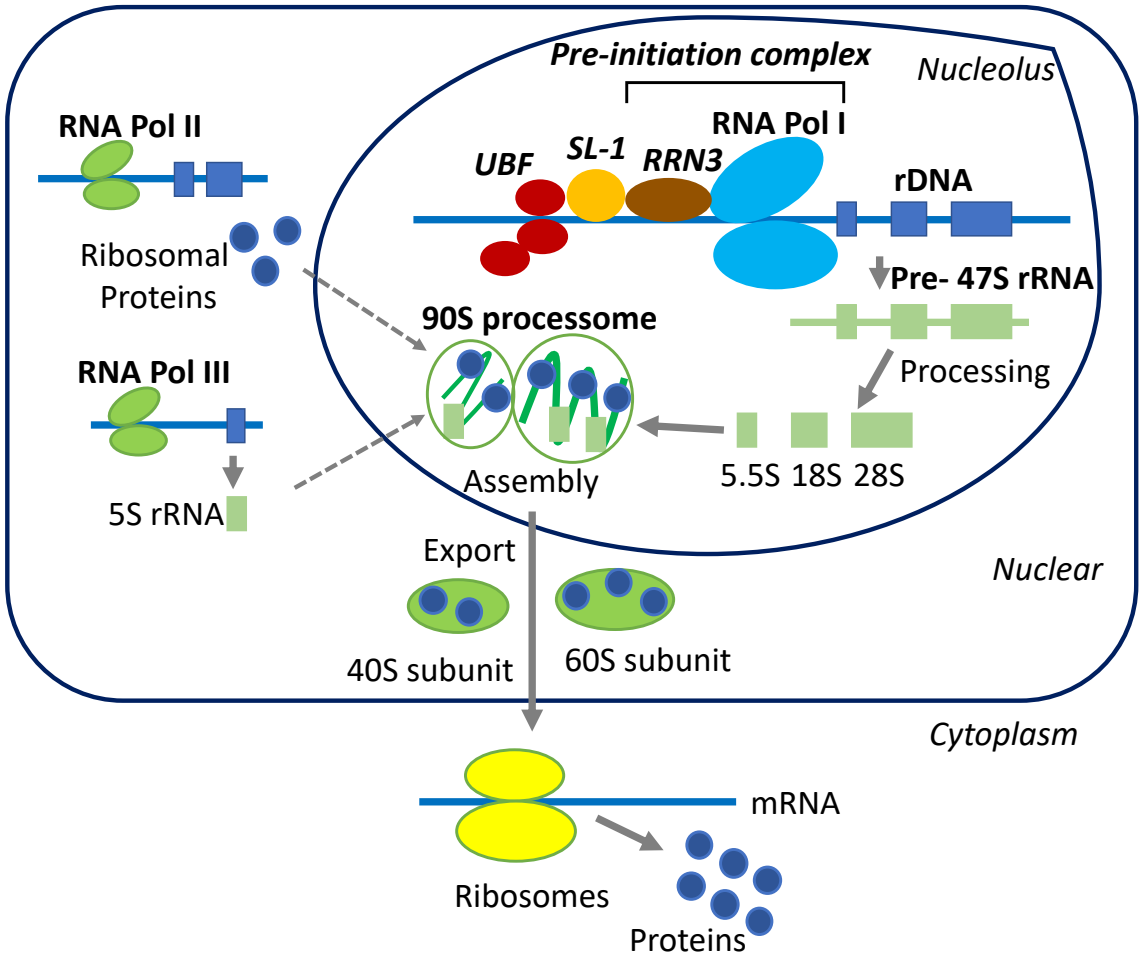

Figure 1.1 Schematic diagram of ribosome biogenesis
All RNA polymerases (RNA polymerase I, II and III) participate in ribosome biogenesis. The main process of ribosome biogenesis occurs within the nucleolus. Under cell growth stimulation, two RNA polymerase I specific factors, upstream binding factor-1 (UBF-1) and promoter selectivity factor (SL-1), bind to rDNA promoter regions. These two factors lead to the formation of the RNA Pol I pre-initiation complex. The recruited RNA Pol I transcribes the pre-47S rRNA precursor (47S pre-rRNA). The 47S pre-rRNA is co-transcriptionally processed into 5.5S, 18S and 28S rRNAs. These are assembled along with the 5S rRNA and RPs, which are transcribed by RNA polymerase III and RNA polymerase II, respectively, within the nucleoplasm to formed the 40S and 60S subunits. Finally, the 40S and 60S are exported to the cytoplasm and form the mature 80S ribosome on an mRNA, which is then translated to generate a protein (Adapted from (Hein et al., 2013, Pelletier et al., 2018, Drygin et al., 2010)).
Abbreviation: RNA Pol I=RNA polymerase I; RNA Pol II=RNA polymerase II; RNA Pol III=RNA polymerase III; UBF=Upstream binding factor; SL-1=Selective factor-1; RRN3=RNA polymerase I-specific transcription initiation factor RRN3; rDNA=ribosomal DNA; rRNA=ribosomal RNA,

1.3 Ribosome biogenesis and RNA Pol I transcription in cancer

Ribosome biogenesis is markedly enhanced in cancer cells and is related to cancer pathogenesis (Pelletier et al., 2018). Compared to normal cells, cancer cells have enhanced growth and proliferation rates, as a consequence of genetic mutation(s) and/or altered signalling pathways (Hanahan and Weinberg, 2011). In order to facilitate growth and proliferation, cancer cells upregulate ribosome biogenesis and RNA Pol I transcription activity (Drygin et al., 2010), which has been reported in numerous cancers (Bywater et al., 2012, Rebello et al., 2016, Xu et al., 2017), and is reflected by enlarged nucleoli (Denais and Lammerding, 2014, Tiku and Antebi, 2018). Influencing ribosome biogenesis, p53 and RB1 can inhibit RNA Pol I transcription by suppressing UBF binding to rDNA, while c-Myc increases RNA Pol I transcription by stimulating UBF and SL-1 binding to the rDNA promoter (Hannan et al., 2000, Zhai and Comai, 2000). Also, PI3K/AKT/mTOR signalling can promote ribosome biogenesis directly or via cooperating with c-Myc (Chan et al., 2011). In cancer cells, all these factors are commonly dysregulated by mutations resulting in their loss or altered function (Hanahan and Weinberg, 2011, Janku et al., 2018, Faivre et al., 2006, Hoxhaj and Manning, 2020, Polivka and Janku, 2014). The result of these genetic anomalies is enhanced RNA Pol I transcription and ribosome biogenesis (Drygin et al., 2010, Grummt, 2013). Based on these findings, the manipulation of ribosome biogenesis in cancer cells was hypothesised as a potential new strategy for cancer therapy (Boisvert et al., 2007, Derenzini et al., 2009).

1.3.1 Ribosome biogenesis and RNA Pol I transcription in OS

Several studies have revealed that factors such as c-Myc, p53, RB1 and ribosomal protein L34 are altered in OS and its been proposed that ribosome biogenesis may be abnormally enhanced (Chen et al., 2018, Montanaro et al., 2007, Luo et al., 2016) . Genetic mutations resulting in the loss of functional p53, the lack of regulator Cyclin-Dependent Kinase 4 (CDK4) causing RB1 inactivation (Miller et al., 1996, Zhou et al., 2018, Kansara et al., 2014), and c-Myc overexpression have all been described in OS (Chen et al., 2018) (Table 1.1). An additional factor, MDM2, a negative regulator of p53, is commonly upregulated in OS and may induce tumorigenesis through the suppression of wild type p53 activity (Miller et al., 1996). Montanaro and colleagues reported that the inhibition of ribosome biogenesis by actinomycin D affects OS cell cycle progression in both p53 and RB1 efficient and deficient conditions (Montanaro et al., 2007). All these results support that ribosome biogenesis and RNA Pol I transcription activity is altered in OS and thus maybe a new effective therapeutic target.

1.4 Novel RNA Pol I transcription inhibitors: CX-5461, PMR-116 and BMH-21

The function of the nucleolus in ribosome biogenesis was revealed in the early 1960's, however, the potential of this as a new target for cancer treatment has not been recognized widely until the 2000's. After confirming a therapeutic efficacy for targeting the ribosome by CX-5461, an RNA Pol I transcription inhibitor, studies were conducted to estimate whether conventional chemotherapies also had inhibitory effects on RNA Pol I transcription activity, such as Actinomycin D (Fetherston et al., 1984, Burger et al., 2010), Doxorubicin and Cisplatin (Burger et al., 2010) (Table 1.2). Interestingly, their inhibitory effects on ribosome biogenesis had been confirmed from many studies with many cancers, but the activities of these drugs are not limited to RNA Pol I transcription activity

(Jordan and Carmo-Fonseca, 1998a). CX-5461 and PMR-116 are a new class of RNA Pol I transcription inhibitors (RNA Pol Ii) with a high therapeutic efficacy on cancer cells. CX-5461, first generation, and PMR-116, second generation, are selective for their primary target, RNA Pol I (rDNA transcription), and have no noticeable effect on DNA (Haddach et al., 2012, Hannan, 2018). BMH-21, a third RNA Pol I transcription inhibitor, also demonstrated inhibitory effects on RNA Pol I transcription activity against a number of tumour cell types including osteosarcoma *in vitro* (Fu et al., 2017, Peltonen et al., 2014, Colis et al., 2014a) and melanoma and colorectal carcinoma *in vivo* (Peltonen et al., 2014, Colis et al., 2014b) . The tolerability and efficacy of BMH-21 remains to be determined in clinical trials.

Table 1.2 Chemotherapies with an additional impact on ribosome biogenesis

Drug	Target	Impact on ribosome biogenesis	Cancer type(s)	Refs
Mitomycin C	Guanosines in 5'-CpG-3' motif	Inhibition of Pol I transcription	Adenocarcinoma, stomach, pancreas, anal, bladder, breast, cervical, colorectal, head, neck and non-	(Burger et al., 2010)
Actinomycin D	GC-rich duplex DNA	Inhibits Pol I transcription at low nanomolar concentrations	Wilms tumour and Ewing sarcoma	(Burger et al., 2010, Fetherston et al., 1984)
Cisplatin	Adjacent guanosines in DNA	Inhibition of Pol I transcription	Testicular, bladder, lung, oesophagus, stomach, ovarian sarcoma, and lymphoma	(Burger et al., 2010, Jordan and Carmo-Fonseca, 1998b)
Doxorubicin	DNA and Topoisomerase II	Inhibition of Pol I transcription	Bladder, breast, stomach, lung, ovarian, and thyroid cancer, leukaemia, myeloma	(Burger et al., 2010)
5-Fluorouracil	Thymidylate synthase	Impairs late rRNA processing	Colon, oesophageal, gastric, rectum, breast, biliary tract, head and neck, cervical, pancreas, renal cell	(Burger et al., 2010, Ghoshal and Jacob, 1997)

(Adapted from (Hein et al., 2013))

1.4.1 CX-5461: The first generation of RNA Pol I transcription inhibitor

CX-5461 was the first developed, orally bioavailable selective RNA Pol Ii which has been used as an anti-cancer therapy in hematologic cancers, lymphoma (Bywater et al., 2012), leukemia and multiple myeloma (Hein et al., 2017). CX-5461 inhibits RNA Pol I transcription by disrupting the interaction between SL-1 and UBF, thus preventing the recruitment of RNA Pol I and formation of the pre-initiation complex at the promoter (Drygin et al., 2011).

The therapeutic efficacy of CX-5461 in human and mouse models of cancer has been reported in many studies (Rebello et al., 2016, Xu et al., 2017, Quin et al., 2016, Negi and Brown, 2015, Drygin et al., 2011, Bywater et al., 2012). In Eμ-Myc driven murine lymphoma, CX-5461 rapidly induced a sub-G1 cell cycle arrest and p53-mediated apoptotic cell death (Bywater et al., 2012). In contrast, in A375 human melanoma cells and MIA Paca-2 human pancreatic cells, CX-5461 mediated its anti-tumour effects via autophagy, in the absence of p53-mediated apoptotic cell death and sub G1 cell cycle arrest (Drygin et al., 2011). While, in acute lymphoblastic leukemia, CX-5461 induced a G2 phase cell cycle arrest mediated by the Ataxia telangiectasia mutated (ATM) and Ataxia telangiectasia and Rad3 related (ATR) kinase pathways, independent of p53 activation (Negi and Brown, 2015).

One publication has reported the anti-cancer effects of CX-5461 on human OS. In this case CX-5461 activated autophagy and inhibited mammalian target of rapamycin (mTOR) signalling pathways in U-2-OS and MNNG/HOS *in-vitro*, and also effectively suppressed U-2-OS tumour growth *in-vivo* (Li et al., 2016).

CX-5461 has been evaluated in a phase I clinical trial with advanced hematologic cancer patients (Khot et al., 2019). In this trial, 170mg/m^2 of CX-5461 once a week for 3 weeks was determined as a maximum tolerable dose and demonstrated a rapid on target inhibition of rDNA transcription with manageable adverse effects in the patients. Also, one patient with a high-grade transformation of lymphoma achieved a clinical response with p53 activation in tumour cells and another one patient with anaplastic large cell lymphoma showed a prolonged partial response. An additional phase I clinical trial of CX-5461 for solid tumour and breast cancer is currently on-going in Canada (ClinicalTrial.gov identifier: NCT02719977).

While CX-5461 is considered a selective inhibitor of rDNA transcription some recent studies have reported off-target activities (Xu et al., 2017, Bruno et al., 2020). Xu and colleagues reported that CX-5461 increased the stability of G-quadruplexes in DNA and induced DNA damage in breast cancer models, which would be considered an off-target effect (Xu et al., 2017). There is also a study suggesting Topoisomerase II activity is dysregulated by CX-5461 (Bruno et al., 2020). Although these off-target effects were not intended, inhibiting topoisomerase II by doxorubicin exhibited a therapeutic benefit (Gill et al., 2013). Thus, inhibiting both topoisomerase II and RNA Pol I with CX-5461 treatment may offer greater therapeutic effects in OS patients.

1.4.2 PMR-116: The second generation of RNA Pol I transcription inhibitor

PMR-116 is a second-generation RNA Pol Ii. Compared to CX-5461, PMR-116 shows improved pharmaceutical properties in the mouse including lower plasma protein binding, a higher oral bioavailability and penetration of the blood-brain barrier, thus would be of benefit for tumours arising in, or metastasising to the central nervous system

(CNS) (Jacus et al., 2016). PMR-116 is less potent mole for mole, but is less toxic compared to CX-5461 (Hannan, Hein, Pimera: unpublished data). Thus, it is predicted that a higher concentration may be given to patients with less toxicity compared to that of CX-5461. The specific mechanism of action for PMR-116 is still to be elucidated.

1.5 Experimental Hypothesis and Aims

To summarise, several studies have revealed that altered pathways contribute to OS development, one of these being enhanced ribosome production, an essential requirement of cell proliferation and growth (Montanaro et al., 2007, Chen et al., 2018, Luo et al., 2016). Increased ribosome biogenesis mediated by RNA Pol I transcription has been identified as a novel target for cancer treatment. In fact, the selective RNA Pol Ii, CX-5461, mediated anti-tumour effects in several cancer models both *in vitro* and *in vivo* and a Phase I clinical trial (Rebello et al., 2016, Xu et al., 2017, Quin et al., 2016, Negi and Brown, 2015, Drygin et al., 2011, Bywater et al., 2012, Khot et al., 2019). One *in-vitro* study demonstrated that the RNA Pol Ii, CX-5461, reduced the proliferation of the OS cell lines, U-2-OS and SaOS. They also confirmed the efficacy of CX-5461 in an *in-vivo* study using the U-2-OS cell line (Li et al., 2016). This publication provided initial evidence for the effect of RNA Pol I inhibition against OS, however, was not sufficient to justify a clinical trial, but it justifies this thesis.

Therefore, based on the above, we hypothesized that the regulation of ribosome biogenesis, through RNA Pol I inhibition with CX-5461 or PMR-116, would prove effective in reducing OS growth and proliferation *in-vitro*, and *in-vivo.*

In order to evaluate this hypothesis, three aims were addressed.

(i) Identify the status of the key regulatory proteins involved in RNA Pol I transcription activity that are frequently altered in the 10 human OS cell lines (Chapter 3);

(ii) Evaluate the effects of RNA Pol Ii, CX-5461 and PMR-116, on the growth and proliferation of 10 human OS cell lines *in-vitro* (Chapter 4);

(iii) Investigate the therapeutic efficacy of RNA Pol Ii against p53 mutant and p53 wild type human OS tumours *in-vivo* (Chapter 5).

Chapter Two

Materials and Methods

2.1 General reagents

2.1.1 Media and buffers

Details of reagents, including cell culture media and buffers used in thesis are listed in Table 2.1

Table 2.1 Media and buffers used in experimental procedures

Name	Catalogue Number	Source
Dulbecco's Phosphate Buffered Saline (PBS)	D8537	Sigma Aldrich, St Louis, MO
Trypsin-EDTA (0.5%), no-phenol	15400054	Gibco, Waltham, MA
Minimum Essential Medium (MEM)	M2279	Sigma Aldrich, St Louis, MO
RPMI 1640	R8758	Sigma Aldrich, St Louis, MO
Dulbecco's Modified Essential Medium (DMEM)	D5671	Sigma Aldrich, St Louis, MO
McCoy's 5A	16600-082	Sigma Aldrich, St Louis, MO
L-glutamine 100M	25030-081	Gibco, Waltham, MA
Sodium Pyruvate 100X	11360-070	Gibco, Waltham, MA
D-Glucose solution 200mg/L	A24940-01	Gibco, Waltham, MA
HEPES 100 mM	15630-080	Gibco, Waltham, MA
Puromycin Streptomycin Neomycin (PSN) 100X	15640-055	Gibco, Waltham, MA
Fetal Bovine Serum (FBS)	F9423	Sigma Aldrich, St Louis, MO

2.2 *In-vitro* techniques

2.2.1 Cell lines

Five human OS cell lines (HOS, 143B, MNNG/HOS, U-2-OS, SJSA-1) in 2017, and five patient-derived human OS cell lines were obtained from Prof Han-Soo Kim from the Seoul National University Hospital in 2017 (KOS-1, KOS-2, KOS-3 KOS-6 and KOS-7) and used in this thesis. Fibroblasts and mesenchymal stem cells share many cellular properties including morphology, cell surface markers, differentiation potential and immunophenotypic properties (Denu et al., 2016). In addition, fibroblasts have been used as a control cell line in osteosarcoma study (Chen et al., 2018, Ando et al., 2005). For these reasons, a human fibroblast (HF) cell line (Lonza, Basel, Switzerland) was used as a control cell line in this study. The SK-UT-1 cell line (purchased from the ATCC in 2017) is a uterine leiomyosarcoma cell line which has been shown to be *TP53* mutant with a high level of p53 protein expression. This cell line was included in these studies as part of another project. Further details on these cell lines are provided in Tables 2.2 and 2.3.

All cell lines were tested annually for mycoplasma contamination using a test kit (Lonza, Basel, Switzerland). The cells were cultured in complete medium (As detailed in Table 2.3) in a Hepa-filtered cell culture incubator at 37°C in a humidified atmosphere containing 5 % CO_2.

The cells were checked daily using an inverted microscope. The cells were sub-cultured when their confluence reached 70 to 80% in the cell culture flask. Cells were washed with 2 ml 1X PBS and trypsinized with 2 ml trypsin-EDTA solution for 5 to 10 min to harvest the cells from the flasks. After trypsin-EDTA treatment, the same volume of complete medium was added, the cells in the solution transferred into 15 ml Falcon tubes and centrifuged (200 *g* for 5 mins at 4° C). The supernatant was removed and cells resuspended in 3 ml of complete medium. Finally, cells were sub-cultured at an appropriate cell density into the cell culture flask. For a 175ml cell culture flaks, all the media volumes were doubled.

Table 2.2 Human sarcoma cell lines

Name	Disease	Ethnicity	Sex	Catalogue number	Source	Reference
HOS	OS	Caucasian	F	CRL-1543	American Type Cell Collection (ATCC), Manassas, VA	(McAllister et al., 1971)
143B*			F	CRL-1543		
MNNG/HOS*			F	CRL-1547		
U-2-OS			F	HTB-96		(Niforou et al., 2008)
SJSA-1		Black	M	CRL2098		(Houghton et al., 1982)
SK-UT-1	LMS	Caucasian	F	HTB-114		(Fogh et al., 1977)
KOS-1	OS	Oriental race	M	Obtained from Seoul National University Hospital, South Korea		(Kim H S, 2005)
KOS-2			M			
KOS-3-			F			
KOS-6			M			
KOS-7			F			
Human fibroblast (HF)		Caucasian		CC-2511	Lonza, Basel, Switzerland	

OS= Osteosarcoma, LMS= Uterine Leiomyosarcoma, M= Male, F= Female

*= 143B and MNNG/HOS cell lines were derived from the HOS cell line

Table 2.3. Complete cell growth media used for cell culture

Cell line	Media	Supplemented components
HOS	MEM	10% FBS 2 mM L-glutamine 1X PSN
143B		
MNNG/HOS		
SK-UT-1		
U-2-OS	McCoy's 5A	10% FBS 1X PSN
SJSA-1	RPMI 1640	10% FBS 1X PSN 2.0 mg/mL D-glucose
KOS-1	DMEM	10% FBS 1X PSN 4 mM L-glutamine
KOS-2		
KOS-3		
KOS-6		
KOS-7		
Human fibroblast (HF)	DMEM	10% FBS 1X PSN 8 mM L-glutamine

2.2.2 Establishment of luciferase-expressing human OS cell lines

MNNG/HOS and SJSA-1 cells were transduced with lentiviral particles containing a luciferase transgene (PerkinElmer™, MA) as per the manufacturer's instructions using the reagents detailed in Table 2.4. Briefly, MNNG/HOS or SJSA-1 cells (2.0 x10^3) in complete cell growth medium containing supplemented components (Table 2.3) were seeded into 2 wells of a 24-well plate and incubated for 24 hr. The medium was replaced with the fresh complete medium containing hexadimethrine bromide (Polybrene) at a final concentration of 4 μg/mL to assist transduction of luciferase transgenes into the cells. Thawed lentiviral particles (30 μL) were directly added to the cells in 1 well (transduced cells) and the same volume of complete medium was added to the other well (control non-transduced cells). All cells were incubated for 24 hr and then the medium was exchanged with 1 mL of fresh complete medium. The cells were incubated for a further 24 hr then the medium was exchanged with fresh complete medium containing puromycin to select the transduced cells. The selection process occurred over a 7-day period with the replacement of medium containing puromycin (1 μg/ml for MNNG/HOS-Luc and 3 μg/ml for SJSA-1-Luc) occurring every 2 days. After 7 days with puromycin, the control non-transduced cells were dead, as confirmed by inverted microscope. The transduced cells were then expanded and frozen in an isopropanol chamber at -80°C overnight. The frozen cells were stored in liquid nitrogen tank. The bioluminescence intensity of the transduced cells was then analysed using an *in-vitro* bioluminescence assay to confirm the luciferase expression in the transduced cells (described in Section 2.2.2.1).

Table 2.4 Reagents for luciferase gene transduction

Name	Catalogue Number	Source
Lentiviral particles (RediFect Rec-Fluc-Puro)	CLS960002	PerkinElmer™, Waltham, MA
Hexadimethrine bromide (Polybrene)	T0083	Canvax Biotech, Cordoba, Spain
Puromycin	58-58-2	InvivoGen, San Diego, CA

2.2.2.1 *In-vitro* assay for bioluminescence signal

After the establishment of the luciferase-expressing OS cells, the bioluminescent signal intensity of each cell line was determined *in-vitro*. Non-transduced ($5.0x10^4$) and transduced cells ($5.0x10^3$, $1.0x10^4$, $2.5x10^4$ and $5.0x10^4$) were seeded into a black 24 well flat-bottom plate (PerkinElmer™, Waltham, MA) (Figure 2.1 and 2.2). The cells were incubated for 12 hr to allow for full recovery and attachment to the bottom of the cell culture flask. D-luciferin solution (150 µg/mL) was added to each well containing cells. After 20 min, bioluminescence intensity readings were obtained using the IVIS Spectrum (PerkinElmer™, Waltham, MA).

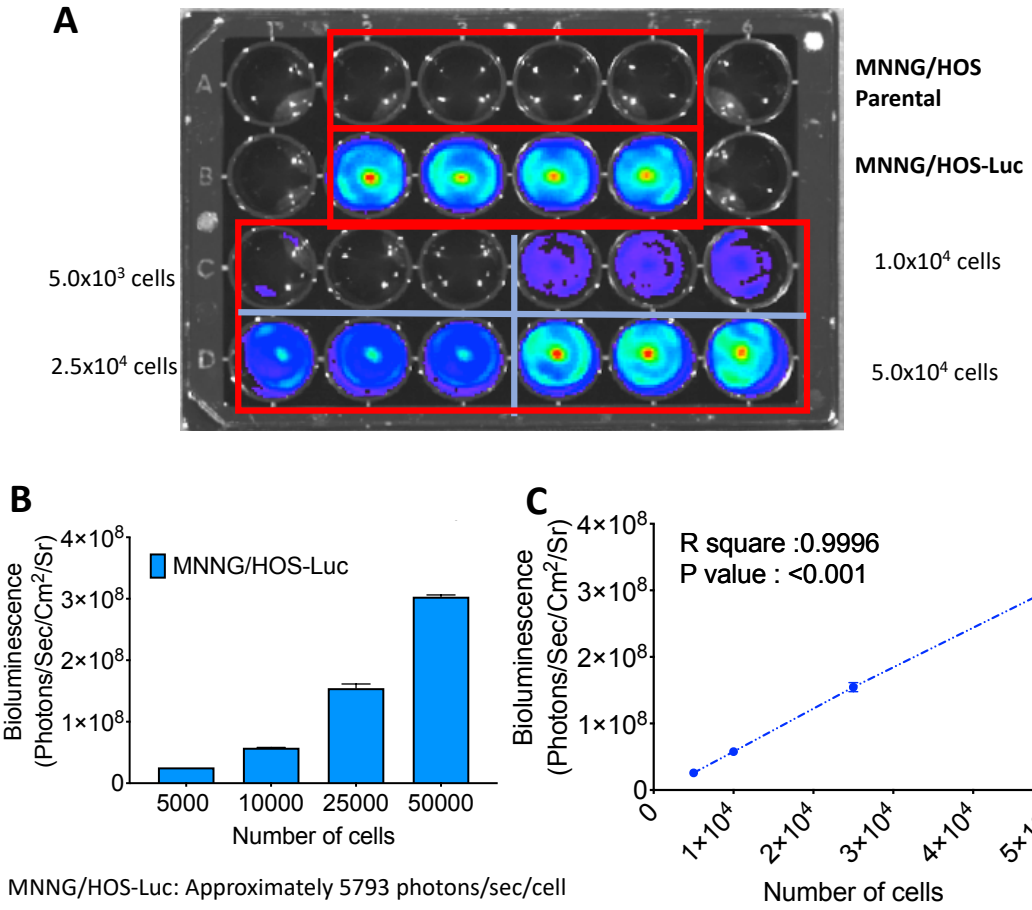

Figure 2.1 Assessment of bioluminescent signal intensity of MNNG/HOS-Luc cells
(A) MNNG/HOS and MNNG/HOS–Luc cells were seeded in a black 24-well flat-bottom plate. The luciferase construct was successfully transduced into MNNG/HOS cells as a bioluminescence signal was emitted following the addition of D-luciferin compared to the non-transduced parental cells. (B) Bioluminescence intensity was quantified across all wells with increasing numbers of transduced cells. (C) A correlation was observed between bioluminescence intensity and the number of transduced cells as determined by Pearson's correlation coefficient. *n*=1

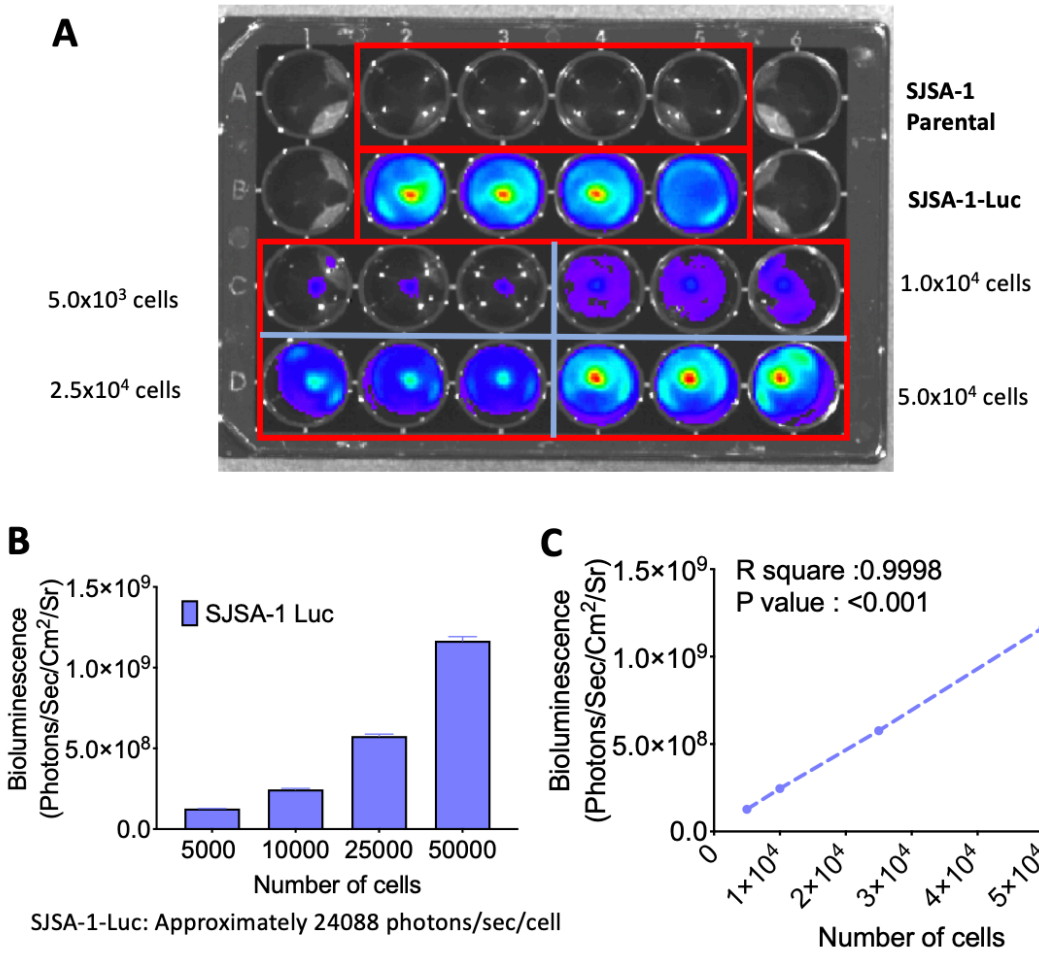

Figure 2.2. Assessment of bioluminescent signal intensity of SJSA-1-Luc cells
(A) SJSA-1 and SJSA-1–Luc cells were plated in a black 24 well flat-bottom plate. The luciferase construct was successfully transduced into the SJSA-1 cells as a bioluminescence signal was emitted following the addition of D-Luciferin compared to the non-transduced parental cells. (B) Bioluminescence intensity was quantified across all wells with increasing numbers of transduced cells. (C) A correlation was observed between bioluminescence intensity and the number of transduced cells as determined by Pearson's correlation coefficient. *n*=1

2.2.3 Cell culture

The cell lines were maintained in culture in a T-75 flask with the recommended complete medium (as detailed in Table 2.3) and incubated in a Hepa-filtered, humidified, cell culture incubator at 37° C with 5% CO_2. The cells were monitored daily using an inverted-microscope. The cells were sub-cultured when their confluence reached 70 to 80% in the cell culture flask as follows: cells were washed once with 2 mL 1X PBS, then lifted off the flask using 2 mL trypsin-EDTA solution and incubated at 37° C with 5% CO_2 for 5 to 10 min following which 2 mL of complete medium was added to the flask. The cells in the solution were then transferred into a 15 mL Falcon tube and centrifuged (200 *g* for 5

mins at room temperature). The supernatant was removed and the pellet resuspended in 3 mL of complete medium. Finally, depending upon the growth rate of the cell line, an appropriate proportion of the cell suspension was added to a new flask and supplemented with additional media. For T-175 cell culture flasks, all the media/reagent volumes were doubled.

2.2.4 Cell metabolic activity-based colorimetric assay (MTT) Assay

MTT (3-(4,5-dimethylthiazol-2yl)-2,5-diphenyltetrazolium bromide) assays were performed to determine the cytotoxicity of RNA Pol Ii (CX-5461 or PMR-116) on the sarcoma and control cell lines. The optimised cell number, was that required to achieve <80 to 90% on the last day of the experiment, was seeded into 96 well flat-bottom microplates (NUNC^{TM}, Thermo Fisher Scientific, Waltham MA) and incubated for 12 hr. The medium was then exchanged with fresh complete medium containing vehicle or various concentrations of CX-5461 and PMR-116 and incubated for 72 hr. After 72hr the drug-containing medium was removed and 100 μL of fresh complete medium plus 10 μL of MTT solution (50mg/ml) (Merck Millipore, Burlington, MA) were added to each well and incubated for 4 hr. Isopropanol containing 0.4 nM of hydrochloric acid, 100 μL, was then added to the well and mixed in thoroughly by repeated pipetting. The absorbance of each well was measured at 570 nm with a reference wavelength of 630 nm using a Thermomax microplate reader. The 50% growth inhibitory concentration of both RNA Pol I inhibitors was determined using non-linear regression analysis in Graph-Pad Prism (Version 8.0).

2.2.5 IncuCyte-based cell proliferation assay and doubling time

Cell proliferation assays were conducted to estimate the anti-proliferation effects of the RNA Pol Ii, CX-5461 and PMR-116, on the sarcoma and control cells. The optimised cell number, was that required to achieve <80 to 90% on the last day of the experiment, was seeded into 96 well flat-bottom plates and incubated for 12 hr after which time the medium was exchanged with fresh complete medium containing vehicle or various concentrations of RNA Pol Ii. The cells were then incubated for 72 hr in an IncuCyte® Live Cell Imaging System and the confluence in each well was recorded every 12 hr. The 50% proliferation inhibitory concentrations of CX-5461 or PMR-116 were estimated using non-linear regression analysis in Graph-Pad Prism (Version 8.0). The doubling time of each untreated cell line was determined using the confluence as measured in the

IncuCyte Live Cell Imaging System and the exponential growth analysis function in Graph Pad Prism (version 8.0).

2.2.6 Quantitative Real-Time PCR

Sarcoma and control cells (1.0 x10^5) were seeded into 100 mm cell culture dishes and incubated for 12 hr following which the medium was exchanged with fresh complete medium containing vehicle or various concentrations of CX-5461 or PMR-116 and incubated for 1 hour. RNA was then extracted from the cells using a RNeasy® Mini Kit (Qiagen, Hilden, Germany) according to the manufacturer's instructions. RNA was quantified using a NanoDrop™ 2000c Spectrophotometer (Thermo Fisher scientific, MA, USA). To degrade any residual DNA within the samples, 500 ng of RNA was treated with DNase (according to kit instructions) then incubated in T100™ Thermocycler (Bio-Rad, CA, USA) using the settings indicated in Table 2.6. Following the DNase treatment, the reagents for cDNA synthesis (Table 2.5) were added to the sample and incubated according to the conditions in Table 2.6 using a Thermocycler. All synthesised cDNA samples were diluted with 80 µL UltraPure™ Distilled Water and stored at -20° C for future use.

To quantify RNA Pol I activity in the samples, 2 sets of primers were used that targeted the Internal Transcribed Spacer 1 (ITS-1) and External Transcribed Spacer-2 (ETS-2) of the pre-47S (Bywater et al., 2012) ribosomal RNA and primers to a housekeeping gene, beta-2-microglobulin (B2M) (Table 2.7) used for normalization. Primer working stocks were prepared using 192 µL of UltraPure™ Distilled water, 4 µL of the forward primer (100 mM) and reverse primer (100 mM). In the qPCR reaction, 12 µL of master mix containing 2 µL of primer working stock and 10 µL of SYBR™ Green master mix (Applied Biosystems, Foster City, CA) and 8 µL of the cDNA sample was loaded into a 96 well PCR plate. The plate was then sealed, spun and transferred to a StepOne™ Plus Real Time (RT) PCR System (Applied Biosystems, Foster City, CA) and RT-PCR was performed using RT-PCR conditions detailed in Table 2.6. Details of the reagents, incubation settings and primer sequences are listed in Tables 2.5, 2.6 and 2.7.

Table 2.5. Reagents for Quantification real-time PCR

Reagents for RNA extraction			
Name	**Company**	**Catalogue number**	
RNeasy mini kit	QIAGEN, Hilden, Germany	74106	
ß-mercaptoethanol	Sigma Aldrich, St Louis, MO	M6025	
Reagents for DNase treatment			
Name	**Company**	**Catalogue number**	**Volume per sample**
RQ1 RNase free DNase	Promega, Madison, WI	M610A	1 µL
Recombinant RNasin® Ribonuclease Inhibitor		N251B	0.2 µL
5X SSIV buffer	Invitrogen, Carlsbad, CA	LT-02241	4.0 µL
0.1M DTT		LT-02241	0.15 µL
Reagents for cDNA synthesis			
UltraPure™ Distilled Water (DNase, RNase free)	Gibco, Waltham, MA	10977	1.5 µL
10 mM dNTPs	Invitrogen, Carlsbad, CA	10297018	1 µL
0.1 M DTT	Invitrogen, Carlsbad, CA	LT-02241	2 µL
0.5 g/L hexamers (Random) primers	Promega, Madison, WI	C118A	0.5 µL
SuperScript™ IV Reverse Transcriptase	Invitrogen, Carlsbad, CA	LT-02241	0.3 µL
Reagents for quantification real-time PCR			
Primer working stock			2 µL
SYBR Green® master mix	Applied Biosystems®, Foster City, CA	4309158	10 µL
cDNA samples			8 µL

Table 2.6. Incubation Settings for Quantification Real-Time PCR

	Time and Temperature setting
DNase treatment	37° C for 15 min -> 70° C for 15 min -> 4° C
cDNA synthesis	20° C for 5 min -> 37° C for 5 min -> 42° C for 75 min -> 70° C for 15 min -> 4° C -> Store at -20° C
RT-PCR	Holding stage: 95° C for 20 sec Cycling Stage (40 cycles): 95° C for 3 sec -> 60° C for 30 sec Melt curve stage (Melt curve 0.7): 95° C for 15 sec -> 60° C for 1 min -> 95° C for 15 sec

Table 2.7. Primer Sequences used in Quantification Real-Time PCR

Name of primer	**Company**	**Sequence**
ETS-2 forward	Integrated DNA Technologies, Coralville, IA	5'-GGCGGTTTGAGTGAGACGAGA-3'
ETS-2 reverse		5'-ACGTGCGCTCACCGAGAGCAG-3'
B2M forward		5'-CCGTGGCCTTAGCTGTGCTCGC-3'
B2M reverse		5'-CCCACTTAACTATCTTGGGCTG-3'

2.2.7 BrdU and PI staining for cell cycle analysis

Bromodeoxyuridine (BrdU) and Propidium iodide (PI) staining was conducted to assess the impact on cell cycle progression in sarcoma and control cells treated with the RNA Pol Ii. The optimised cell number, was that required to achieve < 60% on the last day of the experiment, was seeded into 100 mm cell culture plate with 5 mL of the recommended complete media (Table 2.3) and the plates incubated at 37° C and 5% CO_2 for 12 hr. The media was then exchanged with media containing drug or vehicle, incubated a further 72 hr, then pulse-labelled with 10 μM BrdU (10 mM stock, Sigma-Aldrich) for 30 min at 37° C and 5% CO_2. The cells were then washed with 2 mL of ice-cold 1 X PBS and harvested from the plate using trypsin EDTA as previously described (Section 2.2.1) except that cell pellets were gently resuspended in 100 μL of ice-cold PBS. Cold ethanol (80%; 1mL) was then added to each tube while vortexing and the cell-containing solution was then transferred into 1.5 mL Eppendorf tubes. The samples were stored at 4° C for a minimum of 1 day and a maximum of 2 weeks before staining.

For BrdU detection and PI staining, fixed cells were centrifuged (200 *g* for 5 min at 4° C) and the supernatant carefully removed. The cell pellets were then resuspended with 1 mL 2N HCl containing 0.5% (v/v) Triton X-100 to denature the DNA for 30 min at room temperature following which the cells were centrifuged (200 *g* for 5 mins at 4° C), the supernatant was removed and 1 mL 0.1 M $Na_2B_4O_7.10H_2O$ (pH 8.5) was added into each tube to neutralize the HCl. The cells were centrifuged (200 *g* for 5 min at 4° C) and the supernatant was removed. The pellets were resuspended in 100 μL of PBS containing 2% FBS and 0.5% Tween-20 and anti-BrdU antibody at a concentration of 20 μg/mL and incubated for 30 min at room temperature. Following the addition of 1 mL of PBS containing 2% FBS the tubes were centrifuged (200 *g* for 5 mins at 4° C). The supernatant was removed and the pellets in the unstained and PI-only stained groups were resuspended with 100 μL of PBS containing 2% FBS. For the other samples, the pellets were resuspended in 100 μL Alex Fluor 488 anti-BrdU goat anti-Mouse IgG (H+L) polyclonal antibody at 1:300 dilution in PBS containing 2% FBS and 0.5% Tween-20. All samples were incubated in the dark for 30 min at room temperature then washed by adding 1 mL PBS containing 2% FBS. The cells were centrifuged (200 *g* for 5 mins at 4° C) and the supernatant was removed. The pellets in the unstained and BrdU-only stained groups were resuspended with 200 μL of PBS containing 2% FBS, while for the other

samples the pellets were resuspended in 200 µL PBS containing 2% FBS and 10 µg/mL of PI. All samples were transferred into FACS tubes and incubated in the dark for 20 min at room temperature after which they were analysed using flow cytometry on a Becton Dickinson LSR II FACS machine and the data was analysed using FlowJo software (Version 10). The details of the reagents used for BrdU and PI staining are listed in Table 2.8.

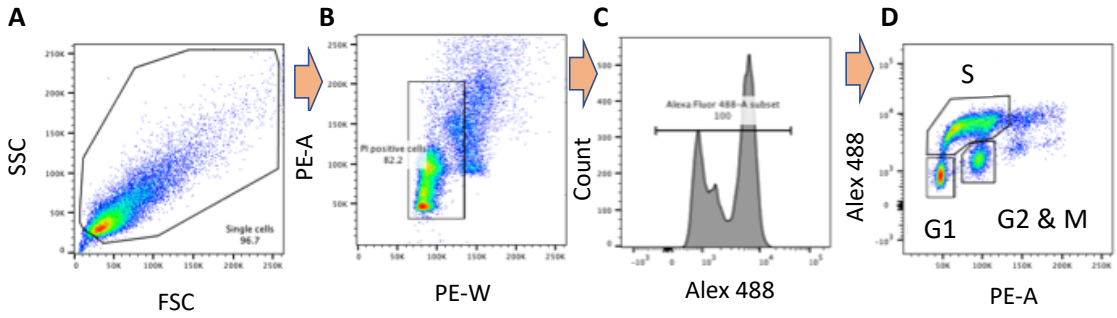

Figure 2.3: Flow Cytometry gating strategy for analysis of cell cycle stage
After treatment with RNA Pol Ii (CX-5461 or PMR-116), BrdU-labelled sarcoma and control cells were analysed by flow cytometry. (A) An initial gate was set for single cells, then (B) a second gate was set for PI stained cells. Subsequently, (C) a third gate was set for BrdU stained cells and (D) 3 final gates were set for G1, S, G2 & M stages of cell cycle.
FSC = forward scatter; SSC = side-scatter; PE-A=Phycoerythrin area, PI-stained cells; PE-W= Phycoerythrin-width, PI-stained cells; Alex 488= BrdU-stained cells.

Table 2.8. Reagents for BrdU and PI staining

Name	Catalogue Number	Source
Anti-BrdU B(44)	347580	BD Biosciences, Franklin Lakes, NJ
Alex fluor 488 goat anti-mouse IgG	A11001	BD Biosciences, Franklin Lakes, NJ
Propidium Iodide	P4170-25MG	Sigma Aldrich, St Louis, MO

2.2.8 Western Blot Analysis

Sarcoma and control cells (~1x10^6 cells) were harvested from culture flasks, washed with 1X cold PBS and lysed in cell lysis buffer (0.5 mM EDTA, 2% SDS, 20 mM HEPES, protease inhibitor (Table 2.9)). The lysates were then transferred to 1.5 mL tubes and incubated for 5 minutes at room temperature to ensure complete membrane disruption. The tubes were then incubated in a heat block at 95°C for 10 minutes to denature the

proteins, then placed at 4°C for 5 minutes. The lysates were then sheared using a 27G needle and syringe. Protein concentration was measured using a Bio-Rad protein assay kit (Table 2.9). Bovine Serum Albumin standard (BSA) was used as a standard curve (Table 2.9). 30 µg of protein was loaded per sample onto a 12% SDS-PAGE gel for protein separation under reducing conditions, according to the manufacturer's instructions. Once separated the protein in the gel was transferred to a PVDF membrane (Bio-Rad, Hercules, CA) using the Bio-Rad semi-dry transfer protocol (1 mA current, 30 V constant voltage for 30 min). The membranes were rinsed in 1X TBST then blocked with 5% non-fat dry milk in 1X Tris-Buffer Saline Tween-20 (TBST) (1X TBS (pH 7.5, 1 mM Tris, 10 mM NaCl) supplemented with 0.1% Tween 20) for one hour at room temperature. The membrane was then probed with specific primary antibodies, diluted in 5% BSA in 1X TBST, overnight at 4°C. The antibody information, dilutions and specific blocking buffers are provided in Table 2.6. After primary antibody incubation, membranes were washed using 1X TBST buffer for 15 mins and incubated with horseradish peroxidase-conjugated (HRP) secondary antibodies (Table 2.10) for one hour at room temperature. The membranes were washed with 1X TBS for 15 mins and developed by enhanced chemiluminescence using Clarity Western ECL Substrate (Bio-Rad, Hercules, CA) reagent. The chemiluminescence blots were imaged with the a ChemiDoc MP Imager (Bio-Rad, Hercules, CA). Densitometric analysis was performed using the ChemiDoc MP Imager Software. ß-actin was used as a loading control by probing the same blots used to determine p53, c-Myc, MDM2 and RB1 abundance. Each replicate was conducted using independently-generated sets of cell lysates.

Table 2.9. Reagents and kits for western blot analysis

Name	Catalogue Number	Source
Protease inhibitor (PhosSTOP)	04906837001	Roche, Basel, Switzerland
Bio-Rad protein assay kit (***DC*™** protein assay kit)	5000112	Bio-Rad, Hercules, CA
Pierce™ Bovine Serum Albumin Standard	23210	ThermoFisherScientific, Waltham, MA
PageRuler™ Prestained Protein Ladder	26616	ThermoFisherScientific, Waltham, MA

Table 2.10. Antibodies used in western blotting

Primary Antibodies									
Human Target Protein	**Isotype (Clonality)**	**Raised in:**	**Clone**	**Recognition site**	**MW of target protein**	**Company**	**Catalogue number**	**Dilution**	**Incubation buffer**
p53	IgG_{2a} (mAb)	Mouse	DO-1	11-25 amino acid residues at N-terminus of p53	53 kDa	Santa Cruz, Dallas, TX	SC-126	1:1000	*5% BSA
c-Myc	IgG_1 (mAb)	Mouse	9E10	171-188 amino acid residues of c-Myc	60-67 kDa	Calbiochem, San Diego, CA	OP10L	1:500	*5% BSA
RB1	IgG (pAb)	Rabbit	C-15	C-terminus of RB	106 kDa	Santa Cruz, Dallas, TX	SC-50	1:1000	*5% BSA
MDM2	IgG_1 (mAb)	Mouse	SMP14	54-167 amino acid residues of MDM2	90 kDa (Full) 60 kDa (Cleaved)	Santa Cruz, Dallas, TX	SC-965	1:1000	*5% BSA
ß-actin	IgG (mAb)	Rabbit	13E5	Amino-terminus of ß-actin	46 kDa	Cell Signaling Technology, Danvers, MA	4970S	1:2000	*5% BSA

Secondary Antibodies						
Target Protein	**Isotype**	**Raised in:**	**Company**	**Catalogue number**	**Dilution**	**Incubation buffer**
Rabbit IgG (HRP conjugated)	IgG	Goat	Bio-Rad, Hercules, CA	1706515	1:3000	*5% non-fat dry milk
Mouse IgG (HRP conjugated)	IgG	Goat	Bio-Rad, Hercules, CA	1706516	1:5000	*5% non-fat dry milk

HRP: horseradish peroxidase; BSA: bovine serum albumin; *Made in TBST=Tris-Buffered Saline Tween-20
mAB; monoclonal antibody; IgG=Immunoglobulin G; kDa: kilodalton

2.3 *In-Vivo* Experiments

Table 2.11. Reagents for *in-vivo* experimental procedures

Name	Catalogue Number	Source
D-Luciferin (XenoLight D-Luciferin)	12799	Perkin Elmer™, Waltham, MA
Hanks' Balanced Salt Solution (HBSS)	24020-117	Gibco, Waltham, MA
Matrigel™ Matrix Basement Membrane	354234	CORNING, Corning, NY

2.3.1 Tumorigenicity of human osteosarcoma cell lines in Rag 2 knockout mouse

The tumorigenic capacity of the human OS cell lines was determined in Rag 2 knockout (KO) mice. The cells were cultured in T-175 cell culture flasks and harvested as previously described in Section 2.2.3. The cell pellets were resuspended in 10 mL of Hank's Balanced Salt Solution (HBSS). The cell concentration was determined using a haemocytometer and averaging triplicate counts, the cells were then centrifuged (200 *g* for 15 mins at room temperature). The pellets were resuspended with HBSS in a volume required to provide the desired concentration for injection. The cells were subcutaneously injected in a volume of 50 µL into the right flank of the mice using a 30G disposable syringe. After tumour injection, mice were checked daily and the tumours measured as detailed in Section 2.3.3.

2.3.2 Tumour measurement

Tumour measurements commenced when the size reached ~2mm and two methods were applied: 1) Digital callipers; 2) *In-vivo* bioluminescence imaging using the IVIS Spectrum imaging system.

2.3.2.1 Tumour measurement using digital callipers

The mice were restrained by hand then the width and length of the tumours measured using digital callipers, these values were automatically entered into an Excel spreadsheet. The following formula was used to determine the tumour volume in mm^3 (Faustino-Rocha et al., 2013):

$$\text{Tumour volume } (mm^3) = \frac{(\text{Tumour width}^2 \times \text{Tumour length})}{2}$$

2.3.2.2 *In-vivo* Bioluminescence Imaging of Tumours

Mice were weighed and received an i.p. injection of D-luciferin solution (150 mg/kg) then placed in a clean cage and monitored for 8 min before being transferred into an anaesthetic induction box. Mice were anaesthetised with an isoflurane-oxygen mixture (Minimum alveolar concentration (MAC) 2.5 with 32% SaO_2) for 4 min, or until pedal reflexes were absent, they were then placed into the imaging chamber of the IVIS® Spectrum in which they continued to receive isoflurane and oxygen via a nose cone. Bioluminescence intensity of the tumours was obtained using an auto-exposure setting in the Living Image® software (version 3.2), then the mice were transferred into a clean heated cage and monitored until fully recovered from anaesthesia following approved ANU ethics protocol (A2017/16).

2.3.3 Maximum Tolerance Dose (MTD) assays

The maximum tolerated dose of the RNA Pol Ii, CX-5461 and PMR-116, was determined using Rag2 KO mice. Various concentrations of each drug and vehicle (Vehicle for CX-5461: 50 mM $Na_2H_2PO_4$ pH 4.5, Vehicle for PMR-116: 50 mM citric acid pH2.0) were administered to mice via oral gavage at the frequencies indicated. To determine tolerance of the dosing schedules, the mice were weighed and checked for signs of illness daily before drug/vehicle was administered. Drug doses were considered not tolerated if a reduction in weight of 20% from the starting weight was observed or the mice received a morbidity score of 3, at which stage the mouse would be humanely euthanised. A morbidity score of 3 is based on signs of ill health such as hunched posture, reduced water drinking, eyelids partly closed or rough fur. The MTD assays and animal monitoring were conducted according to the approved ANU ethics protocol (A2017/16).

2.3.4 Drug studies in tumour-bearing mice

The therapeutic effects of RNA Pol Ii were examined in 2 human OS xenograft mouse models. The cell lines, 143B-Luc and SJSA-1-Luc, were injected into Rag 2 KO as described in Section 2.3.1. Once the tumours had reached ~2 mm in size, bioluminescence imaging was performed as described in Section 2.3.2.2. These measures were considered

the pre-treatment baseline values. The mice were then assigned to treatment or vehicle control groups ensuring that the average tumour volume between the groups was as equal as possible. The group with the lowest average tumour volume always received the vehicle control, whilst the group with the highest average tumour volume always received the active treatment. Drug dosing was according to the dosing schedule indicated in the results section of Chapter 5. In the combined vehicle group, mice were administered a 50:50% mixture of the 2 vehicles thrice weekly. The mice were checked daily for weight and general well-being. Calliper measurements of the tumours were undertaken at the frequencies indicated and bioluminescence imaging was undertaken every 7 days from first drug administration. Ethical cull points were as described for the maximum tolerated dose assays, but in addition, mice were culled when the tumours reached a size of 13 mm in any one direction or a tumour volume of 1000 mm^3. Drug studies were conducted following the approved animal ethics protocol (A2017/16).

2.4 Statistical analysis

Statistical analyses were performed using GraphPad Prism software, Version 8.0 (GraphPad Software, San Diego, CA). Differences between the values of experimental groups were assessed by One-way or Two-way ANOVA, as appropriate. Doubling times of cell lines were obtained using exponential growth analysis function. Comparison of doubling time was assessed by student student's two tailed t test (Nonparametric and welch's correction). Dose-response curve fit and 50% inhibitory values were obtained using non-linear regression analysis. The relationship between 2 variables was assessed using Pearson's correlation co-efficient. Graphs were also generated using GraphPad Prism software.

Chapter Three

Molecular Characterization of Human Osteosarcoma Cell Lines

3.1 Introduction

As discussed in chapter 1 human OS is one of the most common malignant tumours of human bone. While there has been an improvement in survival over the last 30 years, for 30% of OS patients, prognosis is still dismal and novel therapeutic strategies are needed (Kansara et al., 2014). Ribosome biogenesis, more specifically RNA Pol I transcription activity, has been demonstrated to be a valid therapeutic target for human cancer. This is based on such drugs demonstrating anti-tumour effects in many *in vitro* and *in vivo* models of cancer (Drygin et al., 2011, El Hassouni et al., 2019). Most importantly one such drug, CX-5461, has completed a Phase I clinical trial demonstrating tolerability and efficacy in advanced hematologic cancers (Section 1.4.1). There is little data directly determining the effect of drugs such as CX-5461 on OS. By inference however in OS the two tumour suppressors, p53 and RB1, and two oncogenes, MDM2 and c-Myc, are reported as dysregulated which would promote ribosome biogenesis and RNA Pol I transcription activity (Kansara et al., 2014, Drygin et al., 2010). There is one research paper reporting that the RNA Pol Ii CX-5461 mediates an anti-tumour effect in OS via autophagy and up-regulation of the mTOR pathway (Li et al., 2016). While this was demonstrated in 2 commercially available ATCC OS cell lines the authors failed to examine the relationship between the efficacy of RNA Pol Ii and the status of these four key regulatory components. To thoroughly investigate the anti-tumour effects of RNA Pol Ii on OS, a total of 10 human OS cell lines were used in this thesis, including two of the cell lines used by Li et al (2016), and five OS cell lines (KOS) derived from patients attending the Seoul National University hospital. The KOS cell lines were isolated between 2005 and 2010 whereas the ATCC cell lines have been in culture since for considerably longer (HOS:1971, 143B: 1979, MNNG/HOS: 1971, U-2-OS: 1964 and

SJSA-1: 1982). Also, in contrast to the ATCC OS cell lines, the molecular features of the KOS cell lines have not been identified.

The aims of this chapter, therefore, were to

(i) Determine the basal level of protein abundance level of the tumour suppressors (p53 and RB1) and oncogenes (c-Myc and MDM2) that are known regulators of RNA Pol I activity and often dysregulated in OS cell lines.

(ii) Predict the possible mechanisms that could contribute to the alteration of ribosome biogenesis.

3.2 Results

To identify the basal protein abundance of the four proteins of interest, western blot analysis (see section 2.2.6) was performed on all 10 human OS cell lines, one human uterine leiomyosarcoma cell line (SK-UT-1) and one human fibroblast (HF) cell line. Protein samples were generated from exponentially growing cells (Section 2.2.8)

3.2.1 The basal expression of p53 protein in OS cell lines

As mentioned in section 2.2.8 equal protein per cell line was separated by SDS-PAGE and transferred to PVDF membrane. Western blotting analysis determining the abundance of p53 protein in the 10 OS cell lines is shown in Figure 3.1 and Figure A.1. Three OS cell lines, HOS, 143B and MNNG/HOS, demonstrated the highest abundance of p53 protein (HOS: 0.152, 143B: 0.054, MNNG/HOS: 0.416 and HF: 0.005 - Long exposure image in Figure 3.1) while U-2-OS and SJSA-1, and the HF cell line the lowest (U-2-OS: 0.060, SJSA-1: 0.027 and HF: 0.047 - Short exposure image in Figure 3.1). Interestingly all the KOS cell lines expressed what would be considered a low level of

p53, similar to that observed in HF, in fact p53 was undetectable in KOS-7 cells, even with longer exposures. The p53 protein expression patterns in the ATCC cell lines and HF are consistent with their reported genotypes according to (Ottaviano et al., 2010, Zhou et al., 2014). Three ATCC OS expressed mutant p53, HOS, 143B and MNNG/HOS indicated a high level of p53 protein expression. On the other hand, the other two ATCC OS, U-2-OS and SJSA-1, and HF expressed wild type p53 as demonstrated by a low level of abundance. Specifically, cells with mutant p53 cannot be bound by MDM2 so it accumulates in the cell, while those with wild type p53 the level is actively kept low by MDM2 promoting its degradation (Moll and Petrenko, 2003). As would be predicted cells that are null for p53 do not express any p53. Using the ATCC and HF cell lines as reference points, we predict that KOS-1, -2, -3 and -6 are wild type for *TP53*, and KOS-7 is *TP53* null.

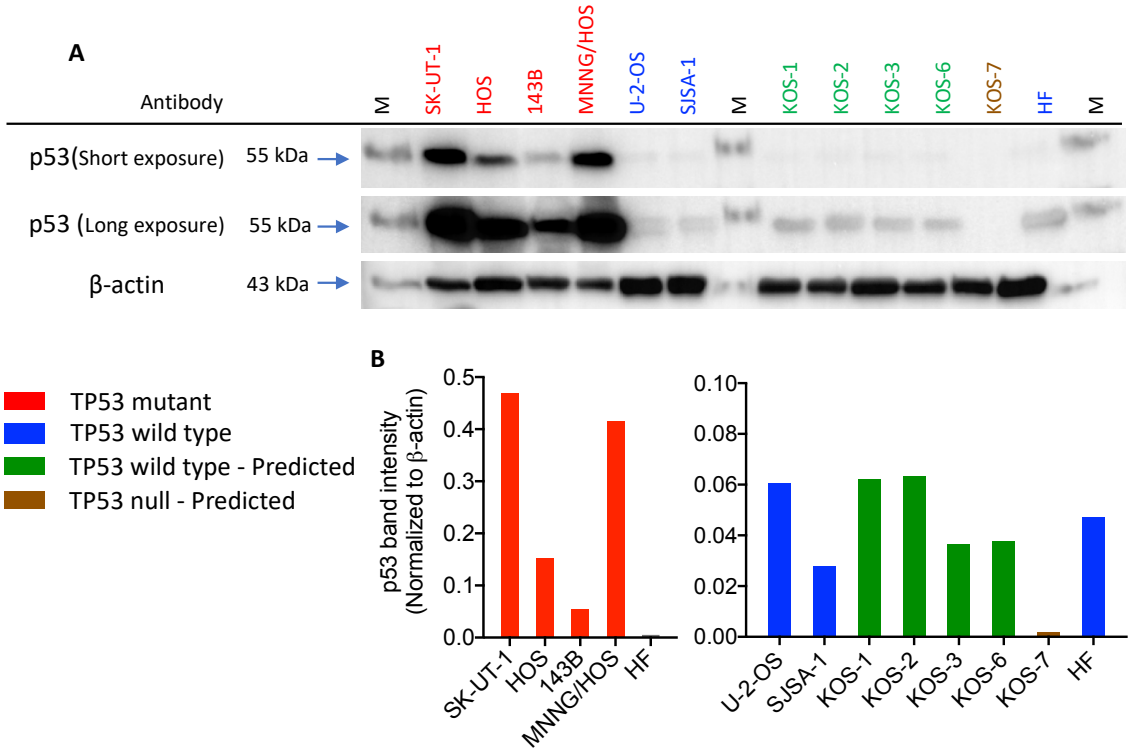

Figure 3.1. **Basal p53 protein expression in exponentially growing OS cell lines, normal human fibroblasts (HF), and leiomyosarcoma SK-UT-1.** (A) p53 protein levels were evaluated by western blot analysis. Representatives of a short and long exposure time are presented to illustrate the full range of expression levels. (B) Quantification of p53 blots. p53 band intensities are shown as a normalized to β-actin on the same blot. The five lines with highest p53 expression were quantitated from the short exposure, and the 8 others from the long exposure image. Colours indicate the *TP53* gene status as listed in molecular characterization of ATCC OS cell lines (Ottaviano et al., 2010), or as predicted from this western blot analysis. M = molecular weight marker (Table 2.9 in Section 2.2.8). The blots shown are representative of 3 independent biological repeats which are all displayed in Appendix Figure A.1. Each replicate was conducted using independently-generated sets of cell lysates.

3.2.2 The basal expression level of MDM2 protein in OS

MDM2 is frequently altered in OS, typically the result is elevated MDM2 expression (Senturk and Manfredi, 2012, Ladanyi et al., 1993). Since the expression level of p53 is regulated by MDM2, we investigated if there was a correlation between p53 and MDM2 protein expression in OS cell lines using western blot analysis (Figure 3.2 and Figure A.2). Of the OS cell lines tested only SJSA-1 showed a detectable band for full length MDM2 (90 kDa). This is consistent with previous reports for SJSA-1 (Freedman and Levine, 1999, Ottaviano et al., 2010). Alternatively spliced variants of MDM2 are usually found along with full-length MDM2 protein (Bartel et al., 2002). Thus, the second band in SJSA-1cells could represent alternatively spliced variants, MDM2-A or MDM2-C. Interestingly however, in the KOS cell lines, leiomyosarcoma SK-UT-1 and HF a cleaved version of MDM2 (55 kDa) was detected. MDM2 can be cleaved by caspase-3 in cancer cells and this has been reported to contribute to tumour development (Pochampally et al., 1998). However, a specific reason for cleaved MDM2 in normal cells has not been revealed. Thus, a cleaved version of MDM2 in the KOS cell lines may have contributed to their tumorigenesis.

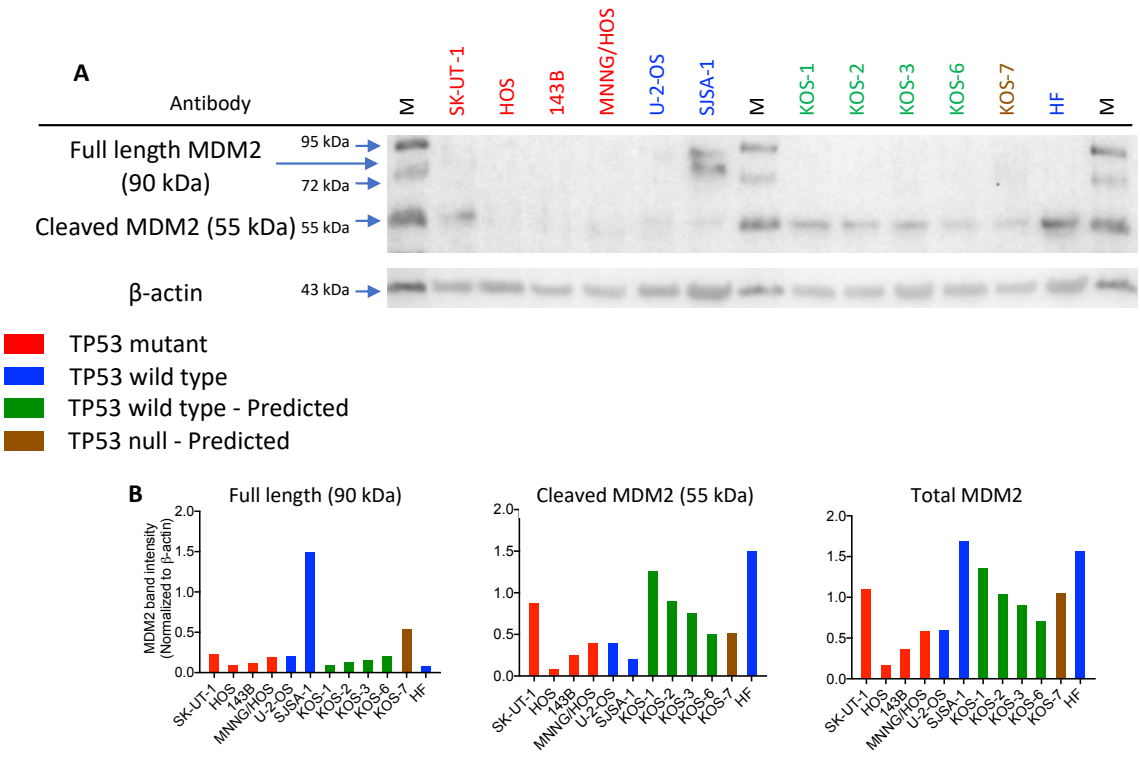

Figure 3.2. **Basal MDM2 protein expression in exponentially growing OS cell lines, normal human fibroblasts (HF) and leiomyosarcoma SK-UT-1.** (A) MDM2 protein levels were evaluated by western blot analysis. (B) Quantification of MDM2 blots. MDM2 band intensities are shown as a normalized to β-actin on the same blot. Colours indicate the *TP53* gene status as listed in molecular characterization of ATCC OS cell lines (Ottaviano et al., 2010), or as predicted from the western blot analysis in Figure 3.1. M = molecular weight markers (Table 2.9 in Section 2.2.8). The blots shown are representative of 3 independent biological repeats which are all displayed in Appendix Figure A.3. Each replicate was conducted using independently-generated sets of cell lysates.

3.2.3 The basal expression of c-Myc protein in OS cell lines

Figure 3.3 and Figure A.3 demonstrate the expression of c-Myc in the OS cell lines. Three OS cell lines (HOS, 143B and MNNG/HOS) which have mutant *TP53* exhibited an elevated c-Myc protein expression compare to the HF cell line which expresses wild type *TP53*. This is consistent with previously published data for HOS, 143B, MNNG/HOS and SK-UT-1 (Feng et al., 2020, Vijayakumar et al., 2011). In contrast, the two OS cell lines (U-2-OS and SJSA-1) expressing wild type *TP53* exhibited a low or undetectable level of c-Myc protein expression. All five KOS cell lines, including the presumptive *TP53* wild type (KOS-1, -2, -3 and -6) and null line (KOS-7), exhibited low or undetectable c-Myc protein expression, similar to that expressing in HF. The leiomyosarcoma cell line SK-UT-1, which also has mutant *TP53,* exhibited the highest level of c-Myc expression of all the cell lines, similar to that expressing in HOS, 143B and MNNG/HOS cell lines. These results suggest c-Myc protein expression is higher in OS cell lines with mutant p53, which is consistent with the correlation reported in (Rochlitz et al., 1995, Niu et al., 2002).

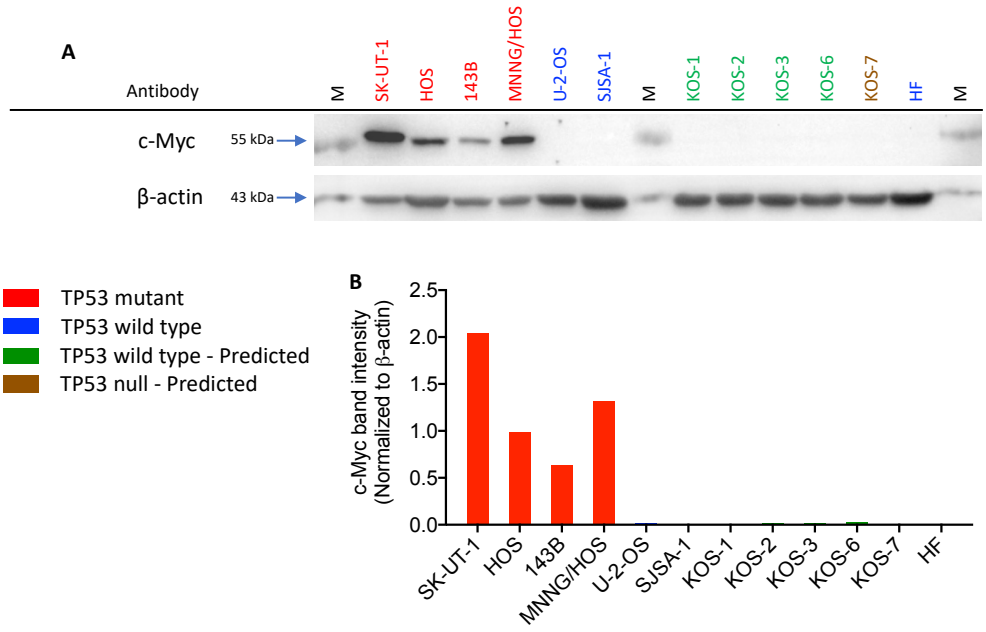

Figure 3.3. Basal c-Myc protein expression in exponentially growing OS cell lines, normal human fibroblasts (HF) and leiomyosarcoma SK-UT-1. (A) c-Myc protein levels were evaluated by western blot analysis. (B) Quantification of c-Myc blots. Band intensities are shown as a normalized to β-actin expression on the same blot. Colours indicate the *TP53* gene status as listed in molecular characterization of ATCC OS cell lines (Ottaviano et al., 2010), or as predicted from the western blot analysis in Figure 3.1. M = molecular weight markers. Table 2.9 in Section 2.2.8). The blots shown are representative of 4 independent biological repeats which are all displayed in Appendix Figure A.2. Each replicate was conducted using independently-generated sets of cell lysates.

3.2.4 The basal expression of RB1 protein in OS cell lines

Similar to p53, the RB1 gene is frequently altered in OS which is proposed to contribute to malignant transformation (Miller et al., 1996, Berman et al., 2008). To evaluate the basal level of RB1 protein in OS, western blot analysis was conducted. Detectable RB1 protein expression was observed in all five ATCC OS cell lines (Figure 3.4 and Figure A.4). The expression of RB1 was highest in the *TP53* mutant OS cell lines (HOS, 143B and MNNG/HOS) compared to those expressing wild type *TP53* (U-2-OS, SJSA-1, HF and SK-UT-1) consistent with previous published data (Zhou et al., 2018). The four KOS cell lines, predicted to be *TP53* wild type (KOS-1, -2, -3 and -6) did not have detectable RB1 under these conditions, whereas the *TP53* null KOS-7 cell line expressed RB1 at a level similar to that for HOS which is mutant for *TP53*.

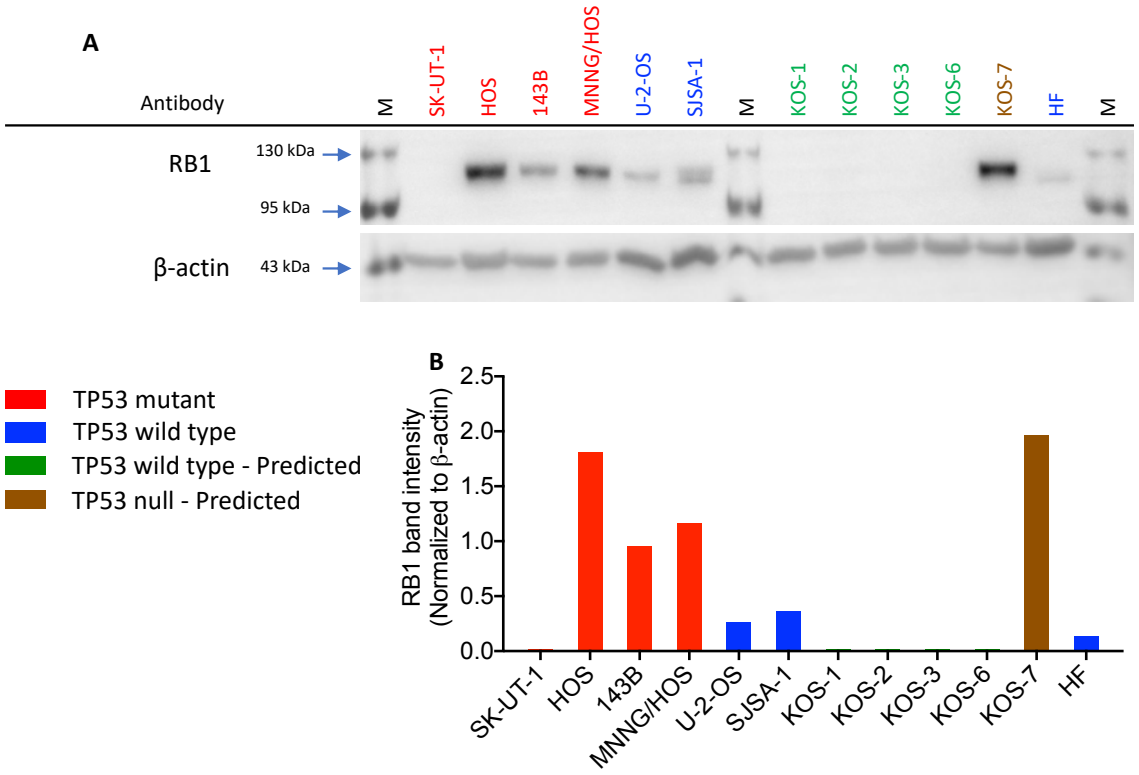

Figure 3.4. Basal RB1 protein expression in exponentially growing OS cell lines, normal human fibroblasts (HF) and leiomyosarcoma SK-UT-1. (A) MDM2 protein levels were evaluated by western blot analysis. (B) Quantification of RB1 blots. RB1 band intensities are shown as a normalized to β-actin on the same blot. Colours indicate the *TP53* gene status as listed in molecular characterization of ATCC OS cell lines (Ottaviano et al., 2010), or as predicted from the western blot analysis in Figure 3.1. M = molecular weight markers (Table 2.9 in Section 2.2.8). The blots shown are representative of 4 independent biological repeats which are all displayed in Appendix Figure A.4. Each replicate was conducted using independently-generated sets of cell lysates.

3.2.5 OS cell proliferation and ribosome biogenesis

The western blotting results demonstrate the OS cell lines included in this project have varying levels of p53, MDM2, c-Myc and RB1 protein expression. These cell lines also showed different doubling times which is likely to be related to the mutation status and expression levels of these four key proteins (Table 3.1). ATCC OS cell lines that have mutant *TP53* (HOS, 143B and MNNG/HOS) had a shorter doubling time than *TP53* wild type ATCC OS cell lines (U-2-OS and SJSA-1) (20 ± 1 vs 29 ± 2 hours, respectively, $p<0.05$). The KOS-7 cell line, that does not express p53, had a shorter doubling time than the ATCC *TP53* wild type OS cell lines (24 hours, $p<0.05$) as well as the other KOS OS cell lines which are predicted to be *TP53* wild type (36 ± 4 hours, $p<0.05$) (Table 3.1).

The rate of ribosome biogenesis has previously been demonstrated to correlate with cell proliferation rate and is influenced by *TP53*, *MDM2*, *c-Myc* and *RB1* mutation status (Montanaro et al., 2007, Li et al., 2016, Chen et al., 2018). Consistent with these reports, the p53 mutant type OS cell lines (HOS, 143B and MNNG/HOS), that also express elevated levels of c-Myc and RB1, had low ΔCt values (high rDNA transcription rate) compared to p53 wild type OS cell line, U-2-OS. In addition, a lack of p53 expression but high RB1 expression (KOS-7), was also associated with a low ΔCt value. In the p53 wild type but MDM2 overexpressed cell line, SJSA-1, lower ΔCt values were measured than U-2-OS (p53 wild type). Although KOS-3 is confirmed as p53 wild type with undetectable levels of MDM2, c-Myc and RB1, the ΔCt value was comparable to that of p53 mutant cell lines (Figure 3.5 A).

A comparison of ΔCt values and doubling time, did not reveal a significant correlation (Figure 3.5B).

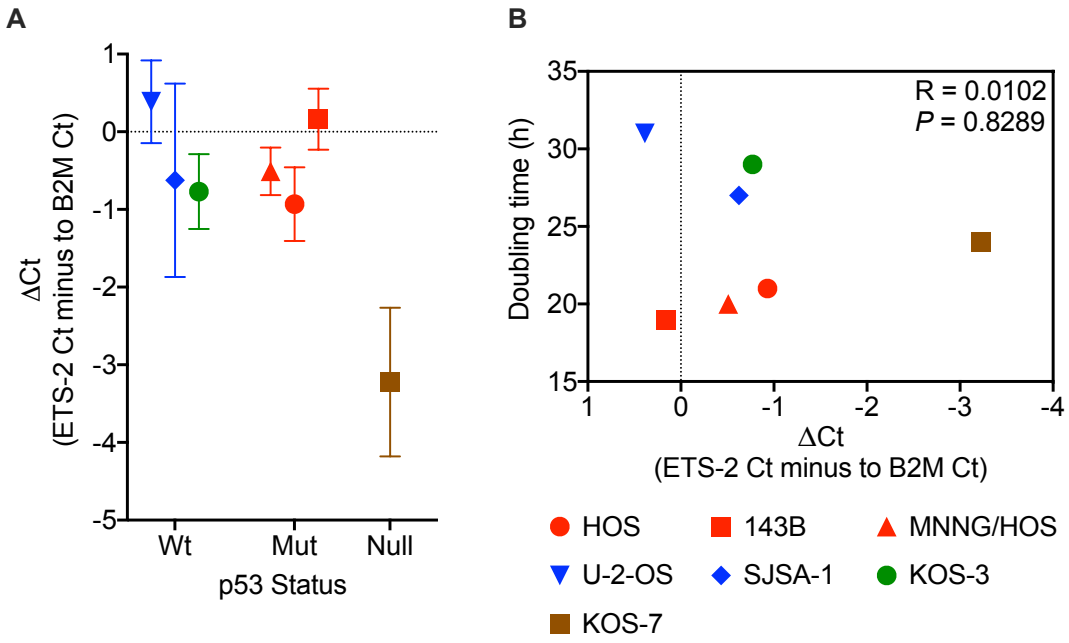

Figure 3.5. Comparison of rDNA transcription rate in untreated OS cell lines
The ΔCt value allows a comparison of the rDNA transcription rates in OS cell lines with a higher ΔCt value indicating a lower rate of rDNA transcription. ΔCt values for each cell line were obtained from the qPCR results by subtracting the Ct value of the house keeping gene (B2M) from the Ct value for the ribosome gene (ETS-2) in the vehicle control-treated cells (Figure 4.6 in Chapter 4). The doubling time for each untreated cell line was determined using the % confluence in the IncuCyte cell proliferation assay (Figure 4.3 in Chapter 4). (A) ΔCt values compared with known and predicted p53 status. (B) ΔCt values compared with doubling time. Colours indicate TP53 gene status as listed in the ATCC information or as predicted from the western blot analysis in Figure 3.1. *n*=6 for ΔCt and n=3 for doubling time, all error bars represent mean +/- standard error of the mean (SEM). Pearson's correlation coefficient in B.

Table 3.1: Cell division, ribosome biogenesis and key protein expression levels in OS

Cell Line *	Doubling time (h)	ΔCt value¤	p53	c-Myc	MDM2#	RB1
Osteosarcoma						
143B	~19 ± 1	-0.93 ± 0.47	+++	+++	+	++
HOS	~21 ± 1	0.16 ± 0.39	+++	+++	+	+++
MNNG/HOS	~20 ± 0	-0.50 ± 0.30	+++	+++	+	++
KOS-7	~23 ± 1	-3.22 ± 0.95	-	-	+	+++
U-2-OS	~31± 1	0.38 ± 0.53	+	-	+	+
SJSA-1	~26 ± 2	-0.62 ± 1.24	+	-	+++	+
KOS-1	~32 ± 2		+	-	+	-
KOS-2	~33 ± 2		+	-	+	-
KOS-3	~29 ± 1	-0.77 ± 0.48	+	-	+	-
KOS-6	~48 ± 3		+	-	+	-
Leiomyosarcoma						
SK-UT-1	~22 ± 0		+++	+++	+	-
Non-cancer						
Human fibroblast	~26 ± 1		+	-	+	+

*Red = *TP53* mutant, Blue = *TP53* wild type, Brown = predicted *TP53* null, Green = predicted *TP53* wild type, #Full length of MDM2 (90 kDa)

¤ ΔCt = Ct ETS-2 minus Ct B2M; ΔCt values are mean +/- standard error of the mean (SEM). *n*=6 for ΔCt values and *n*=3 for doubling times.

3.2.6 Summary

Table 3.1 summarises the findings of this chapter including the cell doubling times, baseline ribosome biogenesis (from results in Chapter 4) and expression of p53, c-Myc, RB1 and MDM2. All p53 mutant OS cell lines (Red: Table 3.1) had a short doubling time compared to p53 wild type OS cell lines (Blue and Green: Table 3.1) which suggests that the proliferation rate in the OS cell lines correlates with p53 status. From the Western blotting results, we predict that 4 of the 5 KOS cells (KOS-1, -2, -3 and -6) express wild type *TP53* and that KOS-7 is *TP53* null. High levels of c-Myc were only detected when mutant *TP53* was present. Expression of full-length MDM2 protein was not common in these OS cell lines, and was only detected in SJSA-1. A cleaved MDM2 protein was observed in SK-UT-1 and KOS cell lines. High levels of RB1 protein were detected in *TP53* mutant OS cell lines (i.e mutant or null *TP53*). An elevated rDNA transcription rate was found to be associated with (i) p53 mutation and elevated c-Myc expression, (ii) overexpression of MDM2, and (iii) the absence of p53 expression and high RB1 expression. These results thus appear to represent three pathways that result in up-regulation of ribosome biogenesis in OS and will be discussed further in Chapter 6.

Chapter Four

In-vitro Effects of RNA Pol I transcription Inhibitors on Human Osteosarcoma Cell Lines

4.1 Introduction

In Chapter 3, the expression of four often altered proteins in OS, p53, RB1, c-Myc and MDM2, were determined for the five commercially available ATCC OS and five patient-derived OS (KOS) cell lines. The expression of these proteins is important as they are known to modulate RNA Pol I transcription activity and thus ribosome biogenesis. Critically RNA Pol I transcription activity has been demonstrated as a new and effective target for cancer therapy, both in experimental models (Drygin et al., 2010, Hein et al., 2013) and now in clinical trial (Khot et al., 2019). The drug CX-5461, a first-in-class selective inhibitor of RNA Pol I transcription, has robust therapeutic effects at low nanomolar ranges in lymphoma, leukemia, prostate cancer, breast cancer and pancreatic cancer (Bywater et al., 2012, Negi and Brown, 2015, Rebello et al., 2016, Xu et al., 2017, El Hassouni et al., 2019). As mentioned in previous (Section 1.4.1), an anti-tumour effect for CX-5461 in human OS *in-vitro* has been reported (Li et al., 2016); however, this publication was limited to 2 commercially available ATCC OS cell lines (MNNG/HOS and U-2-OS) and a micromolar concentration of CX-5461 was used. Furthermore, the effect of CX-5461 on the primary target, rDNA transcription, was not investigated.

The aims of this chapter, therefore, were to evaluate the effect of two RNA Pol Ii, CX-5461 and PMR-116 on: (i) cytotoxicity; (ii) proliferation; (iii) the cell cycle; and (iv) its primary target, rDNA transcription, in the ATCC and patient-derived OS cell lines.

4.2 Results

4.2.1 Cytotoxicity effect of RNA Pol Ii on human OS cell lines

To investigate the anti-tumour potential of the RNA Pol Ii, CX-5461 and PMR-116, an *in-vitro* MTT-based cytotoxicity assay was employed. Specifically, various concentrations of CX-5461, PMR-116 or their corresponding vehicles (50 mM NaH_2PO_4 and 50 mM citric acid respectively) were administered to the OS cell lines then incubated for 72 hrs before 10 μL of MTT (5 mg/ml) added. MTT is reduced to an insoluble purple crystal (with a peak absorbance of 570 nm) only by metabolically active or viable cells (i.e with a functional mitochondria) and then accumulates within the cell. In this case an OD reading at 570 nM is considered a surrogate measure for cell viability. Both RNA Pol Ii reduced the viability of all the OS cell lines tested in a dose dependent manner (Figure 4.1); however, there were differences in sensitivity based on the calculated 50% inhibitory concentrations ($IC_{50:}$ Figure 4.2A). Since p53 status has been reported in numerous cancer models as a marker of sensitivity to CX-5461 (Bywater et al., 2012, Quin et al., 2016, Drygin et al., 2011, Negi and Brown, 2015), we compared the IC_{50} for cell lines with p53 WT, Mutant or null. The IC_{50} for CX-5461 in the p53 mutant (HOS: 242 nM, 143B: 92 nM, MNNG/HOS: 289 nM) or null (KOS-7: 494 nM) OS cell lines were lower compared to those expressing wild type p53 (U-2-OS: 767 nM, SJSA-1: 1404 nM, KOS-1: 721 nM, KOS-2: 2159 nM, KOS-3: 1444 nM, KOS-6: 439 nM). The IC_{50} for PMR-116 showed a similar pattern to CX-5461 with a range from 2185 nM to 244 nM. These results suggest that both RNA Pol Ii are cytotoxic to OS cell lines and there is a correlation with the status of p53 (Figure 4.2 C-D).

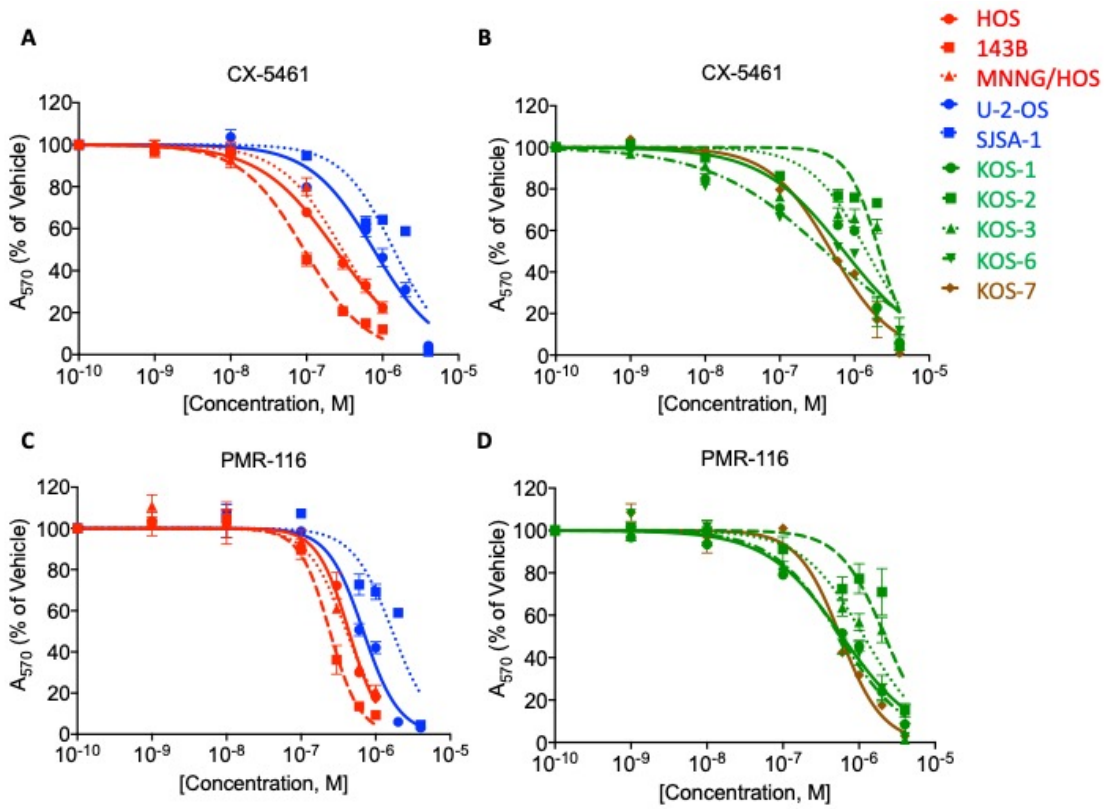

Figure 4.1. RNA Pol Ii reduced OS cell viability in a dose dependent manner.
(A-D) ATCC and KOS OS cell lines were treated with various concentrations of CX-5461, PMR 116 or corresponding vehicle (50 mM NaH_2PO_4 and 50 mM citric acid respectively) for 72 hours and cell viability determined by MTT assay (Section 2.2.4). Colours indicate the *TP53* gene status as predicted by the OS molecular characterization study in chapter 3: Red= p53 mutant, Blue= p53 wild type, Green= p53 wild type, Brown= p53 null. Statistical analysis: *n*=3 per cell line, dose-response curve determined by non-linear regression analysis, graph is mean +/- standard error of the mean (SEM). A: Absorbance.

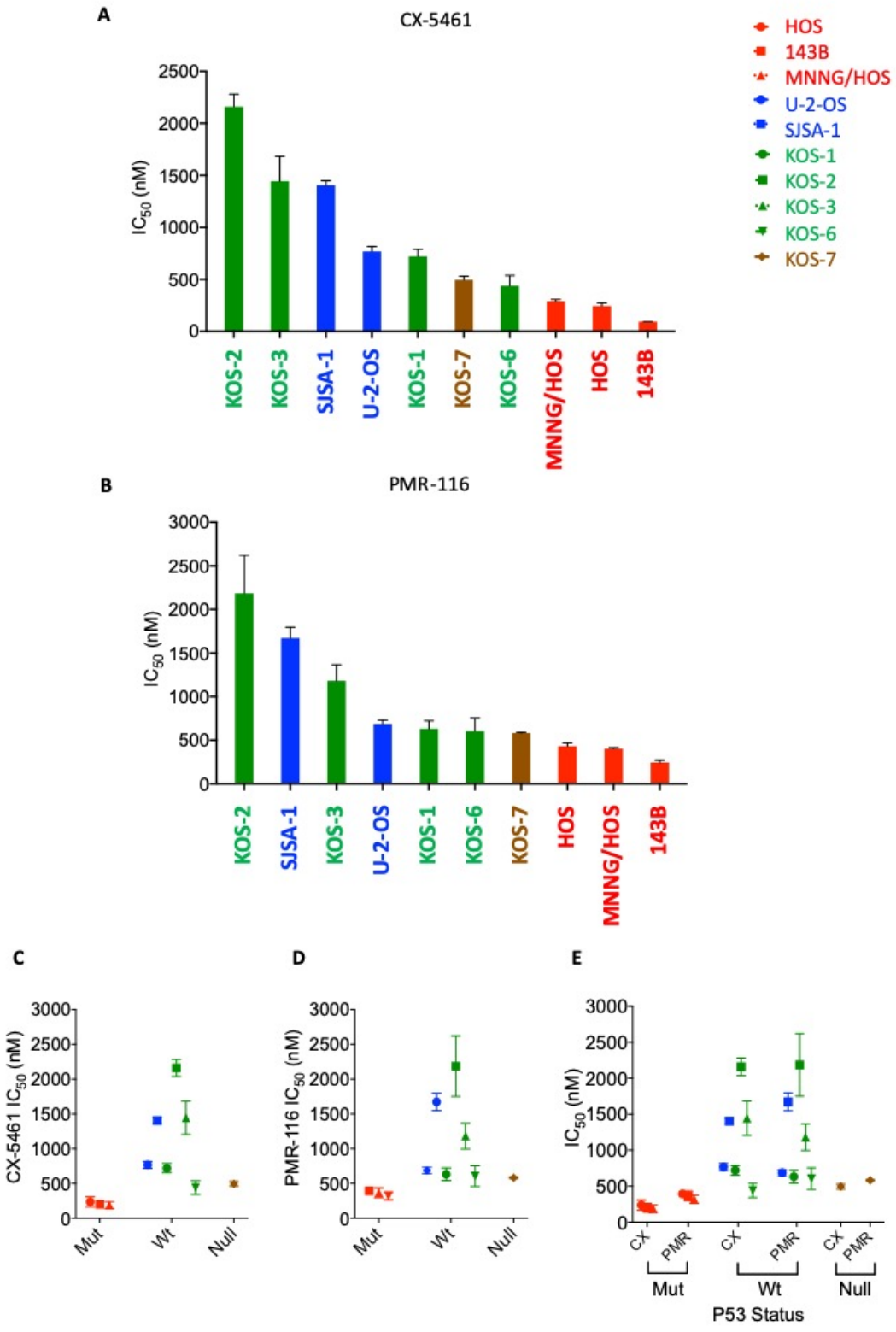
A
CX-5461
HOS
143B
MNNG/HOS
U-2-OS
SJSA-1
KOS-1
KOS-2
KOS-3
KOS-6
KOS-7
IC50 (nM)
2500
2000
1500
1000
500
0
KOS-2
KOS-3
SJSA-1
U-2-OS
KOS-1
KOS-7
KOS-6
MNNG/HOS
HOS
143B
B
PMR-116
3000
2500
2000
1500
1000
500
0
KOS-2
SJSA-1
KOS-3
U-2-OS
KOS-1
KOS-6
KOS-7
HOS
MNNG/HOS
143B
C
CX-5461 IC50 (nM)
Mut
Wt
Null
D
PMR-116 IC50 (nM)
Mut
Wt
Null
E
IC50 (nM)
CX
PMR
Mut
Wt
Null
P53 Status

Figure 4.2. The sensitivity of OS cell lines to RNA Pol Ii - relationship to p53 status
(A-B) The 50% inhibitory concentration (IC_{50}) of the two RNA Pol Ii in the OS cell lines as determined using the MTT assay (Fig. 4-1) are presented as bar graphs with values mean +/- SEM from three independent experiments (*n*=3). (C-D) The same IC_{50} in A (CX-5461) and B (PMR-116) were compared in relation to the *TP53* status of the OS cell lines. Both RNA Pol Ii exhibited a lower IC_{50} in the p53 mutant and null OS cell lines compared to p53 wild type. (E) Across all OS cell lines when grouped based on *TP53* the IC_{50} for CX-5461 and PMR-116 were similar. Colours indicate the *TP53* gene status as predicted in the OS molecular characterization study of chapter 3: Red= p53 mutant, Blue= p53 wild type, Green= p53 wild type, Brown= p53 null. Statistical analysis: *n*=3 per each cell line, graphs are mean +/- standard error of mean (SEM).

4.2.2 Anti-proliferative effect of RNA Pol Ii on human OS cell lines

To evaluate the effect of CX-5461 and PMR-116 on human OS cell line proliferation, cell confluency was analysed using an IncuCyte. Similar to the MTT assay, various concentrations of CX-5461, PMR-116 or corresponding vehicles (50 mM NaH_2PO_4 for CX-5461 and 50 mM citric acid for PMR-116) were added to the panel of OS cell lines and cell confluent determined from 0 to 72 hours of treatment (12 hourly scans). The 50% growth inhibitory concentration (GIC_{50}) was determined at 72 hours treatment as by this time the cells had under gone at least two cell divisions. Similar to the MTT assay results, both CX-5461 and PMR-116 reduced cell confluence in all the OS cell lines tested (Figure 4.3) in a dose dependent manner. In this case cell confluence is the surface area of the well covered by adherent cells (Niepel et al., 2017, Single et al., 2015, Huyck et al., 2012), thus a reduction in cell confluence would suggest a decrease in OS cell proliferation or cell growth. Interestingly, unlike for the IC_{50} values determined using the MTT assay, all the OS cell lines were more sensitive to CX-5461 compared to PMR-116 (Figure 4.3 and Figure 4.4 A-B, E). For example, the highest GIC_{50} for CX-5461 was 188nM for the SJSA-1 cell line, which was similar to the lowest GIC_{50} for PMR-116 which was 214 nM for MNNG/HOS and 238 nM for 143B. Interestingly unlike with the MTT assay results the GIC_{50} for CX-5461 or PMR116 did not correlate with *TP53* status (Figure 4.4. C-D).

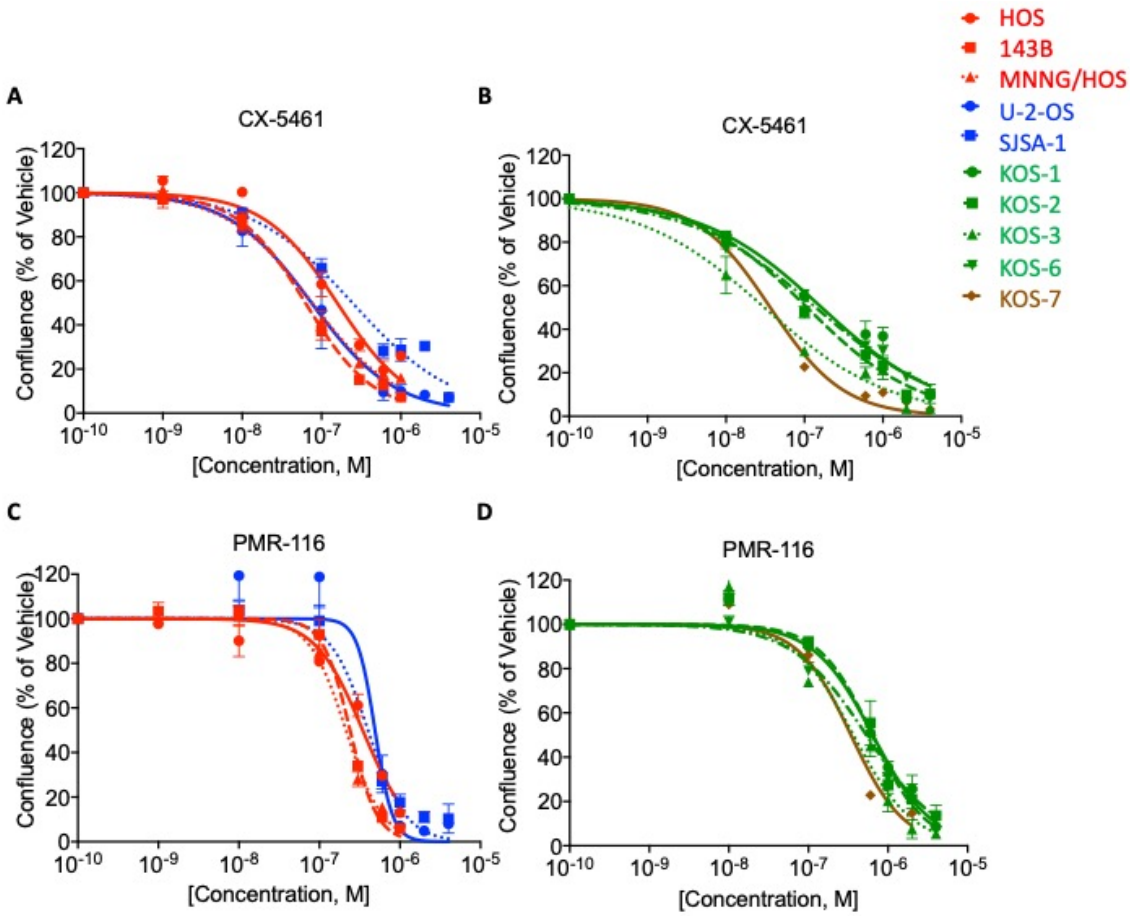

Figure 4.3. The anti-proliferative effect of RNA Pol Ii on OS cell lines
(A-D) ATCC and KOS cell lines were treated with various concentrations of CX-5461, PMR-116 or corresponding vehicle (50 mM NaH_2PO_4 for CX-5461 and 50 mM citric acid for PMR-116) for 72 hours and the confluence of the OS cells in the well of a 96 well plate determined using the IncuCyte®. Cell confluence was used as a readout/measure for cell proliferation (Section 2.2.5). CX-5461 or PMR-116 suppressed the confluence of all the ATCC and KOS cell lines in a dose dependent manner. Colours indicate the *TP53* gene status as predicted in the OS molecular characterization study of chapter 3: Red= p53 mutant, Blue= p53 wild type, Green= p53 wild type, Brown= p53 null. Statistical analysis: *n*=3 per cell line, dose-response curve determined by non-linear regression analysis, graph is mean +/- standard error of the mean (SEM).

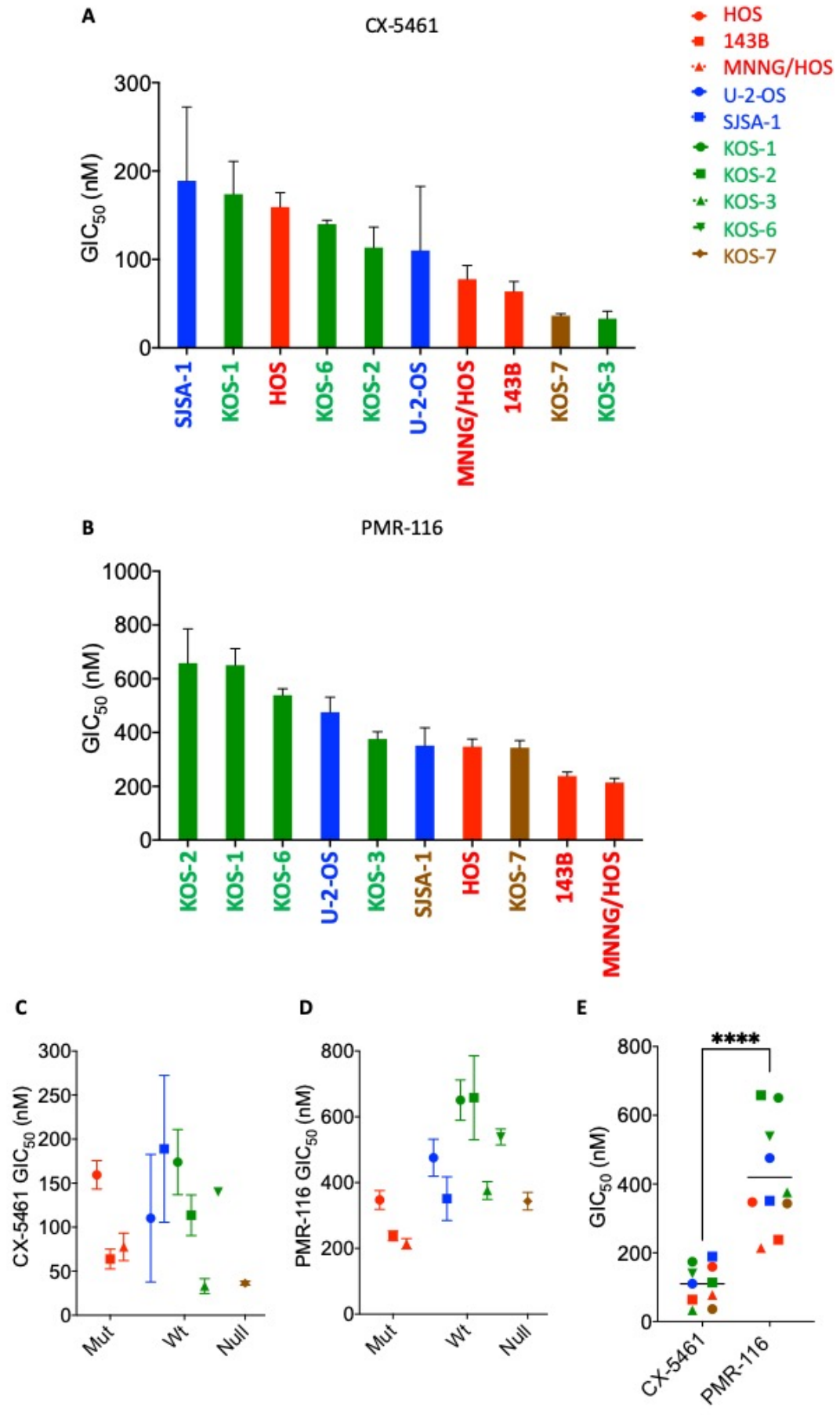
A
CX-5461
HOS
143B
MNNG/HOS
U-2-OS
SJSA-1
KOS-1
KOS-2
KOS-3
KOS-6
KOS-7
GIC50 (nM)
300
200
100
0
SJSA-1
KOS-1
HOS
KOS-6
KOS-2
U-2-OS
MNNG/HOS
143B
KOS-7
KOS-3
B
PMR-116
GIC50 (nM)
1000
800
600
400
200
0
KOS-2
KOS-1
KOS-6
U-2-OS
KOS-3
SJSA-1
HOS
KOS-7
143B
MNNG/HOS
C
CX-5461 GIC50 (nM)
300
250
200
150
100
50
0
Mut
Wt
Null
D
PMR-116 GIC50 (nM)
800
600
400
200
0
Mut
Wt
Null
E
****
GIC50 (nM)
800
600
400
200
0
CX-5461
PMR-116

Figure 4.4. The effect of RNA Pol Ii on OS cell proliferation - relationship to p53 status.
(A, B) The 50% growth inhibitory concentration (GIC_{50}) of the two Pol tis determined using the IncuCyte® cell proliferation assay results in Fig 4-3 are represented as bar graphs with values mean +/-SEM from three independent experiments (*n*=3). (C-D) The same GIC_{50} in A (CX-5461) and B (PMR-116) were compared in relation to the *TP53* status of the OS cell lines. Both RNA Pol Ii GIC_{50} did not indicate the correlation with *TP53* status in OS cell lines. (E) Across all OS cell lines when grouped based on *TP53* the GIC_{50} for CX-5461 showed a significant difference compared to PMR-116. Colours indicate the TP53 gene status as predicted in the OS molecular characterization study of chapter 3: Red= p53 mutant, Blue= p53 wild type, Green= p53 wild type, Brown= p53 null. Statistical analysis: *n*=3 per cell line, graph is mean +/- standard error of the mean (SEM) A-D.

4.2.3 Effect of CX-5461 and PMR-116 on cell cycle progression in human OS cell lines

To evaluate the effect of RNA Pol I transcription inhibition on the cell cycle in the human OS cell lines, uptake of BrdU and PI was evaluated (Section 2.2.7). Five commercially available ATCC OS cell lines and two patient-derived OS cell lines were treated with the GIC_{50} for CX-5461, or PMR-116, or vehicle for 72 hours (Figure 4.5). These were chosen in order to evaluate the different status of p53, specifically U-2-OS, SJSA-1 and KOS-3 are wild type (blue, green), HOS, 143B and MNNG/HOS are mutant (red) and KOS-7 is null (brown) for p53. This was assessed as other publications reported that CX-5461 induces a G1 phase cell cycle arrest in p53 wild type lymphoma cells (Bywater et al., 2012), while it induced G2 phase cell cycle arrest in p53 knockdown cells (Quin et al., 2016).

In all cases CX-5461 mediated an increase in cells in G2 suggesting a G2 phase cell cycle arrest, and this was independent of p53 status (Figure 4.5 A-G). Whereas PMR116 mediated a G2 phase cell cycle arrest in 4 (HOS, U-2-OS, KOS-3 and KOS-7) of the 7 cell lines tested and this was independent of p53 status (Figure 4.5 A-G). For example, of the p53 mutant cell lines HOS responded with an G2 arrest (Figure 4.5 A), 143B demonstrated an S phase arrest and MNNG/HOS cell cycle progression was not affected (Figure 4.5 B-C). The other p53 wild type cell lines exhibited a G2 phase arrest except for SJSA-1 which like MNNG/HOS there was no change in cell cycle progression (Figure 4.5 E). The p53 null type cell line KOS-7 also demonstrated a G2 phase arrest (Figure 4.5 G).

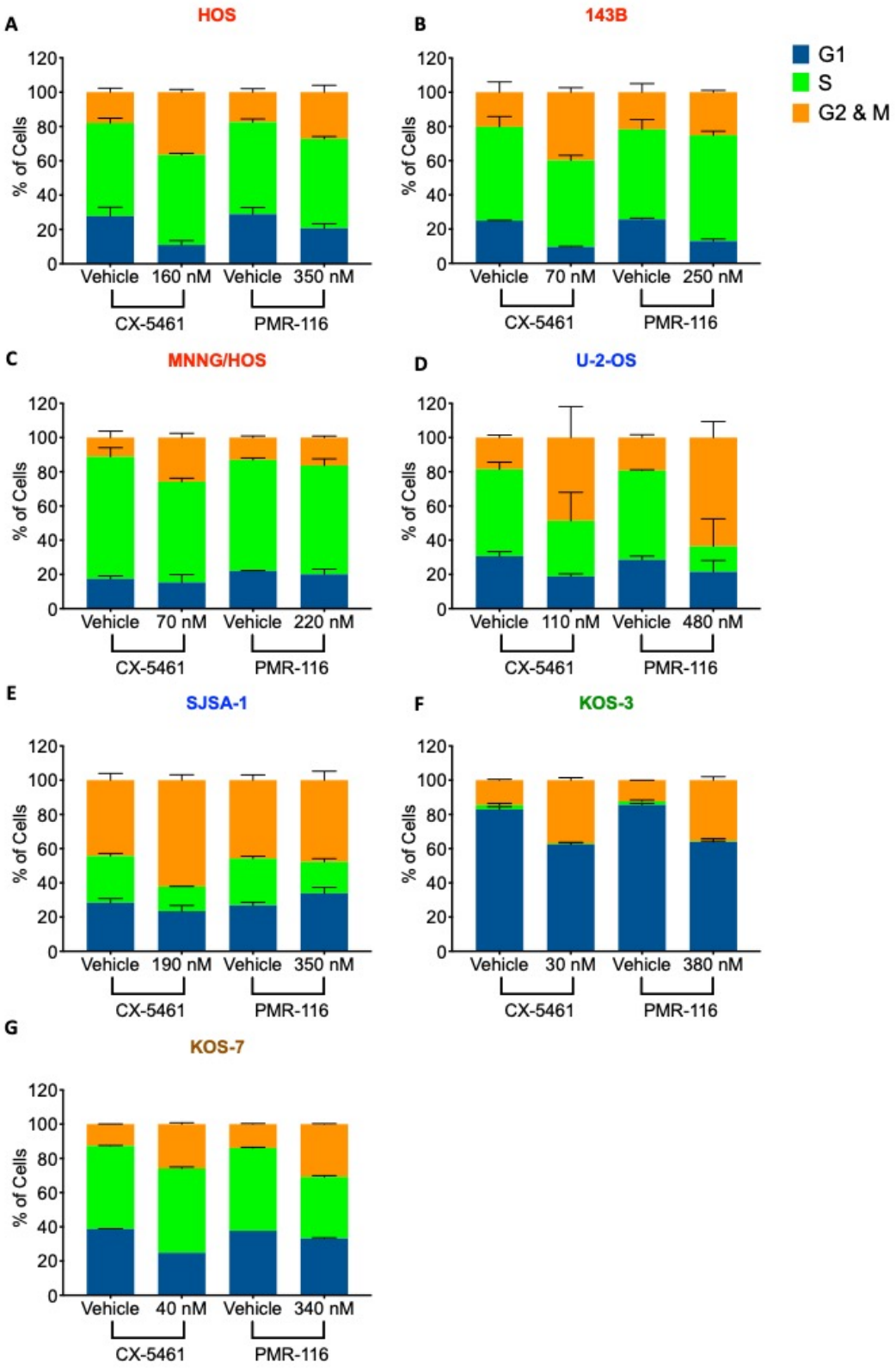
A
HOS
B
143B
G1
S
G2 & M
% of Cells
Vehicle 160 nM Vehicle 350 nM
CX-5461
PMR-116
Vehicle 70 nM Vehicle 250 nM
C
MNNG/HOS
D
U-2-OS
Vehicle 70 nM Vehicle 220 nM
Vehicle 110 nM Vehicle 480 nM
E
SJSA-1
F
KOS-3
Vehicle 190 nM Vehicle 350 nM
Vehicle 30 nM Vehicle 380 nM
G
KOS-7
Vehicle 40 nM Vehicle 340 nM

Figure 4.5. Effects of RNA Pol Ii on cell cycle progression in OS cell lines.
Following 72 hours treatment with the GIC_{50} for CX-5461 or PMR-116 or vehicle the population of cells in each phase of the cell cycle was determined using BrdU and PI staining with FACS analysis (Section 2.2.7). (A-G) Five ATCC OS and two KOS cell lines were analyzed. The colours of the bars in the graphs indicated G0/G1 (blue), S (green) and G2/M (orange) cell populations. The colours of the cell lines name indicate their *TP53* gene status as predicted in the OS molecular characterization study in chapter 3: Red= p53 mutant, Blue= p53 wild type, Green= p53 wild type, Brown= p53 null. The graphs are mean +/-standard error of division (SD) from two independent experiments (*n*=2).

4.2.4 Inhibitory effect of RNA Pol Ii on rRNA synthesis

To determine whether CX-5461 and PMR-116 are effective at hitting their primary target, rDNA transcription, in OS cell lines they were treated with various concentrations of the drug or vehicle for 1 hour. The cells were then harvested, RNA extracted and cDNA synthesis performed based on equal RNA. The abundance of the 5'External Transcript Spacer (ETS), as determined by qPCR (Section 2.2.6), was used as a surrogate measure for rDNA transcription rate as this is the first section of the 47s pre-rRNA that is cleaved and degraded (Bywater et al., 2012). Both CX-5461 and PMR-116 in a dose dependent manner effectively reduced the rate of rDNA transcription in all the OS cell lines compared to vehicle (Figure 4.6 A-B). From these curves, the drug concentration to decrease rDNA transcription rate by 50% (transcription inhibitory concentration: tIC_{50}) was determined. The tIC50s were similar between CX-5461 (300 nM to 100 nM) and PMR-116 (450 nM to 60 nM) across 6 of the cell lines, also there was no correlation with *TP53* status. There was however one exception, the KOS-3 cell line which had a tIC50 for CX-5461 (752 nM) which was 2-12 fold higher compared to that of the other OS cell lines, and higher that the tIC_{50} for PMR-116 which was comparable to the other cell lines. This difference in tIC50 for KOS-3 may mean this cell line requires a longer time for the RNA Pol Ii to accumulate to a concentration that it can inhibit rDNA transcription, perhaps the drug is selectively pumped out. However, the IC_{50} and GIC_{50} for CX-5461were not unusually increased in KOS. This means that suppression of RNA Pol I transcription, cytotoxicity and anti-proliferation were not tracking together and these relationships are unclear in the KOS-3 cell line. Irrespective of the result for CX-5461 in KOS-3 cells, the tIC50 for CX-5461 and for PMR-116 were similar. In the tIC_{50} comparison between CX-5461 and PMR-116, both drugs exhibited a similar mean tIC_{50} (Figure 4-6 E). Thus, for all the cell lines, except for CX-5461 treatment of KOS-3,

suggest that CX-5461 and PMR-116 can effectively inhibit their primary target at similar tIC50, regardless of *TP53* status.

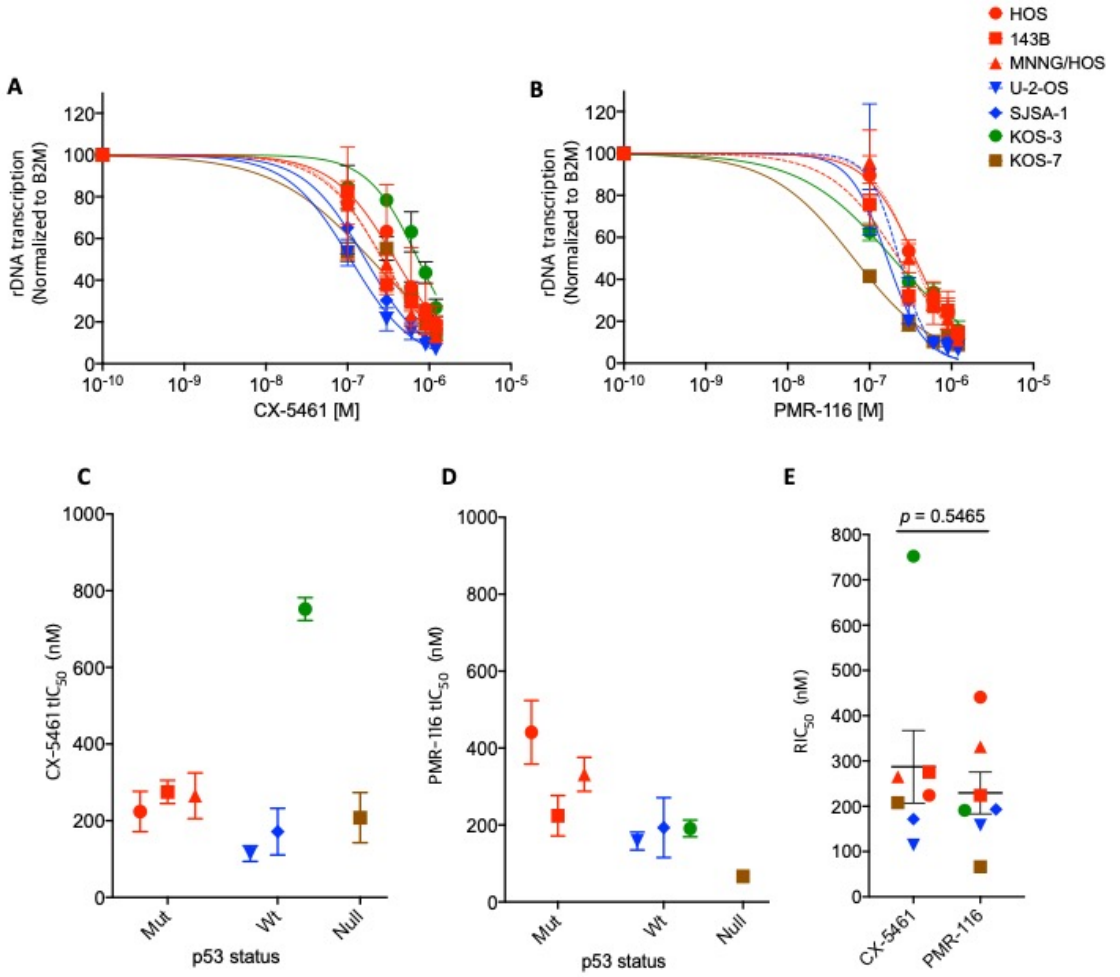

Figure 4.6. Effects of RNA Pol Ii on rDNA transcription in OS cell lines
(A, B) Five ATCC and two KOS OS cell lines were treated with various concentrations of CX-5461, PMR-116 or corresponding vehicle (50 mM NaH_2PO_4 for CX-5461 and 50 mM citric acid for PMR-116) for 1 hour and rDNA transcription rate was determined by quantification real-time PCR (qPCR) of 5'ETS (Section 2.2.1 in chapter 2). The 50% rDNA transcription inhibitory concentration (tIC_{50}) of two Pol Ii was determined using non-linear regression analysis. (C-D) The tIC_{50} of CX-5461 and PMR-116 were analysed in relation to *TP53* status. Both RNA Pol Ii tIC_{50} did not exhibit the correlation with *TP53* status in OS cell lines. (E) Across all OS cell lines when grouped based on *TP53* the tIC_{50} for CX-5461 and PMR-116 were similar. Colours indicate the *TP53* gene status as predicted in the OS molecular characterization study or predicted from western blot analysis in chapter 3: Red= p53 mutant, Blue= p53 wild type, Green= p53 wild type, Brown= p53 null. Statistical analysis: *n*=3 per cell line, dose-response curve determined by non-linear regression analysis A & B, graphs are mean +/-standard error of the mean (SEM) A & E, Student t-test E.

4.2.5 Summary

Both RNA Pol Ii exhibited cytotoxicity and anti-proliferation effects on all OS cell lines. In the MTT assay, p53 mutant OS cell lines showed a higher sensitivity to RNA Pol Ii while this pattern was not observed in the IncuCyte cell proliferation assay results. In the BrdU and PI staining, CX-5461 demonstrated a stronger inhibitory effect on cell cycle progression than PMR-116. All 7 OS cell lines (p53 mutant: HOS, 143B and MNNG/HOS, p53 wild-type: U-2-OS, SJSA-1 and KOS-3 and p53 null-type: KOS-7) showed G2 phase cell cycle arrest with CX-5461 treatment. In contrast, only 4 OS cell lines (HOS, U-2-OS, KOS-3 and KOS-7) exhibited G2 phase cell cycle arrest with PMR-116 treatment. In the qPCR assay, both RNA Pol Ii effectively suppressed their primary target, rDNA transcription activity with similar tIC_{50} irrespective of p53 status. Only the KOS-3 cell line exhibited relatively higher CX-5461 tIC_{50} compared to the other OS cell lines suggesting this cell line may require a longer time to respond to CX-5461 treatment. Further details on the difference between IC_{50}, GIC_{50} and tIC_{50} and the *in-vitro* anti-tumour effects of RNA Pol Ii will be discussed in Chapter 6.

Chapter Five

Therapeutic Efficacy of RNA Pol I transcription Inhibitors *in-vivo*

5.1 Introduction

The potential for RNA Pol Ii, CX-5461 and PMR-116, as a therapy for OS was demonstrated by *in-vitro* assays using 10 different human OS cell lines in chapter 3. However, the effect of RNA Pol Ii on OS *in-vivo* was reported in a single publication which demonstrated that CX-5461 significantly ($p<0.05$) inhibited tumour growth in one mouse model of human OS; specifically U-2-OS (*TP53* wild type OS) grown in nude mice (Li et al., 2016). Since, as mentioned previously, the therapeutic efficacy of CX-5461, for example against lymphoma is dependent on p53 status (Bywater et al., Drygin et al., 2011, Quin et al., 2016, Negi and Brown, 2015) it will be important to evaluate efficacy against a range of OS with different p53 backgrounds as we have in chapter 4. Interestingly in this thesis using human OS cell lines, CX-5461 and PMR-116 exhibited similar potency *in-vitro* irrespective of p53 status (Chapter 4). In order to evaluate our cell lines in a mouse model we chose the recombination activating gene 2 (Rag 2) knockout (KO) mouse strain which has previously been reported to support the growth of many human sarcomas (Nanni et al., Vormoor et al., 2014).

The aims of this chapter, therefore, were to:

(i) Establish the tumorigenic potential of human OS cell lines in Rag 2 KO mice;

(ii) Determine the maximum tolerated doses of CX-5461 and PMR-116 in the Rag 2 KO mice;

(iii) Investigate the therapeutic efficacy of CX-5461 and PMR-116 against tumours of p53 mutant and p53 wild type human OS cell lines in Rag 2 KO mice.

5.2 Results

5.2.1 Tumorigenicity of human OS cell lines in Rag 2 KO mice

Prior to investigating the therapeutic effects of RNA Pol Ii in human OS xenograft mouse models, the tumorigenic capacity of a variety of human OS cells was evaluated in both male and female Rag 2 KO mice (Section 2.3.1). The Rag 2 KO mouse is the immune-deficient strain as the absence of Rag 2 gene prevents B and T lymphocyte maturation (Shinkai et al., 1992). In the initial screening process, 143B-Luc, HOS, MNNG/HOS, U-2-OS and SJSA-1 cell lines were evaluated for tumorigenic capacity in Rag 2 KO mice. A number of conditions were tested such as varying the number of OS cells injected in HBSS buffer or in a Matrigel mixed with HBSS buffer. Only 3 of the 5 OS cell lines, irrespective of optimization, demonstrated robust tumour development (Table 5.1). Out of these 3 MNNG/HOS ($p53^{mut}$) and SJSA-1($p53^{wt}$) were transduced with the luciferase gene (Section 2.2.2) so they can provide accurate tumour volume by bioluminescence imaging. Once single cell clones were successfully transduced with luciferase gene, their tumorigenic capacity was retested and compared with the parental non-transfected cell line. SJSA-1-Luc cell line showed 100% tumour development in both sexes of Rag 2 KO mice within 10 days of tumour inoculation and had a similar tumour growth rate compared to the parental cell line (SJSA-1). In contrast, MNNG/HOS-Luc cell line exhibited a slower tumour growth rate in female of Rag 2 KO mice compared to male mice. Averagely, MNNG/HOS-Luc in female Rag 2 KO mice formed a recognizable tumour (50 mm^3. Measured by a digital calliper. Section 2.3.2.1) 10 days following tumour cell injection. However, MNNG/HOS-Luc in male Rag 2 KO, tumours were not measurable until 20 days post tumour cell injection. Therefore, 143B-Luc and SJSA-1-Luc cell lines were determined as the suitable OS cell lines for *in-vivo* study. The results of the tumorigenicity assays are listed in Table 5.1.

5.2.2 Maximum tolerated dose of RNA Pol Ii

To avoid excessive toxicity of the drug, the maximum tolerated dose (MTD) of CX-5461 and PMR-116 in Rag 2 KO mice was determined (Section 2.3.4). The two RNA Pol Ii were administered via oral gavage to Rag 2 KO mice following the schedules detailed in Table 5.2. From these results the MTD for CX-5461 was determined as 30 mg/kg thrice weekly and for PMR-116 80 mg/kg twice-weekly based on demonstrating that doses higher than these resulted in excessive weight loss (> 20% of baseline) that required euthanasia of the mice (Table 5.2).

Table 5.1 Tumour forming capacity of human OS cell lines in Rag 2 KO mice

Cell line	Tumour cell injection conditions	Tumour development
HOS	3.0×10^6 cells in 50 µL HBSS containing 50% (v/v) Matrigel	No
143B-Luc*	1.0×10^6 cells in 50 µL HBSS	Yes in 100% (F=3, M=2)
MNNG/HOS		Yes in 100% (F=2, M=2)
MNNG/HOS-Luc*		Yes in 100% (F=1, M=2)
U-2-OS	5.0×10^6 cells in 50 µL HBSS containing 50% (v/v) Matrigel	No
SJSA-1		Yes in 100% (F=1, M=1)
SJSA-1-Luc*		Yes in 100% (F=1, M=2)
KOS-2	1.0×10^6 cells in 50 µL HBSS 2.0×10^6 cells in 50 µL HBSS	No
KOS-6	2.0×10^6 cells in 50 µL HBSS	No
KOS-7	5.0×10^6 cells in 50 µL HBSS	No

*: Luc = Luciferase expressing cell line.

F = number of female mice; M= number of male mice.

Table 5.2. Maximum tolerated dose assays of RNA Pol Ii in Rag 2 KO mice

Compound	Concentration	Dosing frequency and period	Weight outcome
PMR-116*Δ	300 mg/kg	Once weekly, 2 weeks	3 of 4 mice had >20% weight loss
	200 mg/kg	Once weekly, 2 weeks	2 of 4 mice had 15% weight loss
	160 mg/kg	Once weekly, 2 weeks	1 of 3 mice had >15% weight loss
	120 mg/kg	Thrice weekly, 2 weeks	1 of 3 mice had 20% weight loss
	100 mg/kg	Twice weekly, 3 weeks	1 of 3 mice had >15% weight loss
	80 mg/kg	Thrice weekly, 3 weeks	2 of 4 mice had >20% weight loss
	80 mg/kg	Twice weekly, 3 weeks	1 of 6 mice had >10% weight reduction
CX-5461*#	40 mg/kg	Thrice weekly, 2 weeks	4 of 4 mice had >20% weight loss
	35 mg/kg	Thrice weekly, 2 weeks	4 of 4 mice had >20% weight loss
	30 mg/kg	Thrice weekly, 2 weeks	3 of 3 mice 10% weight increase

*RNA Pol Ii or vehicle were administered via oral gavage
ΔVehicle for PMR-116: 50 mM Citric acid
#Vehicle for CX-5461: 50 mM $Na_2H_2PO_4$

5.2.3 *In-vivo* therapeutic effects of RNA Pol Ii on human OS tumours in Rag 2 KO mice

Following establishment of the tumorigenic potential of 3 luciferase tagged OS cell lines and the MTD of the RNA Pol Ii in Rag2 KO mice, *in-vivo* experiments were undertaken to determine the therapeutic effects. The cell lines evaluated were 143B-Luc ($p53^{Mut}$) and SJSA-1-Luc ($p53^{Wt}$) so that any possible effect of the RNA Pol Ii based to p53 status could be evaluated.

5.2.3.1 143B-Luc OS

Experiment 1: 143B-Luc cells were subcutaneously injected into 12 male and 12 female Rag 2 KO mice. At 10 days post tumour cell injection, the tumours were measured by digital calliper and IVIS imaging (Section 2.3.2.1 and 2.3.2.2). Based on the bioluminescence signal (BLI), the mice were divided into three groups (vehicle, CX-5461 or PMR-116) to obtain roughly equal average BLI across all groups (Vehicle: 6.12×10^7 +/- 4.47×10^7, SEM), (CX-5461: 6.76×10^7+/- 4.19×10^7, SEM) and (PMR-116: 1.07×10^8+/- 6.17×10^7, SEM). The RNA Pol Ii were administered for a total of 14 days with the experiment concluded when the tumour size in the vehicle group reached a pre-determined ethical end point.

At the termination of the experiment, the average tumour volume measured using digital callipers was significantly ($p<0.05$) reduced in the CX-5461 treated group (58 ± 26 mm) in comparison to the vehicle-treated controls (144 ± 49 mm). The tumour volume in the PMR-116 treated group (94 ± 35 mm) was reduced but not significant when compared to that of the controls ($p=0.14$) (Figure 5.1 A).

The bioluminescent imaging results for the tumours were not as consistent as those obtained using the digital callipers (Figure 5.1 C-D). The average tumour volume using BLI at Day 15 showed the vehicle-treated group with the smallest tumour size and the CX-5461 group with the largest tumour size which was in direct contrast to the digital calliper results. The excised tumour weights, however, correlated significantly with the calliper measurements ($R=0.6766$, $p<0.0001$), but not with the bioluminescent intensity results ($R<0.001$, $p=0.963$) (Figure 5.2). All mice were shaved in the region of tumour cell injection at the commencement of the experiment, however, the hair re-growth in the vehicle-treated group was more rapid than for the RNA Pol Ii treated groups. Surface hair decreases the detection of an internal bioluminescent signal thus it is possible that this factor explains the disparity between the two *in-vivo* tumour measurement techniques (Izumi et al., 2017).

Experiment 2: The above experiment was repeated in two groups, CX-5461 and vehicle groups. 143B-Luc cells were subcutaneously injected into 10 male and 6 female Rag 2 KO mice and divided into two groups (Vehicle group: 5 male and 3 female mice and CX-5461 treated group: 5 male and 3 female mice). Very similar results to Experiment 1 were obtained (Figure 5.1 E-F). At Day 13, one mouse in the CX-5461 cohort was culled as the tumour size reached to ethical end point. At the completion of Experiment 2, the average tumour volume in the CX-5461 treated mice were significantly ($p<0.05$) lower in comparison to those in the vehicle treated mice (269 ± 43 mm vs 519 ± 112 mm, respectively). These results demonstrate a significant and reproducible therapeutic effect of CX-5461 on 143B-Luc OS tumour growth *in vivo* (Figure 5.1 G)

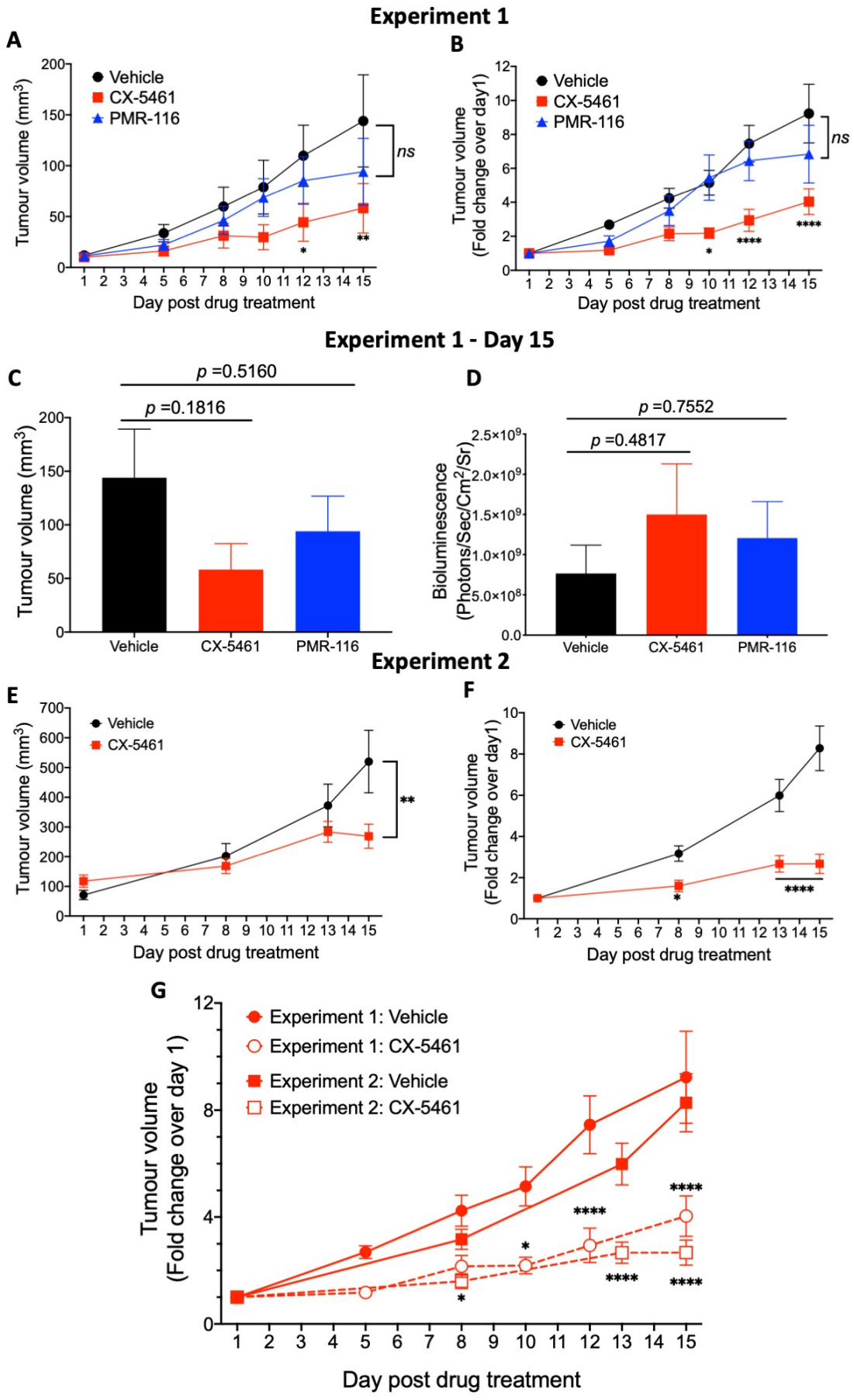
Experiment 1
A
Vehicle
CX-5461
PMR-116
Tumour volume (mm3)
Day post drug treatment
ns
B
Tumour volume (Fold change over day1)
Experiment 1 - Day 15
C
p =0.5160
p =0.1816
D
p =0.7552
p =0.4817
Bioluminescence (Photons/Sec/Cm2/Sr)
Experiment 2
E
F
G
Experiment 1: Vehicle
Experiment 1: CX-5461
Experiment 2: Vehicle
Experiment 2: CX-5461

Figure 5.1 Effect of RNA Pol Ii on Human OS 143B-Luc tumours in Rag 2 KO mice. Following subcutaneous injection of human OS 143B-Luc cells into Rag 2 KO male and female mice: (A) tumour volume (mm^3); and (B) tumour volume expressed as fold-change of Day 1 measurement in mice administered CX-5461 (30 mg/kg thrice weekly), PMR-116 (80 mg/kg twice weekly) or equivalent volume of the combined vehicles (50% of 50 mM NaH_2PO_4 and 50% of 50 mM citric acid, thrice weekly) administered via oral gavage. (C) Tumour volume (mm^3) and (D) bioluminescence signal (Photon/Sec/Cm^2/Sr) at Day 15. (E-F) An experimental repeat with CX-5461 and a single vehicle to the data presented in A and B. (G) Combined CX-5461 data from both experiments, as depicted in B and F, demonstrating the reproducibility of the treatment effect. Statistical analysis: n=6-8 per group with equal sex distribution, Two-way ANOVA A & B; One-way ANOVA C & D; *p<0.05, **p<0.005, ****p<0.0001, error bars represent standard error of the mean (SEM).

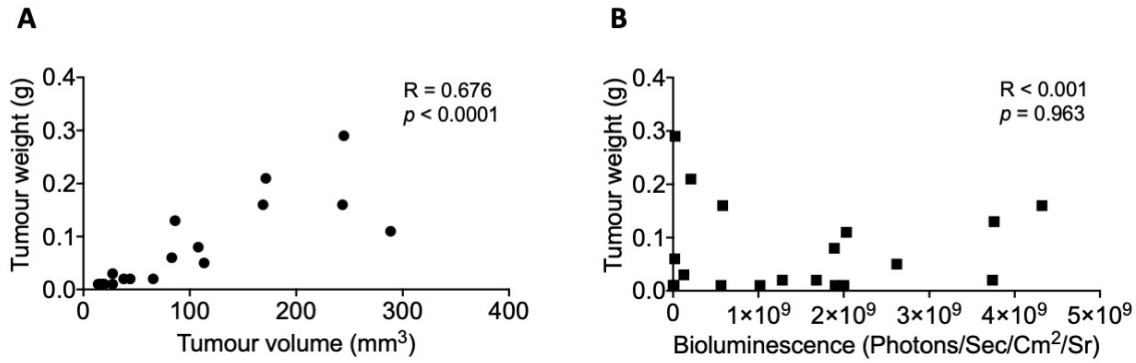

Figure 5.2 Correlation of tumour weight with tumour volume or bioluminescence
(A) In-situ tumour volume was measured using digital callipers and excised tumours were weighed using calibrated scales, and (B) tumour bioluminescence was determined using IVIS imaging prior to excision and weight determined as in A. Statistical analysis: n=18-20 (non-measurable values excluded), Pearson's correlation coefficient A & B.

5.2.3.2 SJSA-1-Luc OS

Experiment 1: SJSA-1-Luc cells were subcutaneously injected into 16 male Rag 2 KO mice which were then randomized into two groups based upon the average tumour BLI at 10 days post tumour cell injection. The mice were treated with CX-5461 or vehicle for a total of 14 days with the experimental end-point determined by the tumour size in the control group. At the completion of the experiment, the average tumour volume in the CX-5461 treated mice was significantly reduced ($p < 0.0001$) in comparison to the vehicle group (49 ± 7 mm vs 239 ± 63 mm, respectively) (Figure 5.3 A-B).

Experiment 2: The above experiment was repeated in 14 female Rag 2 KO mice and similar results were obtained (Figure 5.3 C-D). At the termination of the experiment, the average tumour volume in the CX-5461 treated group was significantly ($p < 0.0001$) lower than the vehicle group (49 ± 7 mm vs 361 ± 66 mm, respectively) (Figure 5.3 C-D). These experiments again demonstrated a significant and reproducible inhibition of SJSA-1-Luc OS tumour growth by CX-5461 *in vivo* (Figure 5.3 E).

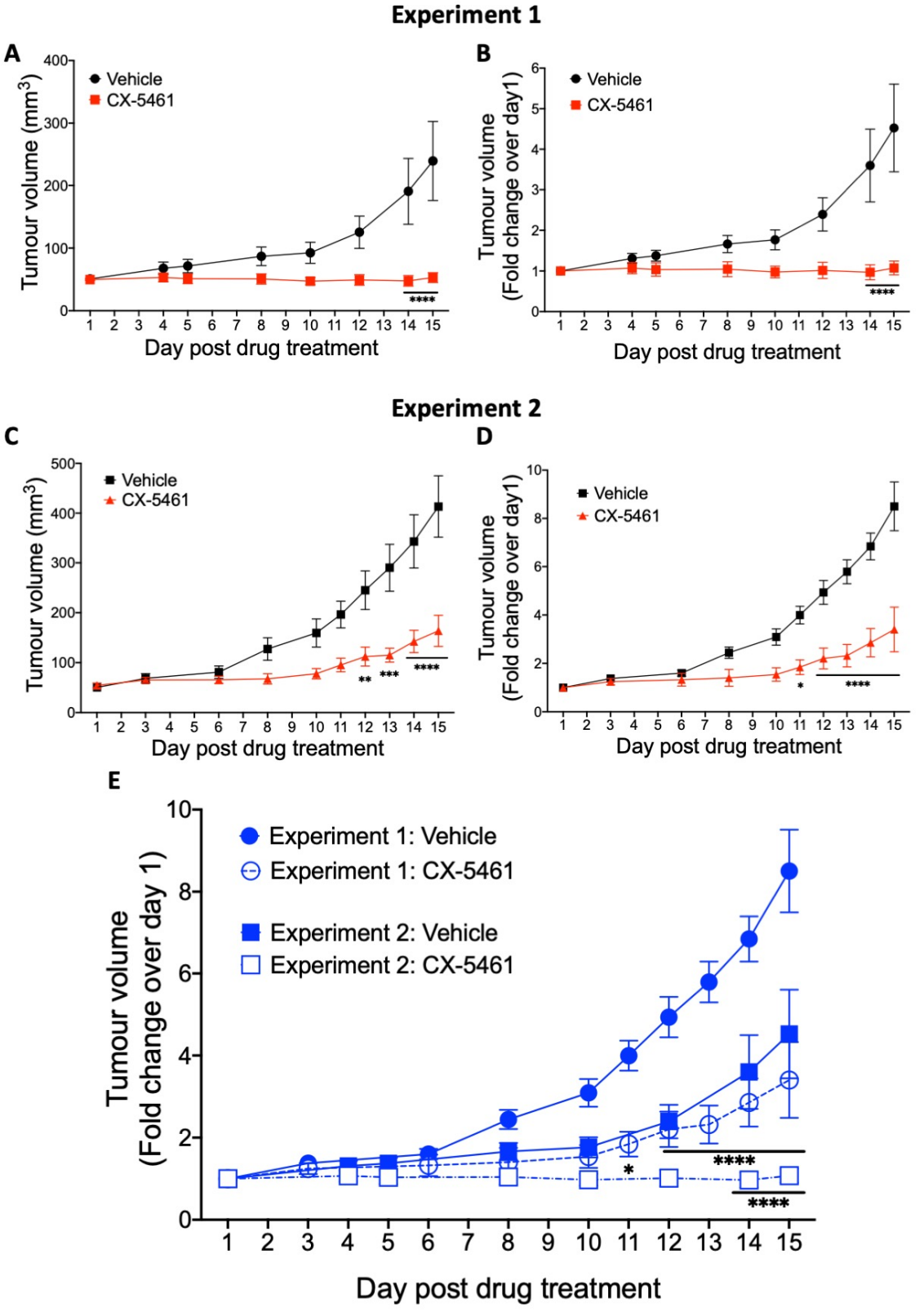
Experiment 1
A
Tumour volume (mm3)
Vehicle
CX-5461
Day post drug treatment
****
B
Tumour volume (Fold change over day1)
Vehicle
CX-5461
Day post drug treatment
****
Experiment 2
C
Tumour volume (mm3)
Vehicle
CX-5461
Day post drug treatment
**
***
****
D
Tumour volume (Fold change over day1)
Vehicle
CX-5461
Day post drug treatment
*
****
E
Tumour volume (Fold change over day 1)
Experiment 1: Vehicle
Experiment 1: CX-5461
Experiment 2: Vehicle
Experiment 2: CX-5461
Day post drug treatment
*
****
****

Figure 5.3 Effects of CX-5461 on Human OS SJSA-1-Luc tumours in Rag 2 KO mice. Following subcutaneous injection of human OS SJSA-1-Luc cells into Rag 2 KO mice (A) Tumour volume (mm^3) and (B) Fold change in tumour volume was measured in SJSA-1-Luc OS bearing male mice administered CX-5461 (30 mg/kg thrice weekly) or equivalent volume of the combined vehicle (50% of 50 mM NaH_2PO_4 and 50% of 50 mM citric acid, thrice weekly) administered via oral gavage. (C-D) An experimental repeat with CX-5461 and a single vehicle but in female mice with data presented as described in A and B. (E) Combined CX-5461 data from both experiments, as depicted in B and D, demonstrating the reproducibility of the treatment effect. Statistical analysis: *n*=6-8 per group, Two-way ANOVA, *$p<0.05$, **$p<0.005$, ***$p<0.0005$, ****$p<0.0001$, error bars represent standard error of the mean (SEM).

Chapter Six

Discussion

6.1 Hypothesis and aims

The overall hypothesis of this thesis is that the inhibition of ribosome biogenesis, through targeting RNA Pol I transcription with CX-5461 or PMR-116, would prove effective in reducing OS cell growth and proliferation *in-vitro* and OS tumour growth *in-vivo*. Thus, inhibition of RNA Pol I transcription could be a new therapeutic strategy for OS treatment.

In order to evaluate this hypothesis, three aims were investigated:

(i) Identify the status of key regulatory proteins which modulate RNA Pol I transcription activity that are frequently altered in OS in 10 human OS cell lines;

(ii) Evaluate the effect of RNA Pol Ii, CX-5461 and PMR-116, on growth and proliferation in 10 human OS cell lines *in-vitro*;

(iii) Investigate the therapeutic efficacy of RNA Pol Ii against p53 mutant and p53 wild type human OS tumours *in-vivo*.

6.2 The molecular characterization of human OS cell lines for genes involved in transcription regulation

The aim of Chapter 3 was to identify the status of key regulatory proteins which modulate RNA Pol I transcription and are frequently altered in OS cell lines, especially for the KOS cell lines as there was no genetic information available. While often the specific cause or initiating factor(s) responsible for the development of OS have not been identified, a number of dysregulated genes or proteins known to alter OS cell proliferation and development have been reported in studies using OS patient samples (Serra and Hattinger, 2017, Ottaviano et al., 2010, Martin et al., 2012). The tumour suppressors p53 and RB1 are known to be frequently altered in OS (Kansara et al., 2014), resulting in impairment

of osteoblast differentiation. Specifically, osteoblast cell cycle progression is dysregulated leading to OS development from immature osteoblasts (Velletri et al., 2016, Berman et al., 2008, He et al., 2015). MDM2 and c-Myc are known to be highly up-regulated oncogenes in OS (Kansara et al., 2014). Elevated MDM2 protein abundance leads to tumorigenesis via the inactivation of wild type p53, while overexpression of c-Myc promotes metastasis of OS cells via stimulating the MEK-ERK pathway (Han et al., 2012, Lonardo et al., 1997). In addition, elevated p53, RB1 and c-Myc protein abundance correlates with a poor response to therapy in OS patients (Chen et al., 2016, Ren and Gu, 2017, He et al., 2014). Recently, several studies reported that increased p53, RB1 and c-Myc expression elevate ribosome biogenesis in OS, whereas inhibition of ribosome biogenesis suppresses OS cell proliferation (Montanaro et al., 2007, Li et al., 2016, Chen et al., 2018). Similar dysregulation has been observed in other cancers. Elevated c-Myc protein expression is common in aggressive prostate cancer and triple negative breast cancer (Gurel et al., 2008, Xu et al., 2010). Upregulated MDM2 protein expression is frequently reported in human sarcoma (Oliner et al., 2016) and elevated mutant p53 protein is common in pancreatic cancer (Jones et al., 2008). Elevated RB1 protein expression has been observed in colorectal cancer (CRC) (Ali et al., 1993, Lai et al., 2006). All these studies suggest that such changes are presenting in a variety of cancers, not limited to OS, and the upregulated ribosome biogenesis could be an effective target for cancer therapy. While the therapeutic efficacy of ribosome inhibition was shown to be dependent on the status of p53, which is also a key regulatory protein in OS, in murine lymphoma model (Bywater et al., 2012, Negi and Brown, 2015) other studies demonstrate efficacy independent of p53 (Quin et al., 2016). Thus, determining the basal expression level of these key tumour suppressors and oncogenes in the ATCC and KOS cell lines and comparing expression with the efficacy of inhibiting ribosome biogenesis with

respect to cytotoxicity, cell proliferation and cell cycle is important for understanding the relationship between these key factors and the efficacy of inhibiting ribosome biogenesis.

The cell line expression data is summarised in Table 3.1, while in Table 6.1 these results are compared to the literature based on OS patient samples. Interestingly the frequency of alterations for the four proteins examined in the cell lines were not always consistent with reports using patient samples (Chen et al., 2014, Lonardo et al., 1997, Stock et al., 2000, Miller et al., 1996). For example, *TP53* mutations occur in 80% of OS patients, and 40% of these exhibited a deletion or loss of heterozygosity for *TP53* (Chen et al., 2014). In our results, 30% of all 10 OS cell lines exhibited upregulated p53 expression which is expected as the consequence of *TP53* mutation. MDM2 amplification is reported to occur in 6 % of OS patients, and c-Myc amplification in 43% (Lonardo et al., 1997, Stock et al., 2000). While only 1 OS cell line of 10 (10%) exhibited detectable full length MDM2 expression, this might be considered similar to the patient data. Although there was no c-Myc expression in the KOS cell lines, taken together 30% of the OS cell lines showed upregulated c-Myc expression, presumably as a consequence of c-Myc amplification, which matches well with the patient data. Whereas 60% of OS patients have an RB1 mutation (Miller et al., 1996, Benassi et al., 1999), but 40% of all 10 OS cell lines exhibited upregulated RB1 expecting as the result of RB1 mutation. Any inconsistency in the frequency of overexpression or mutation for these four proteins between patient samples and our cell lines is likely to be due to the large difference in sample size (16 to 75 of patient samples compared to 10 of cell lines in this thesis) or due to the selection process when the cells were adapted for culture (Table 6.1). None-the-less, our cell line panel does include examples of all 4 common alterations described in OS patients.

Table 6.1 Altered tumour suppressors and oncogenes in human OS

Names	OS Patient		KOS*	ATCC
	Freq (n)	Refs	Expression compared to HF	Expression compared to HF
Tumour protein 53 (TP53)	80 % (28/34) (Mut)	(Chen et al., 2014)	80% Similar (4/5) 20% NE (1/5)	60% up (3/5) 40% down (2/5)
MDM2 p53 binding protein homologue (MDM2)	6% (5/75) (Amp)	(Lonardo et al., 1997)	100% NE (5/5)	20% up (1/5) 80% non (4/5)
Cellular myelocytomatosis (c-Myc)	43 % (7/16) (Amp)	(Stock et al., 2000)	100% NE (5/5)	60% up (3/5) 40% non (2/5)
Retinoblastoma 1 (RB1)	62% (26/42) (Mut) 54% 21/39 (Mut)	(Miller et al., 1996, Benassi et al., 1999)	20% up (1/5) 80% Similar (4/5)	60% up (3/5) 40% down (2/5)

Mut = Mutation Amp = Amplified Freq = Frequency of dysregulation
HF= Human Fibroblast Refs = References NE = Not expressed
Similar = A similar level of expression
*The genetic information for the KOS cell lines has not been determined.

The alterations in the four key proteins examined would be predicted to enhance both OS cell proliferation and RNA Pol I transcription activity. For example, c-Myc is a key upstream regulator of RNA Pol I transcription activity, resulting in elevated ribosome biogenesis (van Riggelen et al., 2010). On the other hand, p53 and RB1 act as suppressors of RNA Pol I transcription activity by disrupting RNA Pol I binding to the rDNA gene promoter (Hannan et al., 2000, Zhai and Comai, 2000). Consistent with these findings, in this study, two p53 mutant OS cell lines (HOS and MNNG/HOS) expressing elevated levels of c-Myc demonstrated high rDNA transcription rates with short doubling times. In addition, MDM2 overexpression, as seen in SJSA-1, and the absence of p53 in combination with high levels of RB1, as in KOS-7, were associated with high rDNA transcription rates and short doubling times. In comparison, when wildtype p53 expression is normal, c-Myc and RB1 expression are absent or low, as in U-2-OS, rDNA

transcription rate and doubling time are also low (Table 3.1 and Figure 3.5). Based on the basal abundance of four key proteins and basal rDNA transcription rates we propose three mechanisms of regulation by which they promote OS cell proliferation, all of which converge on increasing RNA Pol I transcription activity and thus ribosome biogenesis. Specifically, ribosome biogenesis can be up regulated by: i) accumulation of mutant p53 and c-Myc protein (Figure 6.1); ii) suppression of functional p53 by overexpressed MDM2 protein (Figure 6.2); and iii) inhibition of rDNA transcription by RB1 (Figure 6.3).

i) Up-regulation of ribosome biogenesis mediated by elevated mutant p53 and c-Myc protein (Figure 6.1).

When p53 is mutated it loses some functions compared to wild type p53, and typically it is protected from MDM-2 mediated ubiquitination thus will accumulate (Prives and Hall, 1999) (Section 1.1.1). In addition over 80% of mutations in *TP53* occurred in the sequence-specific DNA binding domain which is essential for binding its target gene promoters (Zhou et al., 2019) which would alter the genes expressed (Levine, 1997). Mutant p53 can also form a complex with other transcription factors or proteins, such as a peptidyl-prolyl cis-trans isomerase NIMA-interacting 1 (PIN1) which in turn increases the expression of c-Myc (Liao et al., 2017), and promotes ribosome biogenesis (van Riggelen et al., 2010). Mutant p53 can also lose the ability of wild type p53 to suppress RNA polymerase I transcription (Zhai and Comai, 2000). Thus, together this means that mutant p53 may promote cell proliferation through both altering gene expression, such as increasing c-Myc expression, and also directly releasing suppression of RNA polymerase I transcription (Figure 6.1). The mutant p53 OS cells (HOS, 143B and MNNG/HOS) exhibited elevated c-Myc protein compared to those with wild type p53 (Figure 3.1, 3.2, A.1 and A.2) and these cell lines also had the fastest growth rates in the

cell proliferation assay (Table 3.1). These results are consistent with previous descriptions (Ottaviano et al., 2010). Similarly, SK-UT-1 cell line which is mutant for p53 exhibited elevated c-Myc protein expression and a faster growth rate compared to wild type p53 OS cell lines. In contrast, the p53 null KOS-7 cell line proliferated faster than the p53 wild type OS cells but did not have elevated c-Myc expression. This is consistent with the proposed model of two points of involvement for p53 – one through mutant p53 increasing c-Myc expression and a second via the direct effects of p53 on Pol I transcription activity (Figure 6.1).

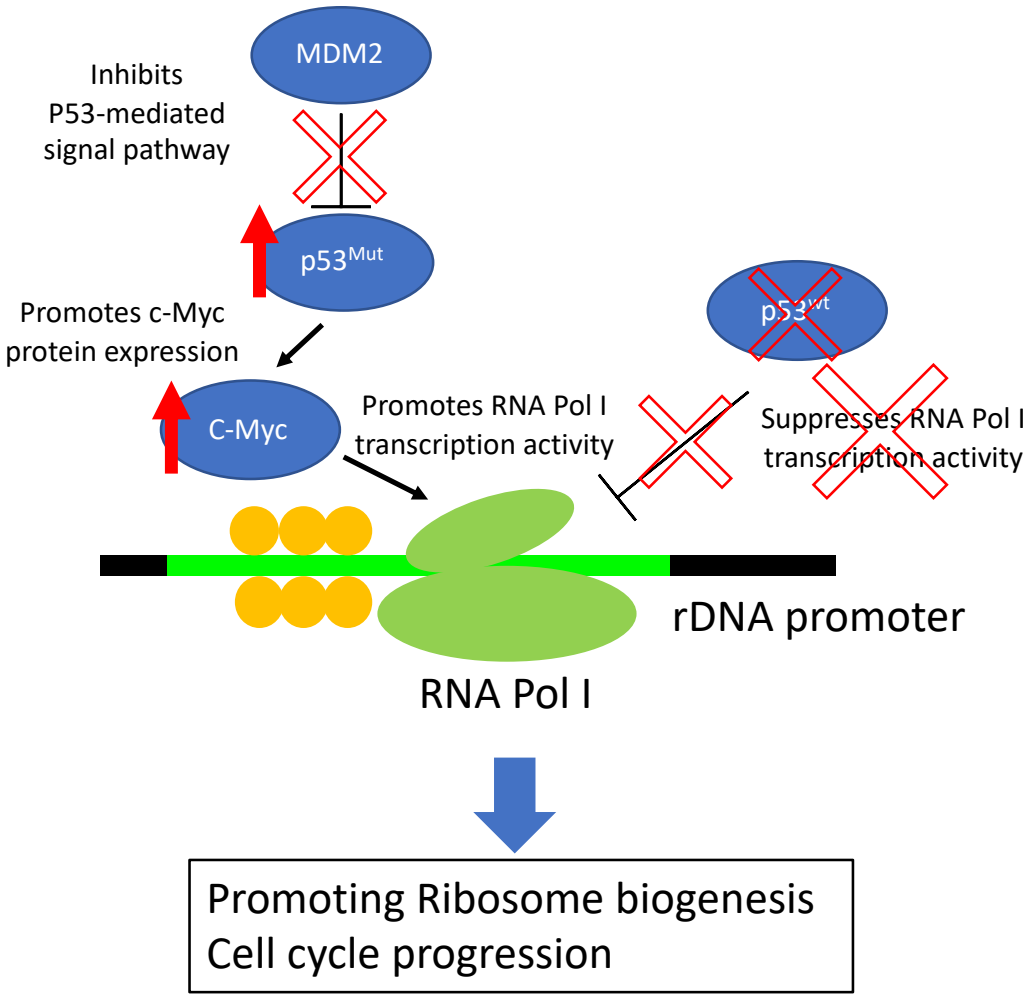

Figure 6.1 Schematic diagram of mutant p53 and c-Myc mechanism of regulating OS
Unlike wild type p53, MDM2 cannot bind mutant p53 which escapes MDM2-mediated ubiquitination and accumulates in the cell. Accumulated mutant p53 promotes c-Myc protein expression via increasing c-Myc mRNA transcription and it subsequently increases RNA Pol I transcription activity. Mutant p53 also lacks the ability to inhibit RNA Pol I transcription activity, further increasing ribosome biogenesis.

ii) Up-regulation of ribosome biogenesis mediated by suppression of p53 function through overexpression of MDM2 protein (Figure 6.2). Upregulated expression of MDM2 can lead to tumorigenesis in the presence of wild type p53 by suppressing the p53-mediated cell protective and apoptotic pathways (Section 1.1.1), and this has been reported in several OS patient analyses (Moll and Petrenko, 2003, Miller et al., 1996, Freedman and Levine, 1999). Elevated MDM2 protein expression has the same effect as lack of the ARF tumour suppressor ($p14^{ARF}$) (Ottaviano et al., 2010). $p14^{ARF}$ is encoded by the *CDKN2A* gene and when expressed it binds MDM2 thus suppressing MDM2-mediated ubiquitination by preventing its exportation from the nucleus to cytoplasm (Orlando et al., 2014, Inoue et al., 1999). Elevated MDM2 protein expression was observed in SJSA-1 cells (Figure 3.3). In SJSA-1, the homozygous deletion of *CDKN2A* gene has been reported and as a result they do not express $p14^{ARF}$, thus MDM2 binds p53 and enhances its degradation resulting in elevated cell proliferation and reduced apoptosis (Silva et al., 2003). Thus, overexpressed MDM2 in this case could promote ribosome biogenesis via inhibiting the function of p53.

Interestingly all the KOS cell lines showed a low level of cleaved MDM2 protein (60 kDa) compared to human fibroblasts (HF) (Figure 3.3 and Figure A.3). It has been reported that MDM2 can be cleaved by caspase-2 in the absence of apoptosis or the p53-mediated cell protective pathway (Oliver et al., 2011, Pochampally et al., 1998). Perhaps in these cases the ability of MDM2 to mediate tumorigenesis has been lost due to it being cleaved. In the SK-UT-1 cell line there was a low or undetectable level of full length or cleaved MDM2 (Figure 3.3 and Figure A.3), suggesting in this case that MDM2 did not mediate tumorigenesis. Thus, in of all the cell lines investigated only SJSA-1 exhibited

the potential for MDM2 to promote cell proliferation via inhibiting p53-mediated signaling pathways and enhancing ribosome biogenesis (Figure 6.2).

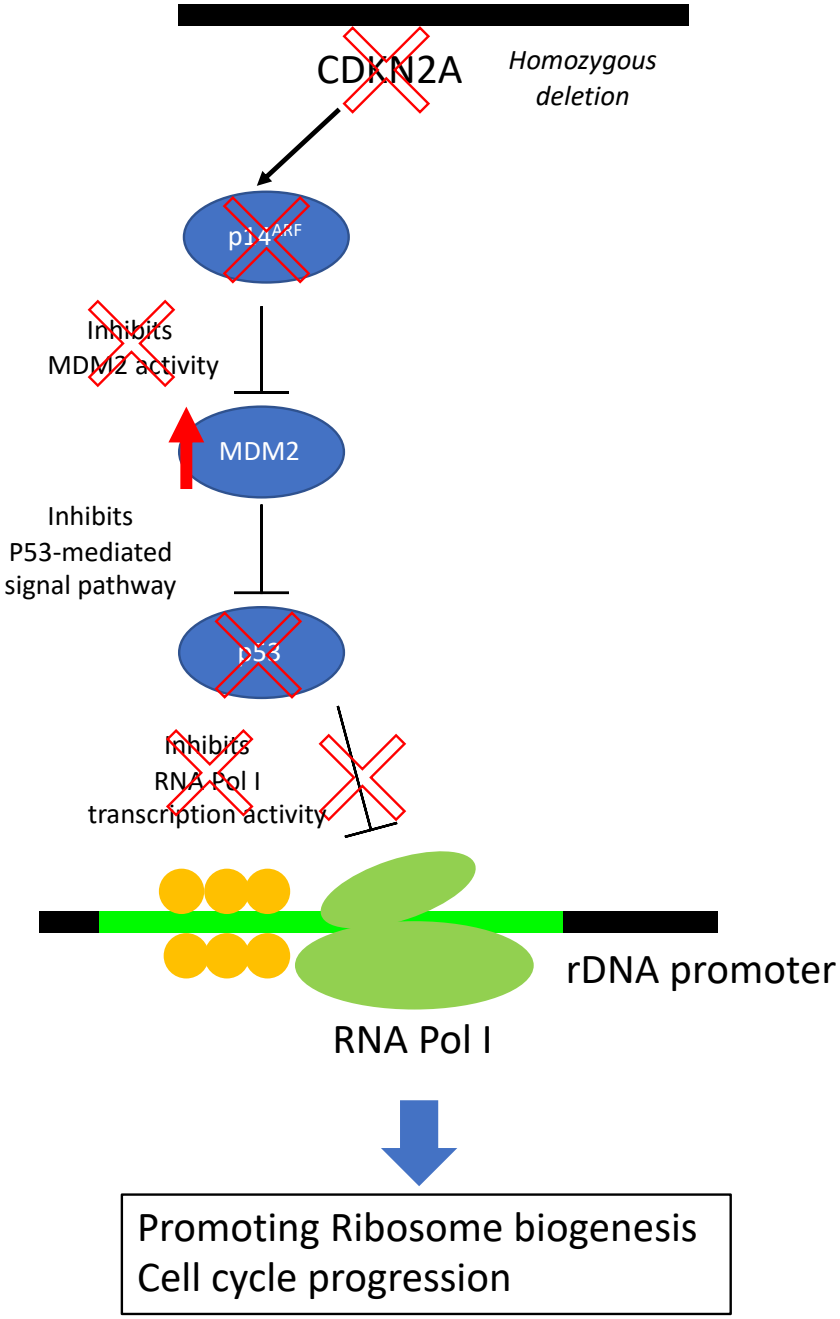

Figure 6.2 Schematic of overexpressed MDM2-mediated mechanism in OS
The predicted overexpressed MDM2-mediated mechanism in MDM2 amplified OS cell line (SJSA-1). SJSA-1, is reported to express wild type p53 and overexpress MDM2, due to a homozygous deletion of the *CDKN2A* gene, which encodes the MDM2-regulator $p14^{ARF}$. The absence of $p14^{ARF}$ promotes MDM2 activity which in turn suppresses the function of wild type p53. Wild type p53 is a negative regulator of RNA Pol I transcription and thus ribosome biogenesis, so overexpression of MDM2 would mediate an increase in RNA Pol I transcription by reducing p53 abundance.

iii) Up-regulation of ribosome biogenesis by inhibition of RB1 (Figure 6.3). The canonical function of RB1 is to control cell cycle progression via inhibitory binding to E2F, which is regulated by phosphorylation of RB1 (Giacinti and Giordano, 2006) (Section 1.1.1). Similar to p53, RB1 suppresses ribosome biogenesis by disrupting the interaction between UBF and SL-1, thus inhibiting RNA Polymerase I transcription (Hannan et al., 2000). This means that RB1 could alter cell proliferation by either regulating cell cycle progression via E2F or ribosome biogenesis via the UBF/SL-1 interaction. In cancers, the function of RB1 is typically inactivated by a genetic mutation or altered phosphorylation (Paternot et al., 2010, Knudsen and Knudsen, 2008). In OS, overexpression of CDK4, which is a RB1 inhibitor, occurs in 8% of patients and correlates with disease progression and poor response to therapeutic treatment (Zhou et al., 2018, Wei et al., 1999). Typically in OS the overexpression of CDK4 is a consequence of the absence of its regulator, $p16^{INK4A}$, due to homozygous deletion of the *CDKN2A* gene (Benassi et al., 1999). In all the ATCC OS cell lines, the homozygous deletion of *CDKN2A* gene has been reported (Ottaviano et al., 2010). The absence of this gene could lead to overexpression of CDK4 and inactivation of RB1 in OS (Nielsen et al., 1998, Zhou et al., 2018, Levine and Fleischli, 2000). Inactivated RB1 can mediate malignant transformation via promoting E2F1-mediated gene expression, while loss of RB1 expression could induce the same result by dysregulating cell cycle progression (Herschkowitz et al., 2008, Dunn et al., 1988, Giacinti and Giordano, 2006). Taken all together, the low or undetectable abundance of RB1 in U-2-OS, SJSA-1 and four of the KOS cell lines could promote OS cell growth and proliferation through increasing RNA Pol I transcription activity and cell cycle progression by E2F1-mediated gene expression. (Figure 3.4, Appendix Figure A.4 and Figure 6.3). Therefore, up-regulation of RNA

Polymerase I transcription and ribosome biogenesis by low levels of RB1 protein expression may regulate OS cell proliferation.

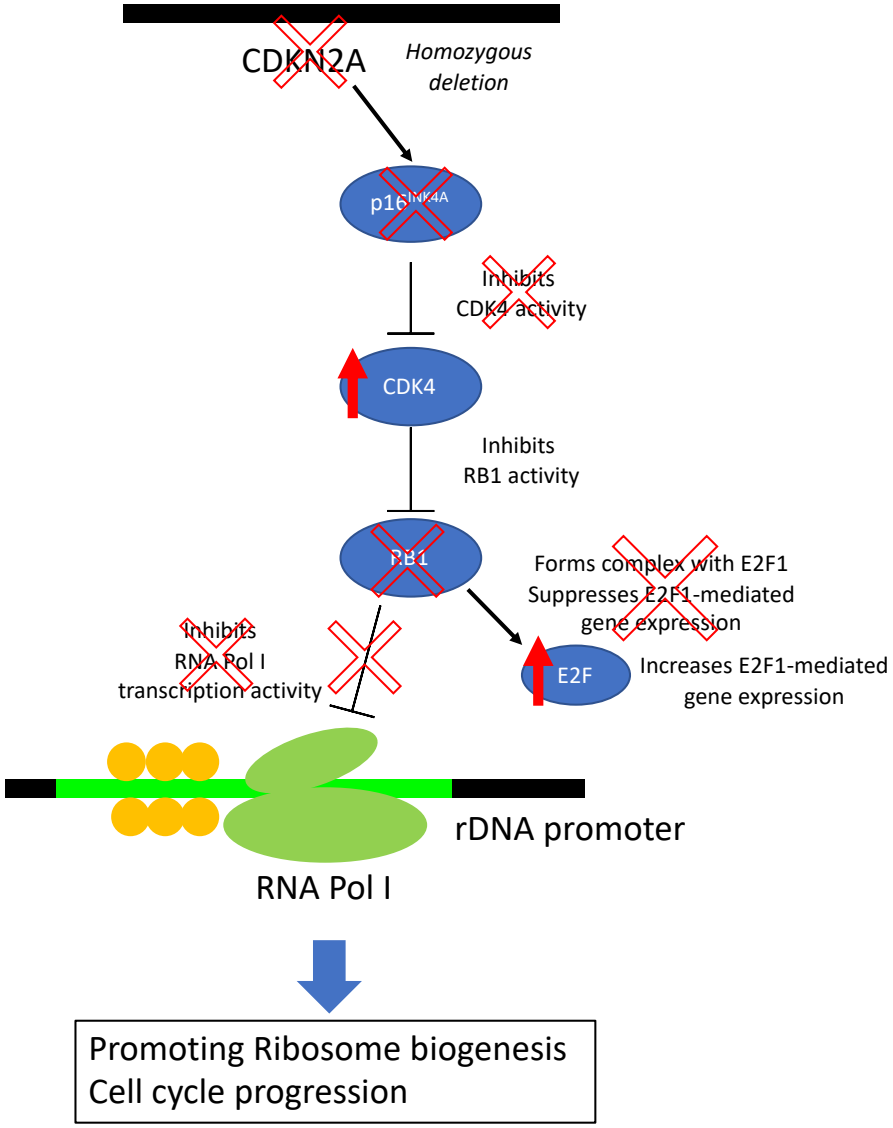

Figure 6.3 Schematic diagram of down-regulated RB1-mediated mechanism in OS
The homozygous deletion of the *CDKN2A* gene, which encodes the inhibitor of CDK4, $p16^{INK4A}$, results in the absence of $p16^{INK4A}$, thus increases CDK4 activity and consequently reduces RB1 activity by phosphorylation. The inactivated RB1 releases transcription factor E2F1 and increases E2F1-mediated gene expression and cell cycle progression. In ribosome biogenesis, RB1 plays as an inhibitor of RNA Pol I transcription, thus inactivation of RB1 would increase RNA Pol I transcription activity.

Thus, these three mechanisms based on the expression of p53, MDM2, MYC and RB1 demonstrate how RNA Pol I transcription activity can be modulated thus impacting on ribosome biogenesis in OS. Furthermore, they support the idea of targeting RNA Pol I as a new effective therapeutic strategy for OS.

6.3 *In-vitro* anti-tumour effects of RNA Pol Ii on human OS cell lines

The aim of Chapter 4 was to investigate the effect of RNA Pol Ii (CX-5461 and PMR-116) on OS cell lines with respect to downstream processes such as cell viability, proliferation and cell cycle progression. Ideally in this system both drugs would reduce cell proliferation, which would indicate a potential benefit for the treatment of OS. We also determined if these drugs were hitting their primary target, rDNA transcription.

Cell viability and proliferation were measured using an MTT assay and IncuCyte® respectively, after 72 hours of drug treatment. The effects of these drugs on cell cycle progression were evaluated by BrdU and PI staining and the impact on rDNA transcription determined by qPCR. Both CX-5461 and PMR-116 demonstrated cytotoxicity and anti-proliferation effects in a dose dependent manner in all of the human OS cell lines tested, irrespective of p53 status. Furthermore, CX-5461 induced a G2 phase cell cycle arrest in 7 OS cell lines but only in 4 OS cell lines with PMR-116 treatment. Additionally, CX-5461 and PMR-116 effectively suppressed 47S pre-rRNA synthesis, the product of RNA polymerase I transcription, with similar tIC_{50} across all the OS cell lines, independent of p53 status.

CX-5461 and PMR-116 reduced both the number of viable cells and cell proliferation in all of the OS cell lines, predominantly via a G2 cell cycle arrest, which supports these drugs as effective anti-cancer agents. Specifically, in the MTT assay, both drugs exhibited cytotoxicity in all the OS cell lines with the p53 mutant cell lines being more sensitive compared to p53 wild type OS cell lines (Figure 4.2). Whereas the IncuCyte data, demonstrated that both drugs reduced cell proliferation, but the GIC_{50} did not correlate with p53 status (Figure 4.4). In addition, the IC_{50} and GIC_{50} for each cell line were not

similar with either drug. Overall, typically the GIC_{50} was lower than the IC_{50} for each cell line. This trend may be attributed to the different target or methodology of the assays used. The MTT assay is designed to measure mitochondrial metabolic activity as a surrogate for cell viability, whereas the IncuCyte measures cell confluence as a surrogate for cell proliferation (Single et al., 2015). Although mitochondrial activity and cell confluence are influenced by the number of viable cells, there are situations where they might not correlate (Niepel et al., 2017, Single et al., 2015, Huyck et al., 2012). One research paper testing the growth inhibitory effects of radiation revealed that mitochondrial activity can actually increase during cell death (Rai et al., 2018). Similar to radiation, the natural compound genistein exhibited a disconnect between the results of an MTT assay and a cell proliferation assay (Pagliacci et al., 1993). These two studies suggest that the MTT assay may underestimate the cytotoxicity of a chemotherapy on cells. Another considerable cause is the effects of RNA Pol Ii on OS cells. In the Li et al (2016) study RNA Pol I inhibition led to the anti-tumour effects on OS cells via autophagy and thy confirmed that CX-5461 induced morphological change compared to non-treated cells, which is a characteristic of autophagy. Autophagy would increase cell size and stopping cell proliferation and these could result in the underestimation in Cell proliferation using IncuCyte® (Miettinen and Björklund, 2015), as it was determined by the cell coverage area no the number of proliferating cells. However, measuring cell confluence have been reported as more suitable *in-vitro* viability assay in evaluating the toxicity of therapeutic compounds compared to estimating metabolic activity (Single et al., 2015). Therefore, the difference between the IC_{50} and GIC_{50} values for CX-5461 and PMR-116 may be due to the assays used, perhaps an underestimate of IC_{50} when using the MTT assay, which means the GIC_{50} values from the cell proliferation assay may be more reliable data. Therefore, based on these reasons, we could interpret that all OS cell

lines are more sensitive to CX-5461 than PMR-116 and the anti-proliferation effects of RNA Pol Ii does not correlate with p53 status.

Several studies using CX-5461 have reported cell cycle arrest depending on p53 status. In lymphoma cells expressing wild type p53, CX-5461 induced a sub-G1 cell cycle arrest, which is a feature of apoptotic cell death (Bywater et al., 2012). In contrast, CX-5461 induced a G2 phase cell cycle arrest in p53 mutant leukaemia cells (Quin et al., 2016, Negi and Brown, 2015). Based on these results, we predicted alterations in the cell cycle based on p53 status. In fact, this was not the case; although CX-5461 did induced a G2 phase cell cycle arrest, it was not dependent on p53 status (Figure 4.5). On the other hand, PMR-116 also induced a G2 cell cycle arrest but not in all the OS cells lines, it was only observed in two ATCC OS (HOS and U-2-OS) and two KOS (KOS-3 and KOS-7) cell lines. The differences in response of the OS cell lines to CX-5461 and PMR-116, as well as this not being dependent on p53 status may be due to the expression of other proteins. For example, the SJSA-1 cell line expresses elevated MDM2 protein mediated by *MDM2* amplification (Freedman and Levine, 1999, Hu et al., 2006). While SJSA-1 express wild type p53, elevated MDM2 may reduce p53 expression enough that it functionally resembles a p53 null cell line. In this case CX-5461 and PMR-116 could only mediate its effects via a p53 independent pathway, thus explaining the observed G2 cell cycle arrest.

CX-5461 and PMR-116, were designed as selective RNA Pol Ii. While the mechanism of action for CX-5461 has been reported to be mediated at the preinitiation complex (PIC) a comprehensive analysis of PMR-116 mechanism of action has not been performed. Our group has preliminary data suggesting, however, that PMR-116 also mediates its effects

at the level of the preinitiation complex (PIC) (Hannan, Hein, Pimera: personal communication). Consistent with the intended primary target of these drugs, both CX-5461 and PMR-116 effectively reduced rDNA transcription in a dose dependent manner in all the OS cell lines with a similar tIC_{50} after 1 hour of treatment (Figure 4.6). This is interesting as the anti-proliferation studies (Figure 4.4 E) demonstrated that the cells were more sensitive to CX-5461 than PMR-116, based on a lower GIC_{50}, (Figure 4.4 E). A recent study reported that CX-5461 can increase the stability of G-quadruplexes in DNA and induce DNA damage in breast cancer cell lines, which would be considered an off-target effect (Xu et al., 2017). There is also a study suggesting Topoisomerase II activity is dysregulated by CX-5461 (Bruno et al., 2020). These off-target activities may also contribute to the efficacy of CX-5461, which in these studies may not be mimicked by PMR-116 and this could explain the discrepancy between the GIC_{50}. Ideally a drug is very selective for its target, issues can arise when off-target effects occur including severe toxicity (Oronsky et al., 2016, Shoshan and Linder, 2008). Thus, the lower GIC_{50} of CX-5461 compared to PMR-116 determined using the cell proliferation assay maybe also the results of both its on- and off-target activities.

In this thesis, all the OS cell lines used were classified based on their *TP53* gene status, that is wild type, mutant or null. Of the two RNA Pol Ii, only CX-5461 increased G2 phase cell cycle in OS cell lines regardless of p53 status. However, further analysis and an increase in the number of OS cell lines, especially those that are p53 null, would be required to be definitive as to what differentiated these responses. Interestingly, as mentioned above, one study reported that CX-5461 induces autophagy and down-regulation of mTOR pathway in OS cell lines, however we did not evaluate this in our experiments. What we can consider, however, is that a concentration of 5 μM was used

in this study which according to our results would be almost 45-fold higher than the tIC_{50} (110 nM) and the GI_{50} (114 nM) we obtained for CX-5461 suggesting their results may have been influenced by cytotoxicity and the potential off-target DNA damage.

6.4 Therapeutic efficacy of RNA Pol Ii *in-vivo* tumour bearing mice model

The key discoveries described in Chapter 5 were that: (i) 143B-Luc and SJSA-1-Luc OS cell lines can be established as a human xenograft model in Rag 2 KO mice for the purpose of therapeutic studies; (ii) the maximum tolerated doses of the RNA Pol Ii, CX-5461 and PMR-116, in the Rag 2 KO mouse strain were determined; and (iii) CX-5461 had a significant and reproducible inhibitory effect against 143B-Luc (p53 mutant) and SJSA-1-Luc (p53 wild type) tumour growth.

The establishment of mouse models of OS, achieved through genetic engineering or allografts or human xenografts, have enabled us to understand the pathogenesis of OS and to assess new treatment strategies. (Uluçkan et al., 2015, Lauvrak et al., 2013). Human xenograft mouse models are considered to be superior to genetically engineered mice models (GEMM) and chemically induced mice models as they are reproducible and more relevant to human disease (Uluçkan et al., 2015, Dass et al., 2007). For example, by utilizing human cancer cells, the complexity of genetic and epigenetic changes can be reproduced and typically tumours in these models develop faster compared to GEMM making experiments feasible. However, human xenograft models cannot recapitulate all the disease features of OS, such as the cancer initiating events and interactions with the tumour microenvironment (Guijarro, 2014, Jacques et al., 2018). Additionally, as immunocompromised mice are required for human xenograft models to prevent graft rejection, the impact of the immune system on tumour growth is missing (Cekanova and

Rathore, 2014). Furthermore, any effect of novel anti-cancer drugs on immune cells cannot be determined.

A number of different immunocompromised mouse strains have been used for human cell xenograft experiments. Nude mice have a defect in the thymus impacting upon T cell maturation as a result of a FOXN1 gene mutation, although they do have functional B- and Natural Killer (NK) cells. Non-obese diabetic (NOD)-severe combined immunodeficiency gamma (NSG) mice have a deficiency in T, B and NK cells as a result of a loss-of-function mutation in the DNA-dependent protein kinase (PRKDC) and a null mutation in the interleukin 2 receptor gamma chain (IL2Rγ) (Shultz et al., 2005, Blunt et al., 1995, Cao et al., 1995). These differences in the immune cell repertoires can influence the ability of a tumour cell line to establish. For example, the OS cell line HOS failed to form solid tumours in nude mice (Luu et al., 2005), but exhibited 100% tumour development in NSG mice (Lauvrak et al., 2013). The immune deficient mouse strain used in these experiments, Rag 2 KO mice, have a deficiency in B and T lymphocyte maturation due to the absence of the recombination activating gene 2 (*Rag2*) which mediates the recombination of immunoglobulin (Ig) and the T cell receptor (TCR) (Shinkai, 1992). This strain has what is known as a severe combined immune deficient (SCID) phenotype as it has a deficiency in B and T cells, but normal NK cells, and is suitable for xenograft experiments (Shinkai et al., 1992). Sarcoma cell lines have been reported to establish as a xenograft model well in this strain, hence it was used in these experiments (Shinkai, 1992, Nanni et al., 2010).

The results obtained with the OS cell lines purchased from the ATCC were consistent with the published literature in that 143B, MNNG-HOS and SJSA-1 were all highly

tumorigenic while Saos-2 and HOS were not (Dass et al., 2007, Luu et al., 2005, Hoffman-Luca et al., 2015). In contrast, 3 of 5 OS cell lines obtained from South Korea (KOS) that were tested in *Rag 2* KO mice lacked tumorigenic capacity (Table 5.1). The Investigator from whom these cell lines were obtained had not previously attempted to inject them into mice (Prof. Hansoo Kim, personal communication). Previous studies revealed that the success rate of tumour development in mice can be influenced by: i) the cancer cell line growth rate; ii) the number of implanted cancer cells; and iii) the ability of the cancer cell to adapt to the host microenvironment (Jung et al., 2018). The KOS cell lines demonstrated relatively slow growth rates *in-vitro* compared to the ATCC OS cell lines (Table 3.1), potentially due to the number of passages that the cell lines have undergone prior to being obtained by us, with a higher number of passages selecting for more rapidly growing cells (Hughes et al., 2007). However, the lack of tumorigenicity could equally be due to their p53 status. Western blotting indicated that 4/5 KOS cell lines were p53 wild type and the 5th cell line, KOS-7, was p53 null (Figure 3.1). The p53 wild type OS cell lines had extended doubling times (30 ± 3.9 hours) compared to the p53 mutant OS cell lines (14 ± 1.7 hours) thus consistent with the function of p53 as a cell-cycle regulator. In agreement with the suggestion that enhanced cell growth rate increases tumorigenic capacity, 2/3 p53 mutant OS cell lines were tumorigenic, whereas, only 1/4 p53 wild type OS cell lines formed tumours in *Rag2* KO mice (Table 5.1). In contrast, the p53 null KOS-7 cell line demonstrated an *in-vitro* growth rate in between that of the p53 mutant and p53 wild type cell lines but also lacked tumorigenic capacity in *Rag2* KO mice under the conditions tested (Table 5.1). Although only one p53 null type OS cell line was tested, this result suggests that an absence of p53 in OS does not mediate the same effect on cell proliferative and tumorigenic potential as the expression of mutant p53.

The finding that cancer cells, in comparison to normal cells, have elevated RNA Pol I transcription rates and ribosome biogenesis to support their rapid growth rates (Drygin et al., 2010), motivated the development of RNA Pol Ii. CX-5461 was the first inhibitor of RNA Pol I transcription developed, showing a 200-fold selectivity for RNA Pol I in comparison to RNA Pol II in cancer cells, and 24% oral bioavailability demonstrated in mice (Haddach et al., 2012). However, adverse effects, including anaemia, skin photosensitivity and palmar-plantar erythrodysesthesia (also known as hand-foot syndrome) were reported in the Phase I study in heavily pre-treated patients with advanced hematologic malignancies (Khot et al., 2019). Furthermore, toxicity studies in CX-5461 treated mice revealed the presence of DNA damage markers, gamma histone 2AX (γ-H2AX) and G-quadruplex stabilization (Haddach et al., 2012, Drygin et al., 2011, El Hassouni et al., 2019, Xu et al., 2017). While the induction of DNA damage would be detrimental to cancer patients what the clinical trial with CX-5461 did demonstrate was that the concept of targeting RNA Polymerase I transcription can provide a therapeutic window.

PMR-116 was developed as a second-generation RNA Pol Ii to improve on the drug like properties of CX-5461. Similar to CX-5461, PMR-116 demonstrated a high selectivity for RNA Pol I compared to RNA Pol II. PMR-116 showed improved pharmaceutical properties, such as a higher bioavailability (82%), penetration of the blood brain barrier (BBB) and low plasma protein binding (Hannan, Hein, Pimera: unpublished data). C57BL/6 mice were substantially more tolerant of PMR116 than *Rag2* KO mice with a maximum tolerated dose of 300 mg/kg once weekly compared to 80mg/kg twice weekly in the *Rag2* KO mice. The MTD dose of CX-5461 was the same in both mouse strains.

the Rag2 KO mice appear to have an enhanced sensitivity to the toxic effects of both CX-5461 and PMR-116 in comparison to other mouse strains for an unknown reason. Routine health screening on this mouse strain have not detected any abnormalities. In C57BL/6 mouse models of acute myeloid leukaemia and B-cell lymphoma, PMR-116 was more effective than CX-5461 when administered at the MTD for this strain (Hannan, Hein, Pimera: unpublished data), thus demonstrating the significant anti-cancer potential of this drug despite the findings in the *Rag2* KO OS studies.

From the *in-vitro* results described in Chapter 4, we expected to observe an inhibition of 143B-Luc ($p53^{mut}$) and SJSA-1-Luc ($p53^{wt}$) tumour growth in *Rag2* KO mice treated with CX-5461 and PMR-116. These expectations were met with CX-5461, as significant reductions in 143B-Luc ($p53^{mut}$) and SJSA-1-Luc ($p53^{wt}$) tumour growth were observed. CX-5461 has been previously reported to inhibit the growth of the p53 wild type, U-2-OS, tumours in nude mice (Li et al., 2016), thus, our results with SJSA-1 ($p53^{wt}$) tumours are consistent with this previous study. In addition, we demonstrated that tumours of the faster growing 143B ($p53^{mut}$) cell line were also sensitive to CX-5461 treatment. In contrast, PMR-116 was not effective in reducing 143B-Luc ($p53^{mut}$) tumour growth and, given the ongoing problems with toxicity in the *Rag2* KO mice manifesting as weight loss, testing of this drug was not continued. In a prior experiment with 143B-Luc in *Rag2* KO mice (data not shown) during which a higher dose of PMR-116 was administered (120 mg/kg thrice weekly), a significant anti-tumour effect was observed, however, again the mice were culled due to an unacceptable level of toxicity. These toxicity issues appear to be specific to the *Rag2* KO mouse strain as other researchers within the same institution have administered higher doses of the same preparation of PMR-116 to C57BL/6 mice without significant toxicity. Future experiments using this drug should be performed in

human OS models established in other immunodeficient mouse strains. Additionally, PMR-116 could be tested against the murine OS cell lines K7M2 in BALB/c mice that have an intact immune system.

The use of digital callipers for the measurement of tumour volume is broadly accepted as the quantitative method for monitoring tumour progress (Faustino-Rocha et al., 2013), however, it measures the tumour in only two dimensions (width and length) and includes all cells within the tumour, such as dead or non-cancerous cells (eg: stromal cells, immune cells and interstitial fluid) (Girit et al., 2008). In contrast, bioluminescence imaging detects the signal emitted from only viable transduced cancer cells (Zinn et al., 2008, Kim et al., 2015). For these reasons, we anticipated that the bioluminescent imaging would yield the most accurate results, however, this was not the case. At the conclusion of Experiment 1 using the 143B-Luc tumours, the average tumour volumes obtained with digital callipers and BLI were compared. The vehicle-treated group exhibited the lowest BLI despite having the largest tumours measured via callipers (Figure 5.1 C-D). The weights of the excised tumours correlated significantly with the digital calliper measurements but not with the BLI results (Figure 5.2). The discrepancy is most likely due to the fact that the vehicle group had rapid hair regrowth in comparison to the drug treated groups and surface hair can reduce the bioluminescence signal from tumours, (Izumi et al., 2011, Izumi et al., 2017, Ahn, 2011). Hair growth occurs in follicles and undergoes three cycles termed anagen, catagen and telogen. Of these phases it is the anagen stage when rapid proliferation occurs to generate the hair fibre (Plikus and Chuong, 2008). As ribosome biogenesis and RNA Pol I transcription activity are increased in fast-growing cells (Laferté et al., 2006, Drygin et al., 2010), the hair follicles at anagen stage may be preferentially killed or arrested by CX-5461 thus reducing hair

production. RNA Pol Ii would, therefore, appear to slow hair growth thus the BLI signal impeding factors were not equal across the groups at the termination of the experiment. If hair growth was influencing the BLI results, shaving the mice before imaging may improve the consistency of the results but could prove difficult around the tumours. Another possible explanation for these results is that differences in the vascularity of the tumours may occur between vehicle and CX-5461 treated groups. This could be determined by staining the tumours for an endothelial marker, such as CD31, to assess the extent of angiogenesis between the control and treated tumours.

In conclusion, the growth of the 143B-Luc and SJSA-1-Luc tumours in *Rag2* KO mice were significantly inhibited by CX-5461, while the mice remained in good health. In contrast, the maximum tolerated dose of PMR-116 in the *Rag2* KO mice was not sufficient to elicit an anti-tumour effect. These data suggest that CX-5461 is a promising novel therapeutic strategy for OS treatment thus warranting studies to be conducted in patients suffering from this aggressive cancer.

6.5 Future directions

The results presented in this thesis suggest that the inhibition of RNA Pol I transcription activity by RNA Pol Ii may provide a new effective therapeutic strategy for human OS treatment. To advance these studies further, the following areas of investigation are suggested.

(i) Sarcomas are cancers that arise in cells of mesenchymal origin and are known to respond quite differently to treatments in comparison to other cancer types (Dancsok et al., 2017, Ordóñez et al., 2008). Given the cell cycle arrest studies and the relationship of

the drug response to p53 status in OS cell lines differed to published studies undertaken in lymphoma and leukaemia cell lines (Bywater et al., 2012, Negi and Brown, 2015), it is important to know what other molecular mechanisms are involved in the OS cellular response to the 2 RNA Pol Ii. Using co-immunoprecipitation and immunofluorescence staining, previous studies in lymphoma revealed that CX-5461 treatment led to the disruption of the nucleolus and cell cycle arrest via the p53-mediated nucleolar stress pathway, with increased association of the nucleolar stress pathway related factors, ribosomal proteins L5 (RPL5) and RPL11, to MDM2 (Quin et al., 2016, Bywater et al., 2012, Drygin et al., 2011). Consequently, it led to cell cycle arrest, senescence or cell cycle arrest depending on the system and severity of insult. Similar methods could be undertaken to elucidate the molecular responses in OS cells. Molecular markers of rDNA transcription (ETS, UBF, POLR1A or RRN3 etc) (Bywater et al., 2013, Drygin et al., 2010), or G2 phase cell cycle, (total and phosphorylated Chk1/2 or cyclin D1) would also be of interest (Bucher and Britten, 2008).

(ii) The therapeutic effects of CX-5461 were demonstrated *in-vivo* using both p53 wild type and mutant OS tumour models (Figures 5.1 and 5.3). The tumours from these experiments have been excised and preserved thus should be examined for gross changes, such as decreased vascularisation, increased immune cell influx, and the extent of tumour necrosis. Additionally, changes at the cellular level such as the size of the nucleolus, evidence of proliferation, and the expression of particular proteins of interest identified in point (i) above could be undertaken using immunohistochemistry to investigate whether CX-5461 induces the same therapeutic effects *in-vivo*.

(iii) The *Rag2* KO mouse strain used in these experiments demonstrated significant sensitivity to PMR-116 in comparison to other mouse strains but comparable sensitivity to CX-5461. This heightened sensitivity to PMR-116 prevented a therapeutic dose from being administered in these studies. To adequately test this drug, the experiments with human OS cell lines could be repeated in NOD/SCID gamma mice which have not demonstrated intolerance to PMR-116 (Dr Kate Hannan, personal communication). Furthermore, as the immune system plays a significant role in both controlling and enhancing tumour growth, and drugs may impact upon these immune effects, it is important to test new anti-cancer drugs in an immune competent mouse model. The K7M2 OS cell line can be grown in wild type BALB/c mice, thus would provide a useful immune competent model for this purpose.

(iv) Due to the chemo-resistance of OS cells, high dose chemotherapy and combination chemotherapy are considered the most effective strategies for OS treatment (Bielack et al., 2015, Luetke et al., 2014). In this study, CX-5461 effectively suppressed rDNA transcription with a tIC50 < 800 nM in all OS cell lines and exhibited anti-tumour effects *in-vivo*. Combining RNA Pol Ii with standard chemotherapies may result in more pronounced therapeutic effects in OS patients and may also permit lower concentrations to be administered to try to reduce any short- or long-term complications of these treatments. This has been achieved with other drugs combinations with CX-5461 for other cancers such as prostate cancer, leukemia and breast cancer (Rebello et al., 2016, Negi and Brown, 2015, Xu et al., 2017).

(v) The five commercially available ATCC OS cell lines used have been the subject of many genetic studies. The mutational status of the four key proteins of interest in these

cell lines is well established and was, therefore, used as a reference for the western blotting analysis to predict their status in the five new KOS cell lines (Chapter 3). To confirm these predictions and to gain additional information on these cell lines, DNA sequencing should be undertaken. This is currently taking place as a collaborative project with paediatric oncology clinicians in Singapore who are performing an in-house Oncomine paediatric panel on the 10 OS cell lines. Preliminary results have shown that KOS cell lines 1, 2 and 3 are wild type *TP53* thus supporting our western blotting results. Additional analysis of the sequencing data will allow us to identify other altered genes in these OS cell lines that will be useful to evaluate the three possible pathways proposed from Chapter 3.

6.6 Conclusion

The aim of this thesis was to investigate the therapeutic potential of RNA Pol Ii as a new treatment for OS patients. As a first step, three possible pathways that may alter RNA Pol I transcription were proposed based on the analysis of 5 commercially available ATCC OS and 5 patient-derived KOS cell lines in Chapter 3. The effects of two RNA Pol Ii, CX-5461 and PMR-116, on these OS cell lines were evaluated *in vitro* in Chapter 4. Both drugs effectively inhibited their primary target, rDNA transcription, and exerted an anti-proliferative effect via G2 cell cycle arrest on the OS cell lines. The *in vivo* effects of RNA Pol Ii were determined using a xenograft model of OS in *Rag2* KO mice in Chapter 5. Although 80 mg/kg of PMR-116 twice-weekly did not reduce the tumour volume, CX-5461 exhibited significant tumour growth inhibitory effects on the human OS cell lines, 143B-Luc and SJSA-1-Luc, that are p53 mutant and p53 wild type, respectively. This research suggests that inhibition of RNA Pol I transcription is certainly worth pursuing as a new therapeutic weapon in the fight against OS.

References

AHN, B. C. 2011. Applications of molecular imaging in drug discovery and development process. *Curr Pharm Biotechnol,* 12**,** 459-68.

ALI, A. A., MARCUS, J. N., HARVEY, J. P., ROLL, R., HODGSON, C. P., WILDRICK, D. M., CHAKRABORTY, A. & BOMAN, B. M. 1993. RB1 protein in normal and malignant human colorectal tissue and colon cancer cell lines. *FASEB J,* 7**,** 931-7.

ANDERSON, P. M., MEYERS, P., KLEINERMAN, E., VENKATAKRISHNAN, K., HUGHES, D. P., HERZOG, C., HUH, W., SUTPHIN, R., VYAS, Y. M., SHEN, V., WARWICK, A., YEAGER, N., OLIVA, C., WANG, B., LIU, Y. & CHOU, A. 2014. Mifamurtide in metastatic and recurrent osteosarcoma: a patient access study with pharmacokinetic, pharmacodynamic, and safety assessments. *Pediatr Blood Cancer,* 61**,** 238-44.

ANDO, T., ICHIKAWA, J., OKAMOTO, A., TASAKA, K., NAKAO, A. & HAMADA, Y. 2005. Gemcitabine inhibits viability, growth, and metastasis of osteosarcoma cell lines. *J Orthop Res,* 23**,** 964-9.

BARTEL, F., TAUBERT, H. & HARRIS, L. C. 2002. Alternative and aberrant splicing of MDM2 mRNA in human cancer. *Cancer Cell,* 2**,** 9-15.

BAYANI, J., SELVARAJAH, S., MAIRE, G., VUKOVIC, B., AL-ROMAIH, K., ZIELENSKA, M. & SQUIRE, J. A. 2007. Genomic mechanisms and measurement of structural and numerical instability in cancer cells. *Semin Cancer Biol,* 17**,** 5-18.

BENASSI, M. S., MOLENDINI, L., GAMBERI, G., RAGAZZINI, P., SOLLAZZO, M. R., MERLI, M., ASP, J., MAGAGNOLI, G., BALLADELLI, A., BERTONI, F. & PICCI, P. 1999. Alteration of pRb/p16/cdk4 regulation in human osteosarcoma. *Int J Cancer,* 84**,** 489-93.

BERMAN, S. D., YUAN, T. L., MILLER, E. S., LEE, E. Y., CARON, A. & LEES, J. A. 2008. The retinoblastoma protein tumor suppressor is important for appropriate osteoblast differentiation and bone development. *Mol Cancer Res,* 6**,** 1440-51.

BIELACK, S. S., SMELAND, S., WHELAN, J. S., MARINA, N., JOVIC, G., HOOK, J. M., KRAILO, M. D., GEBHARDT, M., PÁPAI, Z., MEYER, J., NADEL, H., RANDALL, R. L., DEFFENBAUGH, C., NAGARAJAN, R., BRENNAN, B., LETSON, G. D., TEOT, L. A., GOORIN, A., BAUMHOER, D., KAGER, L., WERNER, M., LAU, C. C., SUNDBY HALL, K., GELDERBLOM, H., MEYERS, P., GORLICK, R., WINDHAGER, R., HELMKE, K., ERIKSSON, M., HOOGERBRUGGE, P. M., SCHOMBERG, P., TUNN, P. U., KÜHNE, T., JÜRGENS, H., VAN DEN BERG, H., BÖHLING, T., PICTON, S., RENARD, M., REICHARDT, P., GERSS, J., BUTTERFASS-BAHLOUL, T., MORRIS, C., HOGENDOORN, P. C., SEDDON, B., CALAMINUS, G., MICHELAGNOLI, M., DHOOGE, C., SYDES, M. R., BERNSTEIN, M. & INVESTIGATORS, E.-. 2015. Methotrexate, Doxorubicin, and Cisplatin (MAP) Plus Maintenance Pegylated Interferon Alfa-2b Versus MAP Alone in Patients With Resectable High-Grade Osteosarcoma and Good Histologic Response to Preoperative MAP: First Results of the EURAMOS-1 Good Response Randomized Controlled Trial. *J Clin Oncol,* 33**,** 2279-87.

BIERMANN, J. S., ADKINS, D. R., AGULNIK, M., BENJAMIN, R. S., BRIGMAN, B., BUTRYNSKI, J. E., CHEONG, D., CHOW, W., CURRY, W. T., FRASSICA, D. A., FRASSICA, F. J., HANDE, K. R., HORNICEK, F. J., JONES, R. L., MAYERSON, J., MCGARRY, S. V., MCGRATH, B., MORRIS, C. D., O'DONNELL, R. J., RANDALL, R. L., SANTANA, V. M., SATCHER, R. L., SIEGEL, H. J., VON MEHREN, M., BERGMAN, M. A., SUNDAR, H. & NATIONAL COMPLREHENSIVE CANCER, N. 2013. Bone cancer. *J Natl Compr Canc Netw,* 11**,** 688-723.

BLUNT, T., FINNIE, N. J., TACCIOLI, G. E., SMITH, G. C., DEMENGEOT, J., GOTTLIEB, T. M., MIZUTA, R., VARGHESE, A. J., ALT, F. W., JEGGO, P. A. & JACKSON, S. P. 1995. Defective DNA-dependent protein kinase activity is linked to V(D)J recombination and DNA repair defects associated with the murine scid mutation. *Cell,* 80**,** 813-23.

BOISVERT, F. M., VAN KONINGSBRUGGEN, S., NAVASCUÉS, J. & LAMOND, A. I. 2007. The multifunctional nucleolus. *Nat Rev Mol Cell Biol,* 8**,** 574-85.

BRUNO, P. M., LU, M., DENNIS, K. A., INAM, H., MOORE, C. J., SHEEHE, J., ELLEDGE, S. J., HEMANN, M. T. & PRITCHARD, J. R. 2020. The primary mechanism of cytotoxicity of the chemotherapeutic agent CX-5461 is topoisomerase II poisoning. *Proc Natl Acad Sci U S A,* 117**,** 4053-4060.

BUCHER, N. & BRITTEN, C. D. 2008. G2 checkpoint abrogation and checkpoint kinase-1 targeting in the treatment of cancer. *Br J Cancer,* 98**,** 523-8.

BURGER, K., MUHL, B., HARASIM, T., ROHRMOSER, M., MALAMOUSSI, A., ORBAN, M., KELLNER, M., GRUBER-EBER, A., KREMMER, E., HOLZEL, M. & EICK, D. 2010. Chemotherapeutic drugs inhibit ribosome biogenesis at various levels. *J Biol Chem,* 285**,** 12416-25.

BYWATER, M. J., PEARSON, R. B., MCARTHUR, G. A. & HANNAN, R. D. 2013. Dysregulation of the basal RNA polymerase transcription apparatus in cancer. *Nat Rev Cancer,* 13**,** 299-314.

BYWATER, M. J., POORTINGA, G., SANIJ, E., HEIN, N., PECK, A., CULLINANE, C., WALL, M., CLUSE, L., DRYGIN, D., ANDERES, K., HUSER, N., PROFFITT, C., BLIESATH, J., HADDACH, M., SCHWAEBE, M. K., RYCKMAN, D. M., RICE, W. G., SCHMITT, C., LOWE, S. W., JOHNSTONE, R. W., PEARSON, R. B., MCARTHUR, G. A. & HANNAN, R. D. 2012. Inhibition of RNA polymerase I as a therapeutic strategy to promote cancer-specific activation of p53. *Cancer Cell,* 22**,** 51-65.

CAO, X., SHORES, E. W., HU-LI, J., ANVER, M. R., KELSALL, B. L., RUSSELL, S. M., DRAGO, J., NOGUCHI, M., GRINBERG, A. & BLOOM, E. T. 1995. Defective lymphoid development in mice lacking expression of the common cytokine receptor gamma chain. *Immunity,* 2**,** 223-38.

CARRLE, D. & BIELACK, S. 2009. Osteosarcoma lung metastases detection and principles of multimodal therapy. *Cancer Treat Res,* 152**,** 165-84.

CEKANOVA, M. & RATHORE, K. 2014. Animal models and therapeutic molecular targets of cancer: utility and limitations. *Drug Des Devel Ther,* 8**,** 1911-21.

CHAN, J. C., HANNAN, K. M., RIDDELL, K., NG, P. Y., PECK, A., LEE, R. S., HUNG, S., ASTLE, M. V., BYWATER, M., WALL, M., POORTINGA, G., JASTRZEBSKI, K., SHEPPARD, K. E., HEMMINGS, B. A., HALL, M. N., JOHNSTONE, R. W., MCARTHUR, G. A., HANNAN, R. D. & PEARSON, R. B. 2011. AKT promotes rRNA synthesis and cooperates with c-MYC to stimulate ribosome biogenesis in cancer. *Sci Signal,* 4**,** ra56.

CHEN, D., ZHAO, Z., HUANG, Z., CHEN, D. C., ZHU, X. X., WANG, Y. Z., YAN, Y. W., TANG, S., MADHAVAN, S., NI, W., HUANG, Z. P., LI, W., JI, W., SHEN, H., LIN, S. & JIANG, Y. Z. 2018. Super enhancer inhibitors suppress MYC driven transcriptional amplification and tumor progression in osteosarcoma. *Bone Res,* 6**,** 11.

CHEN, X., BAHRAMI, A., PAPPO, A., EASTON, J., DALTON, J., HEDLUND, E., ELLISON, D., SHURTLEFF, S., WU, G., WEI, L., PARKER, M., RUSCH, M., NAGAHAWATTE, P., WU, J., MAO, S., BOGGS, K., MULDER, H., YERGEAU, D., LU, C., DING, L., EDMONSON, M., QU, C., WANG, J., LI, Y., NAVID, F., DAW, N. C., MARDIS, E. R., WILSON, R. K., DOWNING, J. R., ZHANG, J., DYER, M. A. & ST. JUDE CHILDREN'S RESEARCH HOSPITAL-WASHINGTON UNIVERSITY PEDIATRIC CANCER GENOME, P. 2014. Recurrent somatic structural variations contribute to tumorigenesis in pediatric osteosarcoma. *Cell Rep,* 7**,** 104-12.

CHEN, Z., GUO, J., ZHANG, K. & GUO, Y. 2016. TP53 Mutations and Survival in Osteosarcoma Patients: A Meta-Analysis of Published Data. *Dis Markers,* 2016**,** 4639575.

CHOU, A. J., KLEINERMAN, E. S., KRAILO, M. D., CHEN, Z., BETCHER, D. L., HEALEY, J. H., CONRAD, E. U., NIEDER, M. L., WEINER, M. A., WELLS, R. J., WOMER, R. B., MEYERS, P. A. & GROUP, C. S. O. 2009. Addition of muramyl tripeptide to chemotherapy for patients with newly diagnosed metastatic osteosarcoma: a report from the Children's Oncology Group. *Cancer,* 115**,** 5339-48.

CIERNIK, I. F., NIEMIERKO, A., HARMON, D. C., KOBAYASHI, W., CHEN, Y. L., YOCK, T. I., EBB, D. H., CHOY, E., RASKIN, K. A., LIEBSCH, N., HORNICEK, F. J. & DELANEY, T. F. 2011. Proton-based radiotherapy for unresectable or incompletely resected osteosarcoma. *Cancer,* 117**,** 4522-30.

COLIS, L., ERNST, G., SANDERS, S., LIU, H., SIRAJUDDIN, P., PELTONEN, K., DEPASQUALE, M., BARROW, J. C. & LAIHO, M. 2014a. Design, synthesis, and structure-activity relationships of pyridoquinazolinecarboxamides as RNA polymerase I inhibitors. *J Med Chem,* 57**,** 4950-61.

COLIS, L., PELTONEN, K., SIRAJUDDIN, P., LIU, H., SANDERS, S., ERNST, G., BARROW, J. C. & LAIHO, M. 2014b. DNA intercalator BMH-21 inhibits RNA polymerase I independent of DNA damage response. *Oncotarget,* 5**,** 4361-9.

DAI, X., MA, W., HE, X. & JHA, R. K. 2011. Review of therapeutic strategies for osteosarcoma, chondrosarcoma, and Ewing's sarcoma. *Med Sci Monit,* 17**,** RA177-190.

DANCSOK, A. R., ASLEH-ABURAYA, K. & NIELSEN, T. O. 2017. Advances in sarcoma diagnostics and treatment. *Oncotarget,* 8**,** 7068-7093.

DASARI, S. & TCHOUNWOU, P. B. 2014. Cisplatin in cancer therapy: molecular mechanisms of action. *Eur J Pharmacol,* 740**,** 364-78.

DASS, C. R., EK, E. T. & CHOONG, P. F. 2007. Human xenograft osteosarcoma models with spontaneous metastasis in mice: clinical relevance and applicability for drug testing. *J Cancer Res Clin Oncol,* 133**,** 193-8.

DELANEY, T. F., PARK, L., GOLDBERG, S. I., HUG, E. B., LIEBSCH, N. J., MUNZENRIDER, J. E. & SUIT, H. D. 2005. Radiotherapy for local control of osteosarcoma. *Int J Radiat Oncol Biol Phys,* 61**,** 492-8.

DENAIS, C. & LAMMERDING, J. 2014. Nuclear mechanics in cancer. *Adv Exp Med Biol,* 773**,** 435-70.

DENU, R. A., NEMCEK, S., BLOOM, D. D., GOODRICH, A. D., KIM, J., MOSHER, D. F. & HEMATTI, P. 2016. Fibroblasts and Mesenchymal Stromal/Stem Cells Are Phenotypically Indistinguishable. *Acta Haematol,* 136**,** 85-97.

DERENZINI, M., MONTANARO, L. & TRERE, D. 2009. What the nucleolus says to a tumour pathologist. *Histopathology,* 54**,** 753-62.

DRYGIN, D., LIN, A., BLIESATH, J., HO, C. B., O'BRIEN, S. E., PROFFITT, C., OMORI, M., HADDACH, M., SCHWAEBE, M. K., SIDDIQUI-JAIN, A., STREINER, N., QUIN, J. E., SANIJ, E., BYWATER, M. J., HANNAN, R. D., RYCKMAN, D., ANDERES, K. & RICE, W. G. 2011. Targeting RNA polymerase I with an oral small molecule CX-5461 inhibits ribosomal RNA synthesis and solid tumor growth. *Cancer Res,* 71**,** 1418-30.

DRYGIN, D., RICE, W. G. & GRUMMT, I. 2010. The RNA polymerase I transcription machinery: an emerging target for the treatment of cancer. *Annu Rev Pharmacol Toxicol,* 50**,** 131-56.

DUNN, J. M., PHILLIPS, R. A., BECKER, A. J. & GALLIE, B. L. 1988. Identification of germline and somatic mutations affecting the retinoblastoma gene. *Science,* 241**,** 1797-800.

EBB, D., MEYERS, P., GRIER, H., BERNSTEIN, M., GORLICK, R., LIPSHULTZ, S. E., KRAILO, M., DEVIDAS, M., BARKAUSKAS, D. A., SIEGAL, G. P., FERGUSON, W. S., LETSON, G. D., MARCUS, K., GOORIN, A., BEARDSLEY, P. & MARINA, N. 2012. Phase II trial of trastuzumab in combination with cytotoxic chemotherapy for treatment of metastatic osteosarcoma with human epidermal growth factor receptor 2 overexpression: a report from the children's oncology group. *J Clin Oncol,* 30**,** 2545-51.

EL HASSOUNI, B., MANTINI, G., IMMORDINO, B., PETERS, G. J. & GIOVANNETTI, E. 2019. CX-5461 Inhibits Pancreatic Ductal Adenocarcinoma Cell Growth, Migration and Induces DNA Damage. *Molecules,* 24.

FAIVRE, S., KROEMER, G. & RAYMOND, E. 2006. Current development of mTOR inhibitors as anticancer agents. *Nat Rev Drug Discov,* 5**,** 671-88.

FAUSTINO-ROCHA, A., OLIVEIRA, P. A., PINHO-OLIVEIRA, J., TEIXEIRA-GUEDES, C., SOARES-MAIA, R., DA COSTA, R. G., COLAÇO, B., PIRES, M. J., COLAÇO, J., FERREIRA, R. & GINJA, M. 2013. Estimation of rat mammary tumor volume using caliper and ultrasonography measurements. *Lab Anim (NY),* 42**,** 217-24.

FENG, W., DEAN, D. C., HORNICEK, F. J., SPENTZOS, D., HOFFMAN, R. M., SHI, H. & DUAN, Z. 2020. Myc is a prognostic biomarker and potential therapeutic target in osteosarcoma. *Ther Adv Med Oncol,* 12**,** 1758835920922055.

FETHERSTON, J., WERNER, E. & PATTERSON, R. 1984. Processing of the external transcribed spacer of murine rRNA and site of action of actinomycin D. *Nucleic Acids Res,* 12**,** 7187-98.

FOGH, J., FOGH, J. M. & ORFEO, T. 1977. One hundred and twenty-seven cultured human tumor cell lines producing tumors in nude mice. *J Natl Cancer Inst,* 59**,** 221-6.

FREEDMAN, D. A. & LEVINE, A. J. 1999. Regulation of the p53 protein by the MDM2 oncoprotein--thirty-eighth G.H.A. Clowes Memorial Award Lecture. *Cancer Res,* 59**,** 1-7.

FU, X., XU, L., QI, L., TIAN, H., YI, D., YU, Y., LIU, S., LI, S., XU, Y. & WANG, C. 2017. BMH-21 inhibits viability and induces apoptosis by p53-dependent nucleolar stress responses in SKOV3 ovarian cancer cells. *Oncol Rep,* 38**,** 859-865.

GHOSHAL, K. & JACOB, S. T. 1997. An alternative molecular mechanism of action of 5-fluorouracil, a potent anticancer drug. *Biochem Pharmacol,* 53**,** 1569-75.

GIACINTI, C. & GIORDANO, A. 2006. RB and cell cycle progression. *Oncogene,* 25**,** 5220-7.

GIANFERANTE, D. M., MIRABELLO, L. & SAVAGE, S. A. 2017. Germline and somatic genetics of osteosarcoma - connecting aetiology, biology and therapy. *Nat Rev Endocrinol,* 13**,** 480-491.

GILL, J., AHLUWALIA, M. K., GELLER, D. & GORLICK, R. 2013. New targets and approaches in osteosarcoma. *Pharmacol Ther,* 137**,** 89-99.

GIRIT, I. C., JURE-KUNKEL, M. & MCINTYRE, K. W. 2008. A structured light-based system for scanning subcutaneous tumors in laboratory animals. *Comp Med,* 58**,** 264-70.

GOORIN, A. M., HARRIS, M. B., BERNSTEIN, M., FERGUSON, W., DEVIDAS, M., SIEGAL, G. P., GEBHARDT, M. C., SCHWARTZ, C. L., LINK, M. & GRIER, H. E. 2002. Phase II/III trial of etoposide and high-dose ifosfamide in newly diagnosed metastatic osteosarcoma: a pediatric oncology group trial. *J Clin Oncol,* 20**,** 426-33.

GRABOWSKI, P. 2009. Physiology of bone. *Endocr Dev,* 16**,** 32-48.

GRONTHOS, S., ZANNETTINO, A. C., GRAVES, S. E., OHTA, S., HAY, S. J. & SIMMONS, P. J. 1999. Differential cell surface expression of the STRO-1 and alkaline phosphatase antigens on discrete developmental stages in primary cultures of human bone cells. *J Bone Miner Res,* 14**,** 47-56.

GRUMMT, I. 2013. The nucleolus-guardian of cellular homeostasis and genome integrity. *Chromosoma,* 122**,** 487-97.

GUIJARRO, M. V. 2014. Osteosarcoma: mouse models, cell of origin and cancer stem cell. *Postdoc J,* 2**,** 19-30.

GUREL, B., IWATA, T., KOH, C. M., JENKINS, R. B., LAN, F., VAN DANG, C., HICKS, J. L., MORGAN, J., CORNISH, T. C., SUTCLIFFE, S., ISAACS, W. B., LUO, J. & DE MARZO, A. M. 2008. Nuclear MYC protein overexpression is an early alteration in human prostate carcinogenesis. *Mod Pathol,* 21**,** 1156-67.

HADDACH, M., SCHWAEBE, M. K., MICHAUX, J., NAGASAWA, J., O'BRIEN, S. E., WHITTEN, J. P., PIERRE, F., KERDONCUFF, P., DARJANIA, L., STANSFIELD, R., DRYGIN, D., ANDERES, K., PROFFITT, C., BLIESATH, J., SIDDIQUI-JAIN, A., OMORI, M., HUSER, N., RICE, W. G. & RYCKMAN, D. M. 2012. Discovery of CX-5461, the First Direct and Selective Inhibitor of RNA Polymerase I, for Cancer Therapeutics. *ACS Med Chem Lett,* 3**,** 602-6.

HAN, G., WANG, Y. & BI, W. 2012. C-Myc overexpression promotes osteosarcoma cell invasion via activation of MEK-ERK pathway. *Oncol Res,* 20**,** 149-56.

HANAHAN, D. & WEINBERG, R. A. 2011. Hallmarks of cancer: the next generation. *Cell,* 144**,** 646-74.

HANNAN, K. M. 2018. RNA polymerase I therapy: the second generation. *In:* HEIN, N. (ed.) *11th international conference on ribosome synthesis.* Orford, Quebec, Canada.

HANNAN, K. M., HANNAN, R. D., SMITH, S. D., JEFFERSON, L. S., LUN, M. & ROTHBLUM, L. I. 2000. Rb and p130 regulate RNA polymerase I transcription: Rb disrupts the interaction between UBF and SL-1. *Oncogene,* 19**,** 4988-99.

HARRIS, S. L. & LEVINE, A. J. 2005. The p53 pathway: positive and negative feedback loops. *Oncogene,* 24**,** 2899-908.

HE, H., NI, J. & HUANG, J. 2014. Molecular mechanisms of chemoresistance in osteosarcoma (Review). *Oncol Lett,* 7**,** 1352-1362.

HE, Y., DE CASTRO, L. F., SHIN, M. H., DUBOIS, W., YANG, H. H., JIANG, S., MISHRA, P. J., REN, L., GOU, H., LAL, A., KHANNA, C., MERLINO, G., LEE, M., ROBEY, P. G. & HUANG, J. 2015. p53 loss increases the osteogenic differentiation of bone marrow stromal cells. *Stem Cells,* 33**,** 1304-19.

HEIN, N., CAMERON, D. P., HANNAN, K. M., NGUYEN, N. N., FONG, C. Y., SORNKOM, J., WALL, M., PAVY, M., CULLINANE, C., DIESCH, J., DEVLIN, J. R., GEORGE, A. J., SANIJ, E., QUIN, J., POORTINGA, G., VERBRUGGE, I., BAKER, A., DRYGIN, D., HARRISON, S. J., ROZARIO, J. D., POWELL, J. A., PITSON, S. M., ZUBER, J., JOHNSTONE, R. W., DAWSON, M. A., GUTHRIDGE, M. A., WEI, A., MCARTHUR, G. A., PEARSON, R. B. & HANNAN, R. D. 2017. Inhibition of Pol I transcription treats murine and human AML by targeting the leukemia-initiating cell population. *Blood,* 129**,** 2882-2895.

HEIN, N., HANNAN, K. M., GEORGE, A. J., SANIJ, E. & HANNAN, R. D. 2013. The nucleolus: an emerging target for cancer therapy. *Trends Mol Med,* 19**,** 643-54.

HERSCHKOWITZ, J. I., HE, X., FAN, C. & PEROU, C. M. 2008. The functional loss of the retinoblastoma tumour suppressor is a common event in basal-like and luminal B breast carcinomas. *Breast Cancer Res,* 10**,** R75.

HOFFMAN-LUCA, C. G., YANG, C. Y., LU, J., ZIAZADEH, D., MCEACHERN, D., DEBUSSCHE, L. & WANG, S. 2015. Significant Differences in the Development of Acquired Resistance to the MDM2 Inhibitor SAR405838 between In Vitro and In Vivo Drug Treatment. *PLoS One,* 10**,** e0128807.

HOUGHTON, J. A., HOUGHTON, P. J. & WEBBER, B. L. 1982. Growth and characterization of childhood rhabdomyosarcomas as xenografts. *J Natl Cancer Inst,* 68**,** 437-43.

HOXHAJ, G. & MANNING, B. D. 2020. The PI3K-AKT network at the interface of oncogenic signalling and cancer metabolism. *Nat Rev Cancer,* 20**,** 74-88.

HU, B., GILKES, D. M., FAROOQI, B., SEBTI, S. M. & CHEN, J. 2006. MDMX overexpression prevents p53 activation by the MDM2 inhibitor Nutlin. *J Biol Chem,* 281**,** 33030-5.

HUGHES, P., MARSHALL, D., REID, Y., PARKES, H. & GELBER, C. 2007. The costs of using unauthenticated, over-passaged cell lines: how much more data do we need? *Biotechniques,* 43**,** 575, 577-8, 581-2 passim.

HUYCK, L., AMPE, C. & VAN TROYS, M. 2012. The XTT cell proliferation assay applied to cell layers embedded in three-dimensional matrix. *Assay Drug Dev Technol,* 10**,** 382-92.

INOUE, R., ASKER, C., KLANGBY, U., PISA, P. & WIMAN, K. G. 1999. Induction of the human ARF protein by serum starvation. *Anticancer Res,* 19**,** 2939-43.

IZUMI, H., ISHIMOTO, T., YAMAMOTO, H. & MORI, H. 2017. Application of hairless mouse strain to bioluminescence imaging of Arc expression in mouse brain. *BMC Neurosci,* 18**,** 18.

IZUMI, H., ISHIMOTO, T., YAMAMOTO, H., NISHIJO, H. & MORI, H. 2011. Bioluminescence imaging of Arc expression enables detection of activity-dependent and plastic changes in the visual cortex of adult mice. *Brain Struct Funct,* 216**,** 91-104.

JACQUES, C., RENEMA, N., LEZOT, F., ORY, B., WALKLEY, C. R., GRIGORIADIS, A. E. & HEYMANN, D. 2018. Small animal models for the study of bone sarcoma pathogenesis:characteristics, therapeutic interests and limitations. *J Bone Oncol,* 12**,** 7-13.

JACUS, M. O., DARYANI, V. M., HARSTEAD, K. E., PATEL, Y. T., THROM, S. L. & STEWART, C. F. 2016. Pharmacokinetic Properties of Anticancer Agents for the Treatment of Central Nervous System Tumors: Update of the Literature. *Clin Pharmacokinet,* 55**,** 297-311.

JAFFE, N. 2009. Osteosarcoma: review of the past, impact on the future. The American experience. *Cancer Treat Res,* 152**,** 239-62.

JAFFE, N., FREI, E., 3RD, TRAGGIS, D. & BISHOP, Y. 1974. Adjuvant methotrexate and citrovorum-factor treatment of osteogenic sarcoma. *N Engl J Med,* 291**,** 994-7.

JANEWAY, K. A. & GRIER, H. E. 2010. Sequelae of osteosarcoma medical therapy: a review of rare acute toxicities and late effects. *Lancet Oncol,* 11**,** 670-8.

JANKU, F., YAP, T. A. & MERIC-BERNSTAM, F. 2018. Targeting the PI3K pathway in cancer: are we making headway? *Nat Rev Clin Oncol,* 15**,** 273-291.

JIMMY, R., STERN, C., LISY, K. & WHITE, S. 2017. Effectiveness of mifamurtide in addition to standard chemotherapy for high-grade osteosarcoma: a systematic review. *JBI Database System Rev Implement Rep,* 15**,** 2113-2152.

JONES, S., ZHANG, X., PARSONS, D. W., LIN, J. C., LEARY, R. J., ANGENENDT, P., MANKOO, P., CARTER, H., KAMIYAMA, H., JIMENO, A., HONG, S. M., FU, B., LIN, M. T., CALHOUN, E. S., KAMIYAMA, M., WALTER, K., NIKOLSKAYA, T., NIKOLSKY, Y., HARTIGAN, J., SMITH, D. R., HIDALGO, M., LEACH, S. D., KLEIN, A. P., JAFFEE, E. M., GOGGINS, M., MAITRA, A., IACOBUZIO-DONAHUE, C., ESHLEMAN, J. R., KERN, S. E., HRUBAN, R. H., KARCHIN, R., PAPADOPOULOS, N., PARMIGIANI, G., VOGELSTEIN, B., VELCULESCU, V. E. & KINZLER, K. W. 2008. Core signaling pathways in human pancreatic cancers revealed by global genomic analyses. *Science,* 321**,** 1801-6.

JORDAN, P. & CARMO-FONSECA, M. 1998a. Cisplatin inhibits synthesis of ribosomal RNA in vivo. *Nucleic Acids Res,* 26**,** 2831-6.

JORDAN, P. & CARMO-FONSECA, M. 1998b. Cisplatin inhibits synthesis of ribosomal RNA in vivo. *Nucleic Acids Research,* 26**,** 2831-2836.

JUNG, J., SEOL, H. S. & CHANG, S. 2018. The Generation and Application of Patient-Derived Xenograft Model for Cancer Research. *Cancer Res Treat,* 50**,** 1-10.

KANSARA, M., TENG, M. W., SMYTH, M. J. & THOMAS, D. M. 2014. Translational biology of osteosarcoma. *Nat Rev Cancer,* 14**,** 722-35.

KHOT, A., BRAJANOVSKI, N., CAMERON, D. P., HEIN, N., MACLACHLAN, K. H., SANIJ, E., LIM, J., SOONG, J., LINK, E., BLOMBERY, P., THOMPSON, E. R., FELLOWES, A., SHEPPARD, K. E., MCARTHUR, G. A., PEARSON, R. B., HANNAN, R. D., POORTINGA, G. & HARRISON, S. J. 2019. First-in-Human RNA Polymerase I Transcription Inhibitor CX-5461 in Patients with Advanced Hematologic Cancers: Results of a Phase I Dose-Escalation Study. *Cancer Discov,* 9**,** 1036-1049.

KIM H S, K. J. H., LEE M R, OH J H, LEE S H 2005. INTEGRIN $av_{ß}3$ IS INVOLVED IN CELL PROLIFERATION IN HUMAN OSTEOSARCOMA. *51st Annual Meeting of the Orthopaedic Research Society.* Washington, DC. 74.

KIM, J. E., KALIMUTHU, S. & AHN, B. C. 2015. In vivo cell tracking with bioluminescence imaging. *Nucl Med Mol Imaging,* 49**,** 3-10.

KLEINERMAN, E. S., JIA, S. F., GRIFFIN, J., SEIBEL, N. L., BENJAMIN, R. S. & JAFFE, N. 1992. Phase II study of liposomal muramyl tripeptide in osteosarcoma: the cytokine cascade and monocyte activation following administration. *J Clin Oncol,* 10**,** 1310-6.

KNUDSEN, E. S. & KNUDSEN, K. E. 2008. Tailoring to RB: tumour suppressor status and therapeutic response. *Nat Rev Cancer,* 8**,** 714-24.

LADANYI, M., CHA, C., LEWIS, R., JHANWAR, S. C., HUVOS, A. G. & HEALEY, J. H. 1993. MDM2 gene amplification in metastatic osteosarcoma. *Cancer Res,* 53**,** 16-8.

LAFERTÉ, A., FAVRY, E., SENTENAC, A., RIVA, M., CARLES, C. & CHÉDIN, S. 2006. The transcriptional activity of RNA polymerase I is a key determinant for the level of all ribosome components. *Genes Dev,* 20**,** 2030-40.

LAI, P. S., CHEAH, P. Y., KADAM, P., CHUA, C. L., LIE, D. K., LI, H. H., EU, K. W., SEOW-CHOEN, F. & LEE, A. S. 2006. Overexpression of RB1 transcript is significantly correlated with 13q14 allelic imbalance in colorectal carcinomas. *Int J Cancer,* 119**,** 1061-6.

LAMPLOT, J. D., DENDULURI, S., QIN, J., LI, R., LIU, X., ZHANG, H., CHEN, X., WANG, N., PRATT, A., SHUI, W., LUO, X., NAN, G., DENG, Z. L., LUO, J., HAYDON, R. C., HE, T. C. & LUU, H. H. 2013. The Current and Future Therapies for Human Osteosarcoma. *Curr Cancer Ther Rev,* 9**,** 55-77.

LAUVRAK, S. U., MUNTHE, E., KRESSE, S. H., STRATFORD, E. W., NAMLØS, H. M., MEZA-ZEPEDA, L. A. & MYKLEBOST, O. 2013. Functional characterisation of osteosarcoma cell lines and identification of mRNAs and miRNAs associated with aggressive cancer phenotypes. *Br J Cancer,* 109**,** 2228-36.

LEVINE, A. J. 1997. p53, the cellular gatekeeper for growth and division. *Cell,* 88**,** 323-31.

LEVINE, A. J. & OREN, M. 2009. The first 30 years of p53: growing ever more complex. *Nat Rev Cancer,* 9**,** 749-58.

LEVINE, R. A. & FLEISCHLI, M. A. 2000. Inactivation of p53 and retinoblastoma family pathways in canine osteosarcoma cell lines. *Vet Pathol,* 37**,** 54-61.

LI, L., LI, Y., ZHAO, J., FAN, S., WANG, L. & LI, X. 2016. CX-5461 induces autophagy and inhibits tumor growth via mammalian target of rapamycin-related signaling pathways in osteosarcoma. *Onco Targets Ther,* 9**,** 5985-5997.

LIAO, P., ZENG, S. X., ZHOU, X., CHEN, T., ZHOU, F., CAO, B., JUNG, J. H., DEL SAL, G., LUO, S. & LU, H. 2017. Mutant p53 Gains Its Function via c-Myc Activation upon CDK4 Phosphorylation at Serine 249 and Consequent PIN1 Binding. *Mol Cell,* 68**,** 1134-1146.e6.

LINDSEY, B. A., MARKEL, J. E. & KLEINERMAN, E. S. 2017. Osteosarcoma Overview. *Rheumatol Ther,* 4**,** 25-43.

LONARDO, F., UEDA, T., HUVOS, A. G., HEALEY, J. & LADANYI, M. 1997. p53 and MDM2 alterations in osteosarcomas: correlation with clinicopathologic features and proliferative rate. *Cancer,* 79**,** 1541-7.

LORENZ, S., BARØY, T., SUN, J., NOME, T., VODÁK, D., BRYNE, J. C., HÅKELIEN, A. M., FERNANDEZ-CUESTA, L., MÖHLENDICK, B., RIEDER, H., SZUHAI, K., ZAIKOVA, O., AHLQUIST, T. C., THOMASSEN, G. O., SKOTHEIM, R. I., LOTHE, R. A., TARPEY, P. S., CAMPBELL, P., FLANAGAN, A., MYKLEBOST, O. & MEZA-ZEPEDA, L. A. 2016. Unscrambling the genomic chaos of osteosarcoma reveals extensive transcript fusion, recurrent rearrangements and frequent novel TP53 aberrations. *Oncotarget,* 7**,** 5273-88.

LUETKE, A., MEYERS, P. A., LEWIS, I. & JUERGENS, H. 2014. Osteosarcoma treatment - where do we stand? A state of the art review. *Cancer Treat Rev,* 40**,** 523-32.

LUO, S., ZHAO, J., FOWDUR, M., WANG, K., JIANG, T. & HE, M. 2016. Highly expressed ribosomal protein L34 indicates poor prognosis in osteosarcoma and its knockdown suppresses osteosarcoma proliferation probably through translational control. *Sci Rep,* 6**,** 37690.

LUU, H. H., KANG, Q., PARK, J. K., SI, W., LUO, Q., JIANG, W., YIN, H., MONTAG, A. G., SIMON, M. A., PEABODY, T. D., HAYDON, R. C., RINKER-SCHAEFFER, C. W. & HE, T. C. 2005. An orthotopic model of human osteosarcoma growth and spontaneous pulmonary metastasis. *Clin Exp Metastasis,* 22**,** 319-29.

MARINA, N. M., SMELAND, S., BIELACK, S. S., BERNSTEIN, M., JOVIC, G., KRAILO, M. D., HOOK, J. M., ARNDT, C., VAN DEN BERG, H., BRENNAN, B., BRICHARD, B., BROWN, K. L. B., BUTTERFASS-BAHLOUL, T., CALAMINUS, G., DALDRUP-LINK, H. E., ERIKSSON, M., GEBHARDT, M. C., GELDERBLOM, H., GERSS, J., GOLDSBY, R., GOORIN, A., GORLICK, R., GRIER, H. E., HALE, J. P., HALL, K. S., HARDES, J., HAWKINS, D. S., HELMKE, K., HOGENDOORN, P. C. W., ISAKOFF, M. S., JANEWAY, K. A., JÜRGENS, H., KAGER, L., KÜHNE, T., LAU, C. C., LEAVEY, P. J., LESSNICK, S. L., MASCARENHAS, L., MEYERS, P. A., MOTTL, H., NATHRATH, M., PAPAI, Z., RANDALL, R. L., REICHARDT, P., RENARD, M., SAFWAT, A. A., SCHWARTZ, C. L., STEVENS, M. C. G., STRAUSS, S. J., TEOT, L., WERNER, M., SYDES, M. R. & WHELAN, J. S. 2016. Comparison of MAPIE versus MAP in patients with a poor response to preoperative chemotherapy for newly diagnosed high-grade osteosarcoma (EURAMOS-1): an open-label, international, randomised controlled trial. *Lancet Oncol,* 17**,** 1396-1408.

MARTIN, J. W., SQUIRE, J. A. & ZIELENSKA, M. 2012. The genetics of osteosarcoma. *Sarcoma,* 2012**,** 627254.

MCALLISTER, R. M., GARDNER, M. B., GREENE, A. E., BRADT, C., NICHOLS, W. W. & LANDING, B. H. 1971. Cultivation in vitro of cells derived from a human osteosarcoma. *Cancer,* 27**,** 397-402.

MEYERS, P. A., HEALEY, J. H., CHOU, A. J., WEXLER, L. H., MEROLA, P. R., MORRIS, C. D., LAQUAGLIA, M. P., KELLICK, M. G., ABRAMSON, S. J. & GORLICK, R. 2011. Addition of pamidronate to chemotherapy for the treatment of osteosarcoma. *Cancer,* 117**,** 1736-44.

MEYERS, P. A., SCHWARTZ, C. L., KRAILO, M., KLEINERMAN, E. S., BETCHER, D., BERNSTEIN, M. L., CONRAD, E., FERGUSON, W., GEBHARDT, M., GOORIN, A. M., HARRIS, M. B., HEALEY, J., HUVOS, A., LINK, M., MONTEBELLO, J., NADEL, H., NIEDER, M., SATO, J., SIEGAL, G., WEINER, M., WELLS, R., WOLD, L., WOMER, R. & GRIER, H. 2005. Osteosarcoma: a randomized, prospective

trial of the addition of ifosfamide and/or muramyl tripeptide to cisplatin, doxorubicin, and high-dose methotrexate. *J Clin Oncol,* 23**,** 2004-11.

MICHAEL, D. & OREN, M. 2003. The p53-Mdm2 module and the ubiquitin system. *Semin Cancer Biol,* 13**,** 49-58.

MIETTINEN, T. P. & BJÖRKLUND, M. 2015. Mevalonate Pathway Regulates Cell Size Homeostasis and Proteostasis through Autophagy. *Cell Rep,* 13**,** 2610-2620.

MILLER, C. W., ASLO, A., WON, A., TAN, M., LAMPKIN, B. & KOEFFLER, H. P. 1996. Alterations of the p53, Rb and MDM2 genes in osteosarcoma. *J Cancer Res Clin Oncol,* 122**,** 559-65.

MIRABELLO, L., TROISI, R. J. & SAVAGE, S. A. 2009. International osteosarcoma incidence patterns in children and adolescents, middle ages and elderly persons. *Int J Cancer,* 125**,** 229-34.

MOLL, U. M. & PETRENKO, O. 2003. The MDM2-p53 interaction. *Mol Cancer Res,* 1**,** 1001-8.

MONTANARO, L., MAZZINI, G., BARBIERI, S., VICI, M., NARDI-PANTOLI, A., GOVONI, M., DONATI, G., TRERE, D. & DERENZINI, M. 2007. Different effects of ribosome biogenesis inhibition on cell proliferation in retinoblastoma protein- and p53-deficient and proficient human osteosarcoma cell lines. *Cell Prolif,* 40**,** 532-49.

MORROW, J. J. & KHANNA, C. 2015. Osteosarcoma Genetics and Epigenetics: Emerging Biology and Candidate Therapies. *Crit Rev Oncog,* 20**,** 173-97.

MURRAY, J. L., KLEINERMAN, E. S., CUNNINGHAM, J. E., TATOM, J. R., ANDREJCIO, K., LEPE-ZUNIGA, J., LAMKI, L. M., ROSENBLUM, M. G., FROST, H. & GUTTERMAN, J. U. 1989. Phase I trial of liposomal muramyl tripeptide phosphatidylethanolamine in cancer patients. *J Clin Oncol,* 7**,** 1915-25.

MUTSAERS, A. J. & WALKLEY, C. R. 2014. Cells of origin in osteosarcoma: mesenchymal stem cells or osteoblast committed cells? *Bone,* 62**,** 56-63.

NANNI, P., NICOLETTI, G., LANDUZZI, L., CROCI, S., MURGO, A., PALLADINI, A., ANTOGNOLI, A., IANZANO, M. L., STIVANI, V., GROSSO, V., MAIRA, S. M., GARCÍA-ECHEVERRÍA, C., SCOTLANDI, K., DE GIOVANNI, C. & LOLLINI, P. L. 2010. High metastatic efficiency of human sarcoma cells in Rag2/gammac double knockout mice provides a powerful test system for antimetastatic targeted therapy. *Eur J Cancer,* 46**,** 659-68.

NEGI, S. S. & BROWN, P. 2015. rRNA synthesis inhibitor, CX-5461, activates ATM/ATR pathway in acute lymphoblastic leukemia, arrests cells in G2 phase and induces apoptosis. *Oncotarget,* 6**,** 18094-104.

NEVINS, J. R. 2001. The Rb/E2F pathway and cancer. *Hum Mol Genet,* 10**,** 699-703.

NIELSEN, G. P., BURNS, K. L., ROSENBERG, A. E. & LOUIS, D. N. 1998. CDKN2A gene deletions and loss of p16 expression occur in osteosarcomas that lack RB alterations. *Am J Pathol,* 153**,** 159-63.

NIEPEL, M., HAFNER, M., CHUNG, M. & SORGER, P. K. 2017. Measuring Cancer Drug Sensitivity and Resistance in Cultured Cells. *Curr Protoc Chem Biol,* 9**,** 55-74.

NIFOROU, K. M., ANAGNOSTOPOULOS, A. K., VOUGAS, K., KITTAS, C., GORGOULIS, V. G. & TSANGARIS, G. T. 2008. The proteome profile of the human osteosarcoma U2OS cell line. *Cancer Genomics Proteomics,* 5**,** 63-78.

NIU, Z. S., LI, B. K. & WANG, M. 2002. Expression of p53 and C-myc genes and its clinical relevance in the hepatocellular carcinomatous and pericarcinomatous tissues. *World J Gastroenterol,* 8**,** 822-6.

OLINER, J. D., SAIKI, A. Y. & CAENEPEEL, S. 2016. The Role of MDM2 Amplification and Overexpression in Tumorigenesis. *Cold Spring Harb Perspect Med,* 6.

OLIVER, T. G., MEYLAN, E., CHANG, G. P., XUE, W., BURKE, J. R., HUMPTON, T. J., HUBBARD, D., BHUTKAR, A. & JACKS, T. 2011. Caspase-2-mediated cleavage of Mdm2 creates a p53-induced positive feedback loop. *Mol Cell,* 43**,** 57-71.

ORDÓÑEZ, J. L., MARTINS, A. S., OSUNA, D., MADOZ-GÚRPIDE, J. & DE ALAVA, E. 2008. Targeting sarcomas: therapeutic targets and their rational. *Semin Diagn Pathol,* 25**,** 304-16.

ORLANDO, G., KHORONENKOVA, S. V., DIANOVA, II, PARSONS, J. L. & DIANOV, G. L. 2014. ARF induction in response to DNA strand breaks is regulated by PARP1. *Nucleic Acids Res,* 42**,** 2320-9.

ORONSKY, B., CARTER, C., SCICINSKA, A., ORONSKY, A., ORONSKY, N., LYBECK, M. & SCICINSKI, J. 2016. Medical Machiavellianism: the tradeoff between benefit and harm with targeted chemotherapy. *Oncotarget,* 7**,** 9041-5.

OTTAVIANO, L., SCHAEFER, K. L., GAJEWSKI, M., HUCKENBECK, W., BALDUS, S., ROGEL, U., MACKINTOSH, C., DE ALAVA, E., MYKLEBOST, O., KRESSE, S. H., MEZA-ZEPEDA, L. A., SERRA, M., CLETON-JANSEN, A. M., HOGENDOORN, P. C. W., BUERGER, H., AIGNER, T., GABBERT, H. E. & POREMBA, C. 2010. Molecular Characterization of Commonly Used Cell Lines for Bone Tumor Research: A Trans-European EuroBoNet Effort. *Genes Chromosomes & Cancer,* 49**,** 40-51.

PAGLIACCI, M. C., SPINOZZI, F., MIGLIORATI, G., FUMI, G., SMACCHIA, M., GRIGNANI, F., RICCARDI, C. & NICOLETTI, I. 1993. Genistein inhibits tumour cell growth in vitro but enhances mitochondrial reduction of tetrazolium salts: a further pitfall in the use of the MTT assay for evaluating cell growth and survival. *Eur J Cancer,* 29A**,** 1573-7.

PATERNOT, S., BOCKSTAELE, L., BISTEAU, X., KOOKEN, H., COULONVAL, K. & ROGER, P. P. 2010. Rb inactivation in cell cycle and cancer: the puzzle of highly regulated activating phosphorylation of CDK4 versus constitutively active CDK-activating kinase. *Cell Cycle,* 9**,** 689-99.

PELLETIER, J., THOMAS, G. & VOLAREVIC, S. 2018. Ribosome biogenesis in cancer: new players and therapeutic avenues. *Nat Rev Cancer,* 18**,** 51-63.

PELTONEN, K., COLIS, L., LIU, H., TRIVEDI, R., MOUBAREK, M. S., MOORE, H. M., BAI, B., RUDEK, M. A., BIEBERICH, C. J. & LAIHO, M. 2014. A targeting modality for destruction of RNA polymerase I that possesses anticancer activity. *Cancer Cell,* 25**,** 77-90.

PLIKUS, M. V. & CHUONG, C. M. 2008. Complex hair cycle domain patterns and regenerative hair waves in living rodents. *J Invest Dermatol,* 128**,** 1071-80.

POCHAMPALLY, R., FODERA, B., CHEN, L. H., SHAO, W. J., LEVINE, E. A. & CHEN, J. D. 1998. A 60 kd MDM2 isoform is produced by caspase cleavage in non-apoptotic tumor cells. *Oncogene,* 17**,** 2629-2636.

POLIVKA, J. & JANKU, F. 2014. Molecular targets for cancer therapy in the PI3K/AKT/mTOR pathway. *Pharmacol Ther,* 142**,** 164-75.

PRIVES, C. & HALL, P. A. 1999. The p53 pathway. *J Pathol,* 187**,** 112-26.

QUIN, J., CHAN, K. T., DEVLIN, J. R., CAMERON, D. P., DIESCH, J., CULLINANE, C., AHERN, J., KHOT, A., HEIN, N., GEORGE, A. J., HANNAN, K. M., POORTINGA, G., SHEPPARD, K. E., KHANNA, K. K., JOHNSTONE, R. W., DRYGIN, D., MCARTHUR, G. A., PEARSON, R. B., SANIJ, E. & HANNAN, R. D. 2016. Inhibition of RNA polymerase I transcription initiation by CX-5461 activates non-canonical ATM/ATR signaling. *Oncotarget,* 7**,** 49800-49818.

RAI, Y., PATHAK, R., KUMARI, N., SAH, D. K., PANDEY, S., KALRA, N., SONI, R., DWARAKANATH, B. S. & BHATT, A. N. 2018. Mitochondrial biogenesis and metabolic hyperactivation limits the application of MTT assay in the estimation of radiation induced growth inhibition. *Sci Rep,* 8**,** 1531.

REBELLO, R. J., KUSNADI, E., CAMERON, D. P., PEARSON, H. B., LESMANA, A., DEVLIN, J. R., DRYGIN, D., CLARK, A. K., PORTER, L., PEDERSEN, J., SANDHU, S., RISBRIDGER, G. P., PEARSON, R. B., HANNAN, R. D. & FURIC, L. 2016. The Dual Inhibition of RNA Pol I Transcription and PIM Kinase as a New Therapeutic Approach to Treat Advanced Prostate Cancer. *Clin Cancer Res,* 22**,** 5539-5552.

REN, W. & GU, G. 2017. Prognostic implications of RB1 tumour suppressor gene alterations in the clinical outcome of human osteosarcoma: a meta-analysis. *Eur J Cancer Care (Engl),* 26.

RIBI, S., BAUMHOER, D., LEE, K., EDISON, TEO, A. S., MADAN, B., ZHANG, K., KOHLMANN, W. K., YAO, F., LEE, W. H., HOI, Q., CAI, S., WOO, X. Y., TAN, P., JUNDT, G., SMIDA, J., NATHRATH, M., SUNG, W. K., SCHIFFMAN, J. D., VIRSHUP, D. M. & HILLMER, A. M. 2015. TP53 intron 1 hotspot rearrangements are specific to sporadic osteosarcoma and can cause Li-Fraumeni syndrome. *Oncotarget,* 6**,** 7727-40.

ROCHLITZ, C. F., HEIDE, I., THIEDE, C., HERRMANN, R. & DE KANT, E. 1995. Evidence for a mutual regulation of p53 and c-myc expression in human colorectal cancer metastases. *Ann Oncol,* 6**,** 981-6.

ROODMAN, G. D. 1999. Cell biology of the osteoclast. *Exp Hematol,* 27**,** 1229-41.

ROSENBERG, A. E. 2013. WHO Classification of Soft Tissue and Bone, fourth edition: summary and commentary. *Curr Opin Oncol,* 25**,** 571-3.

SADIKOVIC, B., YOSHIMOTO, M., CHILTON-MACNEILL, S., THORNER, P., SQUIRE, J. A. & ZIELENSKA, M. 2009. Identification of interactive networks of gene expression associated with osteosarcoma oncogenesis by integrated molecular profiling. *Hum Mol Genet,* 18**,** 1962-75.

SCHWARZ, R., BRULAND, O., CASSONI, A., SCHOMBERG, P. & BIELACK, S. 2009. The role of radiotherapy in oseosarcoma. *Cancer Treat Res,* 152**,** 147-64.

SENTURK, E. & MANFREDI, J. J. 2012. Mdm2 and tumorigenesis: evolving theories and unsolved mysteries. *Genes Cancer,* 3**,** 192-8.

SERRA, M. & HATTINGER, C. M. 2017. The pharmacogenomics of osteosarcoma. *Pharmacogenomics J,* 17**,** 11-20.

SHEN, P. S., PARK, J., QIN, Y., LI, X., PARSAWAR, K., LARSON, M. H., COX, J., CHENG, Y., LAMBOWITZ, A. M., WEISSMAN, J. S., BRANDMAN, O. & FROST, A. 2015. Protein synthesis. Rqc2p and 60S ribosomal subunits mediate mRNA-independent elongation of nascent chains. *Science,* 347**,** 75-8.

SHINKAI, Y. 1992. RAG-2-deficient mice lack mature lymphocytes owing to inability to initiate V(D)J rearrangemen.

SHINKAI, Y., RATHBUN, G., LAM, K. P., OLTZ, E. M., STEWART, V., MENDELSOHN, M., CHARRON, J., DATTA, M., YOUNG, F. & STALL, A. M. 1992. RAG-2-deficient mice lack mature lymphocytes owing to inability to initiate V(D)J rearrangement. *Cell,* 68**,** 855-67.

SHOSHAN, M. C. & LINDER, S. 2008. Target specificity and off-target effects as determinants of cancer drug efficacy. *Expert Opin Drug Metab Toxicol,* 4**,** 273-80.

SHULTZ, L. D., LYONS, B. L., BURZENSKI, L. M., GOTT, B., CHEN, X., CHALEFF, S., KOTB, M., GILLIES, S. D., KING, M., MANGADA, J., GREINER, D. L. & HANDGRETINGER, R. 2005. Human lymphoid and myeloid cell development in NOD/LtSz-scid IL2R gamma null mice engrafted with mobilized human hemopoietic stem cells. *J Immunol,* 174**,** 6477-89.

SILVA, J., SILVA, J. M., DOMINGUEZ, G., GARCIA, J. M., CANTOS, B., RODRIGUEZ, R., LARRONDO, F. J., PROVENCIO, M., ESPANA, P. & BONILLA, F. 2003. Concomitant expression of p16INK4a and p14ARF in primary breast cancer and analysis of inactivation mechanisms. *J Pathol,* 199**,** 289-97.

SIMS, N. A. & MARTIN, T. J. 2014. Coupling the activities of bone formation and resorption: a multitude of signals within the basic multicellular unit. *Bonekey Rep,* 3**,** 481.

SINGLE, A., BEETHAM, H., TELFORD, B. J., GUILFORD, P. & CHEN, A. 2015. A Comparison of Real-Time and Endpoint Cell Viability Assays for Improved Synthetic Lethal Drug Validation. *J Biomol Screen,* 20**,** 1286-93.

SMITH, J., BOTET, J. F. & YEH, S. D. 1984. Bone sarcomas in Paget disease: a study of 85 patients. *Radiology,* 152**,** 583-90.

STOCK, C., KAGER, L., FINK, F. M., GADNER, H. & AMBROS, P. F. 2000. Chromosomal regions involved in the pathogenesis of osteosarcomas. *Genes Chromosomes Cancer,* 28**,** 329-36.

THOMAS, D. M., JOHNSON, S. A., SIMS, N. A., TRIVETT, M. K., SLAVIN, J. L., RUBIN, B. P., WARING, P., MCARTHUR, G. A., WALKLEY, C. R., HOLLOWAY, A. J., DIYAGAMA, D., GRIM, J. E., CLURMAN, B. E., BOWTELL, D. D., LEE, J. S., GUTIERREZ, G. M., PISCOPO, D. M., CARTY, S. A. & HINDS, P. W. 2004. Terminal osteoblast differentiation, mediated by runx2 and p27KIP1, is disrupted in osteosarcoma. *J Cell Biol,* 167**,** 925-34.

TIKU, V. & ANTEBI, A. 2018. Nucleolar Function in Lifespan Regulation. *Trends Cell Biol,* 28**,** 662-672.

ULUÇKAN, Ö., SEGALINY, A., BOTTER, S., SANTIAGO, J. M. & MUTSAERS, A. J. 2015. Preclinical mouse models of osteosarcoma. *Bonekey Rep,* 4**,** 670.

VAN RIGGELEN, J., YETIL, A. & FELSHER, D. W. 2010. MYC as a regulator of ribosome biogenesis and protein synthesis. *Nature Reviews Cancer,* 10**,** 301-309.

VELLETRI, T., XIE, N., WANG, Y., HUANG, Y., YANG, Q., CHEN, X., CHEN, Q., SHOU, P., GAN, Y., CAO, G., MELINO, G. & SHI, Y. 2016. P53 functional abnormality in mesenchymal stem cells promotes osteosarcoma development. *Cell Death Dis,* 7**,** e2015.

VIJAYAKUMAR, S., LIU, G., RUS, I. A., YAO, S., CHEN, Y., AKIRI, G., GRUMOLATO, L. & AARONSON, S. A. 2011. High-frequency canonical Wnt activation in multiple sarcoma subtypes drives proliferation through a TCF/β-catenin target gene, CDC25A. *Cancer Cell,* 19**,** 601-12.

VORMOOR, B., KNIZIA, H. K., BATEY, M. A., ALMEIDA, G. S., WILSON, I., DILDEY, P., SHARMA, A., BLAIR, H., HIDE, I. G., HEIDENREICH, O., VORMOOR, J., MAXWELL, R. J. & BACON, C. M. 2014. Development of a preclinical orthotopic xenograft model of ewing sarcoma and other human malignant bone disease using advanced in vivo imaging. *PLoS One,* 9**,** e85128.

WEI, G., LONARDO, F., UEDA, T., KIM, T., HUVOS, A. G., HEALEY, J. H. & LADANYI, M. 1999. CDK4 gene amplification in osteosarcoma: reciprocal relationship with INK4A gene alterations and mapping of 12q13 amplicons. *Int J Cancer,* 80**,** 199-204.

WHELAN, J., PATTERSON, D., PERISOGLOU, M., BIELACK, S., MARINA, N., SMELAND, S. & BERNSTEIN, M. 2010. The role of interferons in the treatment of osteosarcoma. *Pediatr Blood Cancer,* 54**,** 350-4.

WUNDER, J. S., GOKGOZ, N., PARKES, R., BULL, S. B., ESKANDARIAN, S., DAVIS, A. M., BEAUCHAMP, C. P., CONRAD, E. U., GRIMER, R. J., HEALEY, J. H., MALKIN, D., MANGHAM, D. C., ROCK, M. J., BELL, R. S. & ANDRULIS, I. L. 2005. TP53 mutations and outcome in osteosarcoma: a prospective, multicenter study. *J Clin Oncol,* 23**,** 1483-90.

XU, H., DI ANTONIO, M., MCKINNEY, S., MATHEW, V., HO, B., O'NEIL, N. J., SANTOS, N. D., SILVESTER, J., WEI, V., GARCIA, J., KABEER, F., LAI, D., SORIANO, P., BANATH, J., CHIU, D. S., YAP, D., LE, D. D., YE, F. B., ZHANG, A., THU, K., SOONG, J., LIN, S. C., TSAI, A. H., OSAKO, T., ALGARA, T., SAUNDERS, D. N., WONG, J., XIAN, J., BALLY, M. B., BRENTON, J. D., BROWN, G. W., SHAH, S. P., CESCON, D., MAK, T. W., CALDAS, C., STIRLING, P. C., HIETER, P., BALASUBRAMANIAN, S. & APARICIO, S. 2017. CX-5461 is a DNA G-quadruplex stabilizer with selective lethality in BRCA1/2 deficient tumours. *Nat Commun,* 8**,** 14432.

XU, J., CHEN, Y. & OLOPADE, O. I. 2010. MYC and Breast Cancer. *Genes Cancer,* 1**,** 629-40.

ZHAI, W. & COMAI, L. 2000. Repression of RNA polymerase I transcription by the tumor suppressor p53. *Mol Cell Biol,* 20**,** 5930-8.

ZHOU, D., ZHANG, Z., HE, L. M., DU, J., ZHANG, F., SUN, C. K., ZHOU, Y., WANG, X. W., LIN, G., SONG, K. M., WU, L. G. & YANG, Q. 2014. Conversion of fibroblasts to neural cells by p53 depletion. *Cell Rep,* 9**,** 2034-42.

ZHOU, X., HAO, Q. & LU, H. 2019. Mutant p53 in cancer therapy-the barrier or the path. *J Mol Cell Biol,* 11**,** 293-305.

ZHOU, Y., SHEN, J. K., YU, Z., HORNICEK, F. J., KAN, Q. & DUAN, Z. 2018. Expression and therapeutic implications of cyclin-dependent kinase 4 (CDK4) in osteosarcoma. *Biochim Biophys Acta Mol Basis Dis,* 1864**,** 1573-1582.

ZINN, K. R., CHAUDHURI, T. R., SZAFRAN, A. A., O'QUINN, D., WEAVER, C., DUGGER, K., LAMAR, D., KESTERSON, R. A., WANG, X. & FRANK, S. J. 2008. Noninvasive bioluminescence imaging in small animals. *ILAR J,* 49**,** 103-15.

Appendix

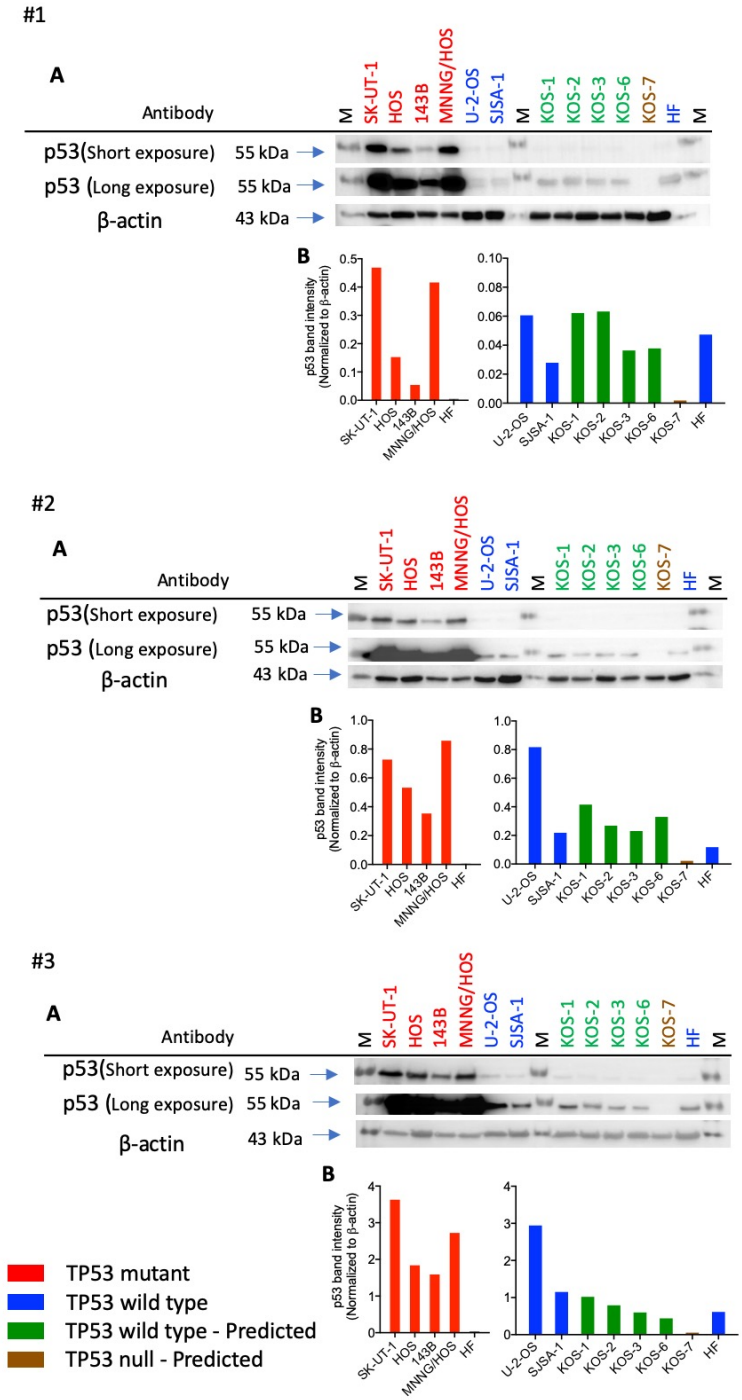

Figure A.1. Western analysis of basal p53 protein expression in exponentially growing OS cell lines, normal human fibroblasts (HF) and leiomyosarcoma SK-UT-1, for 3 independent biological repeats. (#1 is also presented in Figure 3.1.) (A) p53 protein levels were evaluated by western blot analysis. Representatives of a short and long exposure time are presented to illustrate the full range of expression levels. (B) Quantification of p53 blots. p53 Band intensities are shown as a ratio normalized to β-actin on the same blot. The five lines with highest p53 expression were quantitated from the short exposure, and the 8 others from the long exposure. Colours indicate the *TP53* gene status as listed in the ATCC information (Ottaviano et al., 2010), or as predicted from this western blot analysis. M = molecular weight markers. Each replicate was conducted using independently-generated sets of cell lysates.

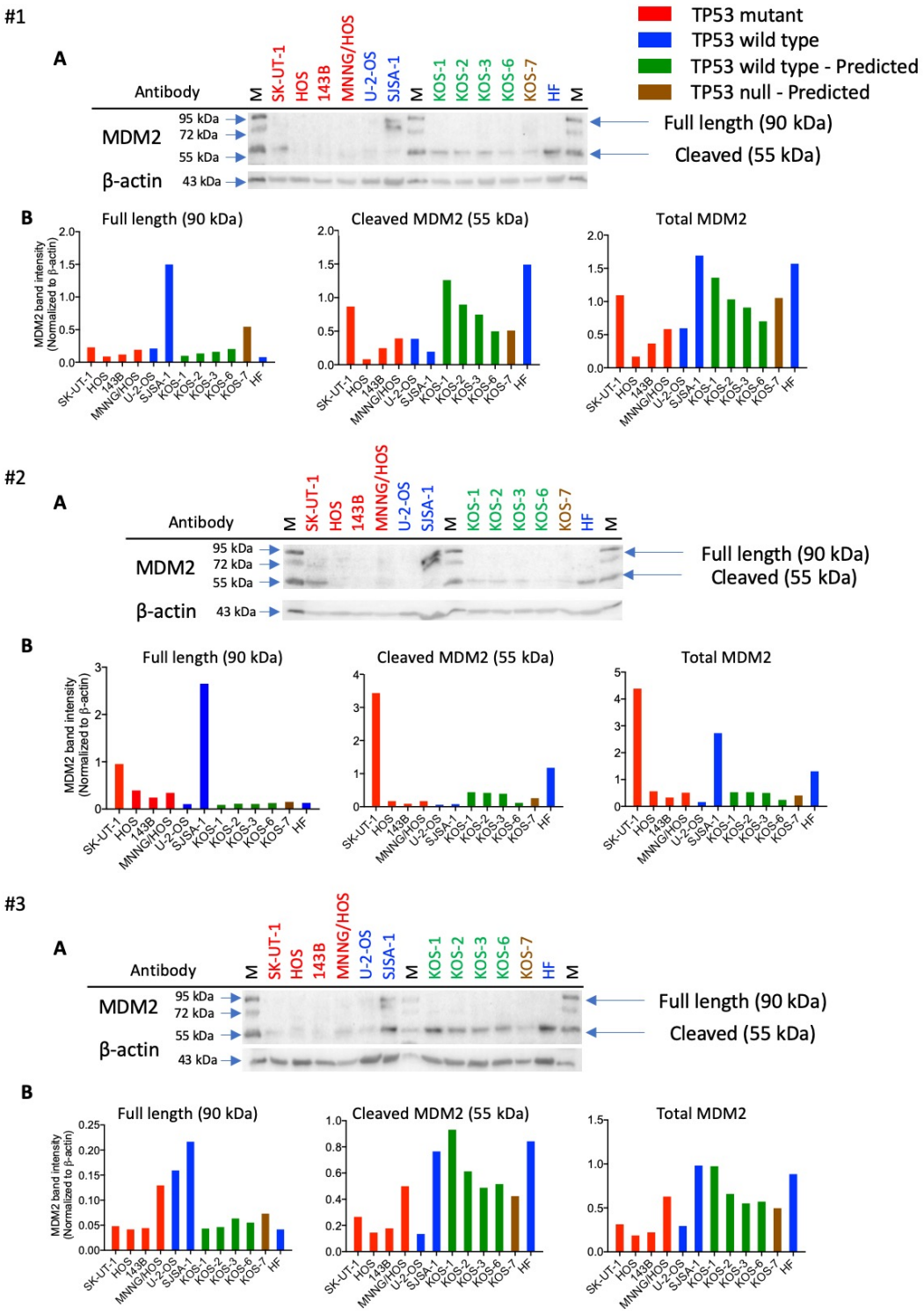

Figure A.2. Western blot analysis of basal MDM2 protein expression in exponentially growing OS cell lines, normal human fibroblasts (HF) and leiomyosarcoma SK-UT-1, for 3 independent biological repeats. (#1 is also presented as Figure 3.3.) (A) MDM2 protein levels were evaluated by western blot analysis. (B) Quantification of MDM2 blots. MDM2 band intensities are shown as a ratio normalized to β-actin on the same blot. Colours indicate the *TP53* gene status as listed in the ATCC information (Ottaviano et al., 2010), or as predicted from the western blot analysis in Figure 3.1. M = molecular weight markers. Each replicate was conducted using independently-generated sets of cell lysates.

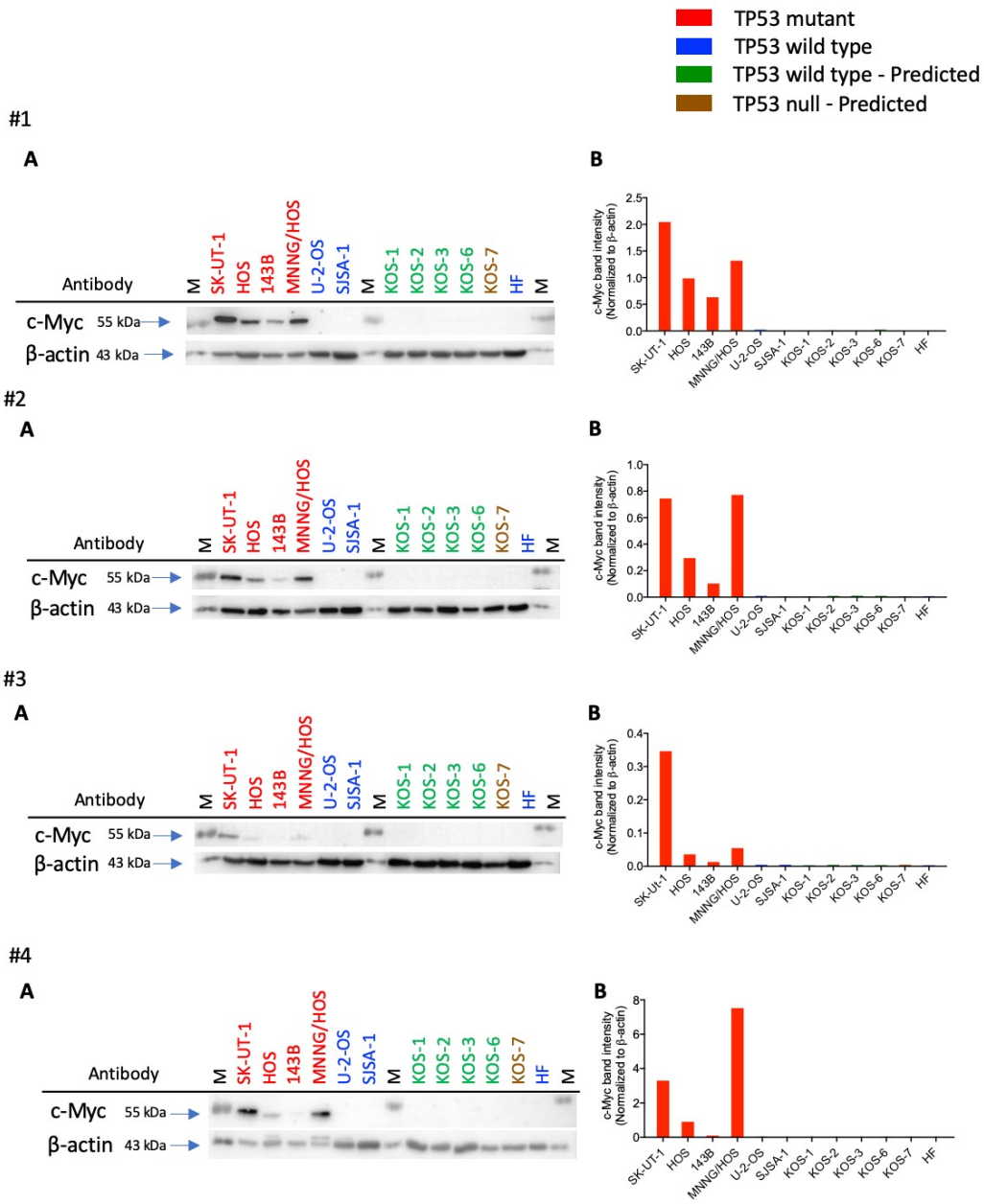

Figure A.3. **Western analysis of basal c-Myc protein expression in exponentially growing OS cell lines, normal human fibroblasts (HF) and leiomyosarcoma SK-UT-1, for 4 independent biological repeats.** (#1 is also presented as Figure 3.2.) (A) c-Myc protein levels were evaluated by western blot analysis. (B) Quantification of c-Myc blots. c-Myc band intensities are shown as a ratio normalized to β-actin on the same blot. Colours indicate the *TP53* gene status as listed in the ATCC information (Ottaviano et al., 2010), or as predicted from the western blot analysis in Figure 3.1. M = molecular weight markers. Each replicate was conducted using independently-generated sets of cell lysates.

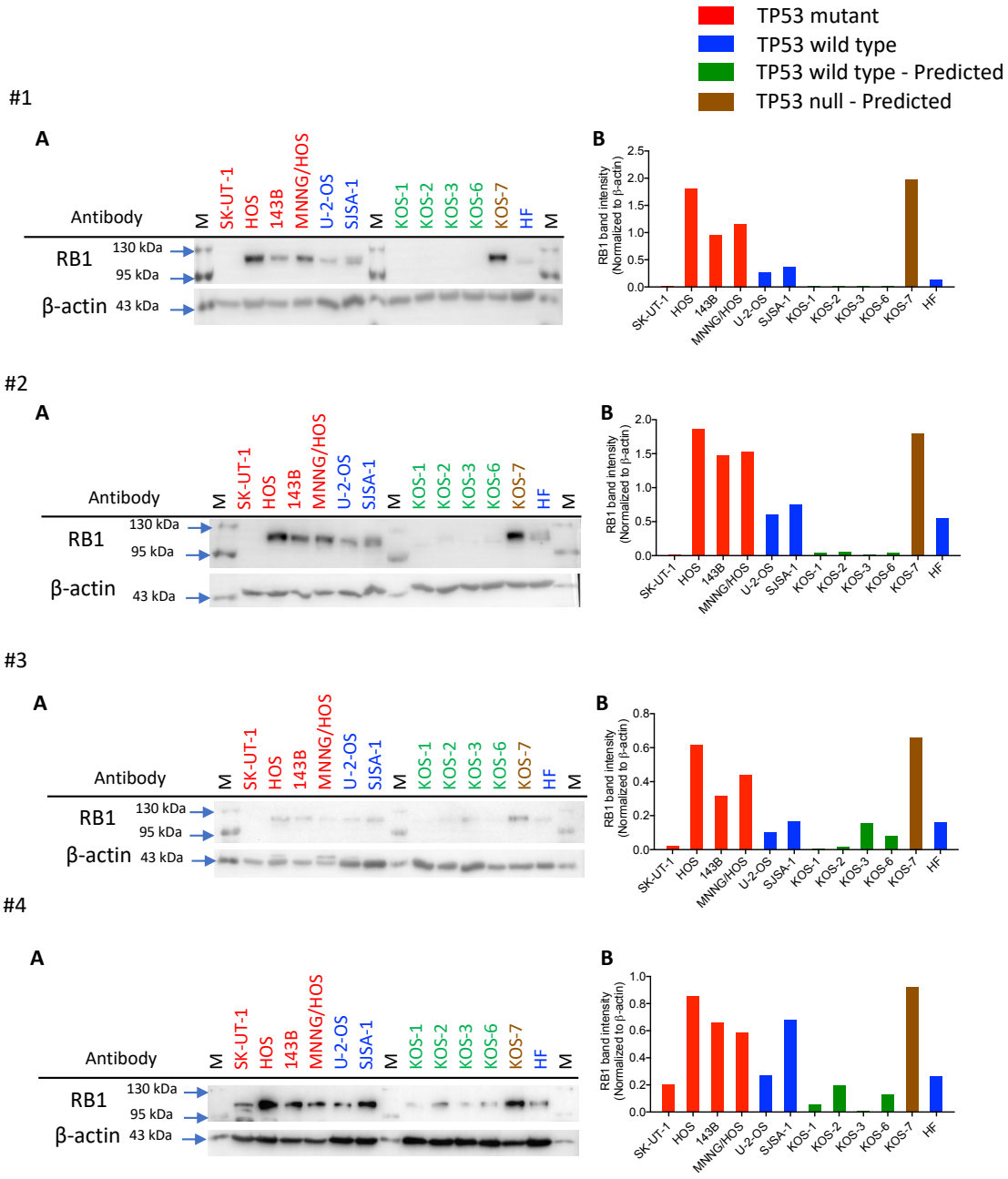

Figure A.4. Western blot analysis of basal RB1 protein expression in exponentially growing OS cell lines, normal human fibroblasts (HF) and leiomyosarcoma SK-UT-1, for 4 independent biological repeats. (#1 is also presented as Figure 3.4.) (A) RB1 protein levels were evaluated by western blot analysis. (B) Quantification of RB1 blots. RB1 band intensities are shown as a ratio normalized to β-actin on the same blot. Colours indicate the *TP53* gene status as listed in the ATCC information (Ottaviano et al., 2010), or as predicted from the western blot analysis in Figure 3.1. M = molecular weight markers. Each replicate was conducted using independently-generated sets of cell lysates.